Gauge theory and nematic order : the rich landscape of orientational phase transition

Liu, K.

Gauge Theory and Nematic Order

The rich landscape of orientational phase transition

Proefschrift

ter verkrijging van
de graad van Doctor aan de Universiteit Leiden,
op gezag van Rector Magnificus
prof. mr. C.J.J.M. Stolker,
volgens besluit van het College voor Promoties
te verdedigen op dinsdag 6 september 2016
klokke 13:45 uur

door

Ke Liu

geboren te Jize (Hebei), China in 1987

Promotor:	Prof. Dr. J. Zaanen
Promotiecommissie:	Prof. Dr. H. T. C. Stoof (Utrecht University)
	Dr. J. van Wezel (University of Amsterdam)
	Prof. Dr. E. R. Eliel
	Dr. D. J. Kraft
	Prof. Dr. K. E. Schalm
	Prof. Dr. V. Vitelli

Casimir PhD series 2016-19
ISBN 978-90-8593-263-5
An electronic version of this thesis can be found at
https://openaccess.leidenuniv.nl

The work described in this thesis is carried out at the Lorentz Institute, Leiden University. The author was supported by a state scholarship program funded by China Scholarship Council (CSC).

The cover shows an oriental landscape excerpted from a classical Chinese drawing, Dwelling in the Fuchun Mountains. The work was created by Gong-Wang Huang in 1300s and now is in public domain. The patterns of seals show my name and signature in ancient Chinese.

To My Family and Fuzi

Contents

Chapter 1

Introduction

Breaking a symmetry down to a subgroup

Spontaneous symmetry breaking refers to the breaking of the symmetry of the underlying physical laws by states of matter, without any asymmetric external disturbances. However, it also acts as a guiding principle to explore physical laws in many fields of modern physics, such as those govering magnetism [1, 2], superfluidity [3, 4], superconductivity [5, 6] and mass generation of fundamental particles [7–10]. Nevertheless, there is an aspect which is obvious but has been somewhat overlooked: there are rich hierarchies of the symmetry broken phases.

Following the symmetry principle, a symmetry can break down to any of its subgroups. Each of these subgroups corresponds to a long range order which has its own ground state manifold and supports distinct rigidity and topological excitations. The associated phase transitions may have different nature in, for instance, the continuity of thermodynamic quantities and, if continuous, the type of critical properties. Moreover, the original symmetry G_0 can break to a symmetry G_1 having non-trivial subgroups, and the latter one can further break, $G_0 \to G_1 \to G_2 \to ...$, with new orders having their own rigidity and topological defects developing from the previous one. This in turn means that, next to the breaking of a symmetry directly to a smaller group, one can break it step by step as well, leading to a rich landscape of intermediate phases.

In this thesis we will use the three-dimensional orthogonal group $O(3)$ as the parent symmetry and discuss spontaneous breaking of $O(3)$ to its subgroups, the three-dimensional point groups. Since $O(3)$ is a rotational group, breaking it will generally lead to orientational orders. In many instances, such as in crystals, these orientational orders may be accompanied with a translational order. However, for simplicity we will only consider

situations where translational symmetries are not broken or not relevant. Following the terminology developed in the field of liquid crystals [11], the associated symmetry broken phases may be called generalized nematics, where "generalized" refers to a richer landscape of symmetries and degrees of freedom. The symmetry associated with a nematic order will relate to an arbitrary point group, and constituents of the system are not necessarily mesogens as in a classical liquid crystals, but can also comprise electrons and spins, as in electronic quantum liquid crystals [12–14] and spin nematics [15, 16].

Why $O(3)$?

$O(3)$ is of practical importance. It is the rotational group of our three-dimensional world, $O(3)$ broken orders can emerge from alignments of real objects. For instance, the familiar uniaxial nematic liquid crystal, which has been commonly used in industry in making display screens, is a phase of aligned cylindrical molecules. Moreover, $O(3)$ also describes the effective degrees of freedom of many magnetic systems. E.g., in the Heisenberg model, although $\frac{1}{2}$-spins are usually parameterized by $SU(2)$ fields, the Hamiltonian is invariant under $O(3)$.

On the other hand, the group structure of $O(3)$ is also sufficiently complex and rich. The subgroups of $O(3)$ are classified as three dimensional point groups: they provide a vast family of candidates for symmetry broken phases (see Fig. 1.1 for a selection). The nature of the associated phase transitions are unclear or unexplored for most of them, and the few well-studied instances evidence that they do have different critical properties. For example, the transition $O(3) \to C_{\infty v}$ [17] and $O(3) \to C_1$ [18] fall into the Heisenberg and the $O(4)$ universality class, respectively, while the transition $O(3) \to D_{\infty h}$ [11] is weakly first order. Moreover, apart from the C_1 symmetry, where $O(3)$ is fully broken, each of these point groups can break further, thereby leaving room for various intermediate phases and transition sequences. E.g., if we choose the D_2 symmetry to break, both the direct $O(3) \to D_2$ transition, and transition sequences like

$$O(3) \to D_{\infty h} \to D_2, \tag{1.1}$$

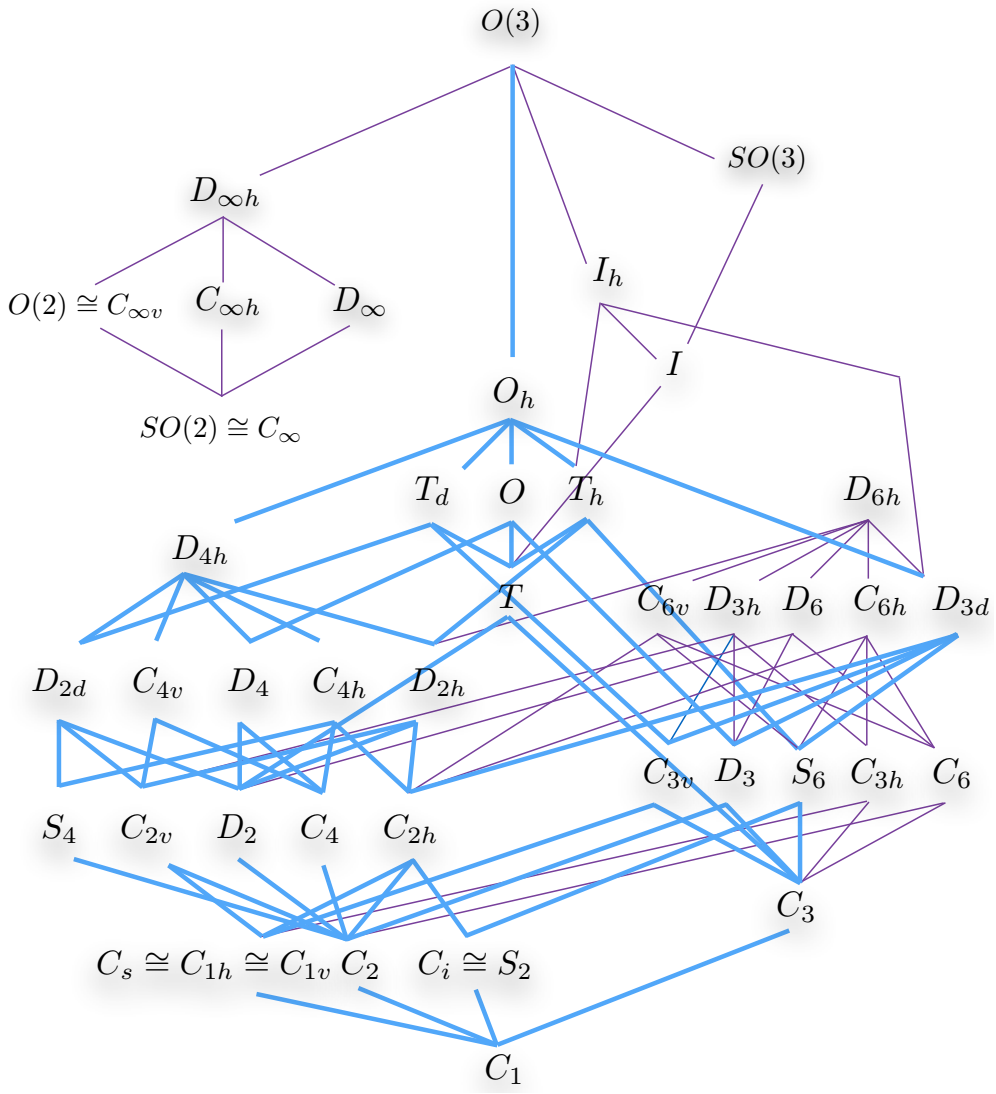

Figure 1.1. A selection of three-dimensional point groups. Following from the symmetry principle, each point group can correspond to an orientational order. The lines indicate subgroup relations (not unique) and spontaneous symmetry breaking may occur between any two groups connected by them. Here the O_h case is highlighted as an example, showing that one can descend all the way down to C_1 corresponding to full symmetry breaking; all orientationally ordered (generalized nematic) phases related to the symmetries connected by the thick lines are allowed. The Schönflies notation is used.

and

$$O(3) \to O_h \to D_{4h} \to D_4 \to D_2 \tag{1.2}$$

can in principle occur. Furthermore, $O(3)$ broken orders support rich topological defects. According to homotopy classifications [19, 20], these defects are in general non-Abelian and can lead to new exotic (non-Abelian) statistics. They can also be excited individually or simultaneously, producing various configurations of order parameter fields and even possibly interfering with the nature of a phase transition.

Discrete non-Abelian gauge theory

$O(3)$ symmetry is not mysterious, and the physics of nematic orders has been subject to intensive research since the late 19th century [21, 22]. However, why does our understanding remain largely limited to a few simple examples, like $C_{\infty v} \cong O(2)$ (Heisenberg magnets), $D_{\infty h}$ (uniaxial nematics) and D_{2h} (biaxial nematics)? Apart from the experimental challenges, from the theory point of view, a central issue is the lack of an efficient theoretical tool to cope with highly symmetric orders.

Though in principle we can employ the standard Landau paradigm to study generalized nematic orders, there are couple of obstacles. The Landau theory of phase transitions uses a functional of order parameters with a certain symmetry. This means that order parameters are required before we can actually write down the Landau free energy. However, such order parameters are generally non-trivial to construct. Moreover, to be able to reflect the unbroken symmetry, the order parameters are in general complicated tensors of high rank, which makes the resulting Landau theory very involved and difficult to solve. Finally, the topological defects of interests are usually not explicitly encoded in a Landau theory, unless they are added artificially.

The central result of this thesis is the introduction of an alternative theory that can efficiently cope with all $O(3)$ broken nematic orders and fit them in a unified framework [23]. The theory revolves around a discrete non-Abelian gauge theory, namely a discrete version of Yang-Mills theory [24], generalizing the Lammert-Rokshar-Toner model of an Abelian Z_2 gauge symmetry [25, 26]. Here the term "discrete" does not only mean that the theory is defined on a lattice [27], but also that the gauge group

is discrete. This gauge group is a three-dimensional point group symmetry. Based on the fact that a gauge symmetry cannot break [28], it can effectively realize the symmetry breaking of $O(3)$ to arbitrary point group symmetries. Since in the theory a point group is used for fixing degrees of freedom of the gauge symmetry, the theory is highly flexible and convenient for all point groups symmetries. It also can act as an order parameter generator for generalized nematic phases [29], rather than requiring order parameters as inputs. Moreover, in terms of gauge couplings, tuning parameters of topological defects are hardwired into the theory.

Outline of this thesis

Before coping with the full complexity of $O(3)$ broken nematic orders, we first discuss in Chapter 2 nematic orders breaking $SO(2)$ symmetry [30] as a preliminary example. $SO(2)$ is the two-dimensional proper rotational group and is Abelian, breaking it can lead to two-dimensional nematic orders characterized by cyclic groups C_N. We will start with reviewing the topological melting of two dimensional crystals at zero temperature [31], where such C_N nematic phases emerge as rotational symmetry broken superfluids. We then construct an order parameter theory, an Abelian $SO(2)/Z_N$ gauge theory, for these quantum C_N nematics and discuss the associated phase transitions. We demonstrate how vectors can be turned into C_N symmetric fields by coupling to Z_N gauge fields, and show that the C_N nematic phase can be realized by the Higgs phase in a gauge theory. The core idea of implementing the nematic symmetry by a gauge symmetry is clarified in this chapter.

In Chapter 3, we begin with the main topic of this thesis: three-dimensional generalized nematic orders and their description with a non-Abelian gauge theory [23]. We show that as a single vector is not sufficient to describe these orders, we have to depart from $O(3)$ matrix fields. This leads to a non-Abelian $O(3)/G$ gauge theory, where G specifies the point group symmetry. The advantages of this theory in comparison with traditional Landau methods are discussed in detail here. We also apply it to various nematic orders and examine their phase transitions. With the benefit that this gauge -theoretical description provides a common reference for all point-group-symmetric nematic orders, we uncover the giant

fluctuations in highly symmetric orders and identify a fluctuation-driven chiral liquid phase.

Chapter 4 focuses on the order parameter tensors of these generalized nematics, being three-dimensional orientational ordering tensors [29]. We first discuss the difficulty in constructing such tensors and then develop a systematic way of deriving them from the $O(3)/G$ gauge theory. Ordering tensors of the physically most interesting cases, including all the crystallographic point groups, the icosahedral groups and the five infinite axial groups, are presented in explicit form. We analyze the structure of these order parameters and their relation with the $O(3)$ subgroup structure. Additionally, the way to measure these tensor order parameters and of using them in determining the symmetry of a phase is discussed.

In Chapter 5, we futher examine the structure of nematic order parameters and the intermediate phases emerging when breaking $O(3)$ [32]. We show that, various intermediate phases can be easily realized in our gauge theory with anisotropic couplings. This anisotropy is in analogy with the biaxiality in the context of biaxial liquid crystals, and is allowed for all finite axial point groups $\{C_n, C_{nv}, S_{2n}, C_{nh}, D_n, D_{nh}, D_{nd}\}$. We thus generalize the well-known biaxial-uniaxial transition of D_{2h}-biaxial nematics to a much broader realm.

Finally, we conclude our study with an outlook in Chapter 6.

Core concepts and necessary background information will be presented whenever needed.

Chapter 2

Preliminary: C_N Quantum nematics in $2+1$ dimensions

In this chapter, we will discuss nematics of two dimensional cyclic symmetries at zero temperature, as a preliminary example of the general three-dimensional point-group-symmetric nematics. These are quantum C_N nematics which are Abelian and can be obtained from quantum crystalline states by dislocation mediated melting in two spatial dimensions. We first recollect some results of the melting procedure in a duality language and then construct an order parameter theory for the resulting nematic orders and discuss the realization of nematic orders by discrete gauge theories.

2.1 Topological melting of a crystal

2.1.1 Topological defects in crystals

Crystalline orders can be perturbed by excitations of the ground state. Ordinary excitations like external shear forces and propagating phonons are smooth disturbances of the order parameter. However, there are also excitations that diminish the order in the form of local singularities in the order parameter fields. Because the order parameter field is smooth everywhere outside of the singularity, the influence of the singularity can be noticed throughout the rest of the system. As this influence does not depend on local details, these singularities are called topological defects. As crystals break both translation and rotation symmetry of the real space, there are two topologically distinct excitations: dislocations and disclinations. They are point and line defects in two and three spatial dimensions, respectively, and are classified by homotopy theory [19, 20].

The topological defects associated with translational order are called dislocations, which can be visualized by the so-called Volterra process: making an imaginary cut in the material and inserting a half-line of particles ending at the dislocation core (Fig. 2.1) [33, 34]. If one traverses

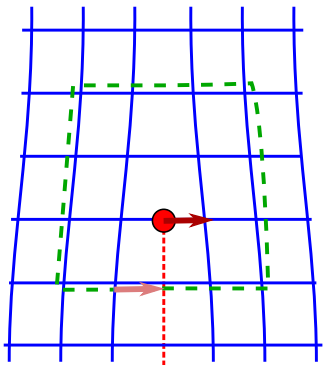

Figure 2.1. Dislocation in a 2D square lattice crystal. In the Volterra processes, a dislocation is a half-line insertion, indicated by the dashed red line. Its topological charge is a Burgers vector, indicated by an arrow. This charge can be picked up by traversing a contour around the defect as indicated by the dotted line.

a circuit around the dislocation core, we notice that there is a deficient displacement. In other words, the lattice distance becomes ill-defined near the dislocation. It is in this sense that dislocations perturb translational order. In the extreme case, dislocations proliferate and completely destroy translational order. The deficient lattice displacement is a vector quantity called the Burgers vector $\mathbf{B} = B^a$ [35],

$$\oint_{\mathcal{C}} \mathrm{d}x^m \partial_m u^a = B^a. \tag{2.1}$$

It is the topological charge associated with the dislocation. The circuit $\mathcal{C}$ around the dislocation core used to measure the displacement is called Burgers circuit (Fig. 2.1). In three dimensions the dislocation core is a line. If the Burgers vector is orthogonal to the line, it is called an edge dislocation, and when the Burgers vector is parallel to the dislocation it is called a screw dislocation. By viewing a 2D system as a planar cut orthogonal to the defect line, 2D dislocations can be said to be edge dislocations.

The topological defects associated with rotational order are called disclinations. The Volterra process for creating a disclination is making a cut and inserting or removing a whole wedge of material (Fig. 2.2) [33, 34]. In a crystal, the operation must always be an element of the point group (e.g. a multiple of $\frac{\pi}{2}$-rotation in a square lattice) to ensure the gluing together of the deformed lattice is locally smooth. The topological charge is obtained by the angle of rotation in parallel transporting

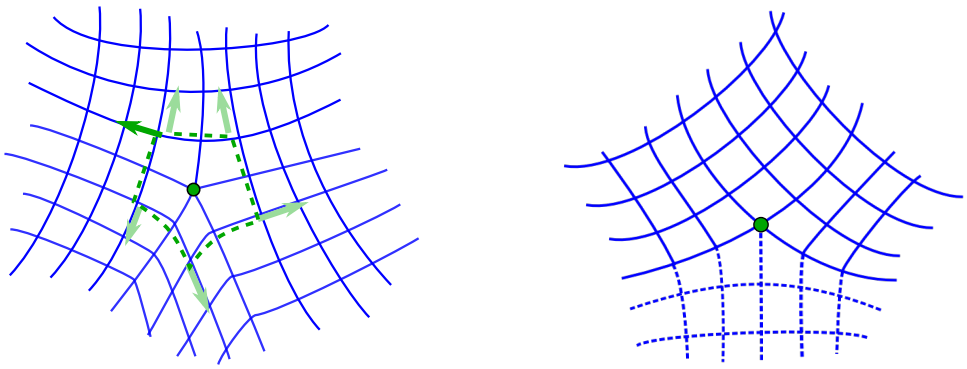

(a) disclination (b) Volterra construction

Figure 2.2. Disclinations in a 2D square lattice crystal. (a) A disclination is the insertion of a wedge. The site at the defect core has five instead of four neighboring sites, therefore the Frank charge is $\frac{\pi}{2}$. This can be picked up by parallel transport of a vector along a closed circuit around the disclination core, indicated by the dotted line. (b) The Volterra construction of a disclination. The inserted material us indicated by dashed lines.

of a vector around the disclination core, see Fig. 2.2(a). It is called the Frank tensor $\Omega^{c_1\cdots c_{D-2}}$ [36],

$$\oint_{\mathcal{C}} \mathrm{d}x^m \partial_m \epsilon_{c_1\cdots c_{D-2}ab}\omega^{ab} = \Omega^{c_1\cdots c_{D-2}}. \tag{2.2}$$

In D spatial dimensions, the Frank tensor has $D-2$ components. So in 2D it is a scalar Ω and in 3D a vector Ω^c. The Frank tensor points perpendicular to the plane of rotation, and its magnitude denotes the deficient angle. In 3D, the straightforward generalization of a 2D disclination is to have the disclination line pointing out of the plane in Fig. 2.2(a), that is, parallel to its Frank vector. This is called a wedge disclination for obvious reasons. When the Frank vector is orthogonal to the disclination line it is called a twist disclination.

However, dislocations and disclinations are not independent. A dislincation can be viewed as an infinite set of dislocation and is energetically much more costly, and a dislocation can be viewed as the disclination and anti-dislicnation pair.

2.1.2 Defect mediated melting

As the influence of the topological defect perturbs is noticeable even at long distances from the singularity, the energy of a single defect grows with

distance, as the energy of a vortex in a superfluid grows logarithmically with distance. Therefore, one hardly finds isolated defects in long-range ordered materials; instead one finds pairs of defects–antidefects that together are topologically neutral at length scales larger than that of defect separation. The creation of such a pair costs a finite amount of energy.

In imaginary time, the creation and subsequent annihilation of such a defect pair can be represented by a closed loop in spacetime. Upon increasing quantum fluctuations, the number of these loops increases and the size of these loop grows. At a critical point, these loops blow out and single defects appears and proliferate. This lead to the destruction of the ordered state.

However, due to the hierarchy of the topological defects of translations and rotations, dislocations are intrinsically easier to produce than disclinations. Therefore, the proliferation of disclinations and dislocation can happen separately, although *a priori* one cannot exclude the possibility that the disclinations will proliferate together with the dislocations giving rise to the first-order transition directly from the solid to the isotropic liquid.

Only dislocations proliferating but disclinations staying massive will lead to a state where the translational symmetry is restored but the breaking of the rotational symmetry of the solid is maintained, i.e., a nematic or liquid crystal phase. Since the dislocation does not take the responsibility for rotational symmetry breaking, their proliferation will still broken as characterized by the point group of the 'parent' crystal. These form the family of 'nematic-like' liquid crystals. In 2 spatial dimensions, these nematics are classfied by the subgroup of $O(2)$, leading to chiral or non-chiral nematic with p-fold symmetry [30]. The classical correspondance for this phase is the hexatic phase with D_6 symmetry [37].

2.2 Quantum field theory description of dislocation melting and quantum nematics

2.2.1 Stress-strain duality

The above procedure of topological melting can be well described by utilizing the stress-strain duality in elasticity [31, 38, 14, 39], which is an extended version of the familiar vortex-boson duality [33].

In the stress-strain duality, the strain variables $\partial_m u^a$ are the original

fields in the Lagrangian describing the low lying excitations of a crystal,

$$\mathcal{L}_{\text{original}}[\partial_m u^a] = \frac{1}{2}\partial_\mu u^a C_{\mu\nu ab}\partial_\nu u^b. \tag{2.3}$$

Here u^a is a displacement in two spatial dimensions with $a = x, y$. $\mu = \tau, x, y$, however, is the index of spacetime, so dynamical case with imaginary-time derivatives $\partial_\tau u^a$ taken into account [14]. Correspondingly, the standard textbook spatial elasticity tensor is now expanded to a spatio-temporal variant $C_{\mu\nu ab}$. The stresses are the canonical momenta conjugate to the generalized velocities that the strains represent,

$$\sigma^a_\mu = -\mathrm{i}\frac{\delta\mathcal{S}}{\delta(\partial_\mu u^a)} = -\mathrm{i}C_{\mu\nu ab}\partial_\nu u^b. \tag{2.4}$$

The factor $-i$ stems from the imaginary-time formalism.

In the duality, we will take the stresses as the principal variables and express the strains $\partial_\nu u^b$ in terms of stress σ^a_μ,

$$\begin{aligned}\mathcal{L}_{\text{dual}}[\sigma^a_\mu, \partial_\mu u^a] &= \mathcal{H} + \mathrm{i}\sigma^a_\mu\partial_\mu u^a \\ &= \tfrac{1}{2}\sigma^a_\mu C^{-1}_{\mu\nu ab}\sigma^b_\nu + \mathrm{i}\sigma^a_\mu\partial_\mu u^a.\end{aligned} \tag{2.5}$$

$C^{-1}_{\mu\nu ab}$ denotes the inverse of the elasticity tensor. When the underlying solid is isotropic, $C_{\mu\nu ab}$ can be diagonalized and requires only two elasticity moduli, and can be easily inverted [31]. For anisotropic solids, $C_{\mu\nu ab}$ contains off-diagonal entries and requires extra moduli, and is difficult to invert. However, it is anticipated that this anisotropy can be reproduced by the anisotropy in the dislocation condensate.

Next we separate the displacement field into smooth and singular parts $u^a(x) = u^a_{\text{smooth}}(x) + u^a_{\text{sing}}(x)$. On the smooth part we perform integration by parts, and then integrate it out as a Lagrange multiplier for the constraint

$$\partial_\mu\sigma^a_\mu = 0. \tag{2.6}$$

This relation represents the well-known fact that stress is locally conserved in a solid.

In two spatial dimensions, Eq. (2.6) can be explicitly enforced by expressing the stress as the curl of a gauge field called the dual stress gauge field,

$$\sigma^a_\mu(x) = \epsilon_{\mu\nu\lambda}\partial_\nu b^a_\lambda(x), \tag{2.7}$$

where $b^a_\mu = (b^a_\mathrm{t}, b^a_m) = (\frac{1}{c_\mathrm{T}} b^a_\tau, b^a_m)$ with c_T being the phonon velocity. b^a_λ is a flavored vector with six components. However, there are two independent gauge transformations which leave the stress tensor invariant,

$$b^a_\lambda(x) \to b^a_\lambda(x) + \partial_\lambda \varepsilon^a(x), \tag{2.8}$$

where ε^x and ε^y are two arbitrary scalar fields. The number of physical degrees of freedom is then reduced to four, corresponding to Eq. (2.6). Moreover, by enforcing the Ehrenfest constraint [40]

$$\epsilon_{\mathrm{t}am}\sigma^a_m = \partial_m b^m_\mathrm{t} - \partial_\mathrm{t} b^n_n = 0, \tag{2.9}$$

one can further reduces b^a_λ to three degrees of freedom, which correspond to the three independent components of symmetric strains in two spatial dimensions.

Substituting the definition Eq. (2.7) into the Lagrangian Eq. (2.5) we find

$$\begin{aligned}\mathcal{L}_\mathrm{dual} &= \tfrac{1}{2}(\epsilon_{\mu\kappa\lambda}\partial_\kappa b^a_\lambda) C^{-1}_{\mu\nu ab}(\epsilon_{\mu\rho\sigma}\partial_\rho b^b_\sigma) + \mathrm{i}(\epsilon_{\mu\kappa\lambda}\partial_\kappa b^a_\lambda)\partial_\mu u^a \\ &= \tfrac{1}{2}(\epsilon_{\mu\kappa\lambda}\partial_\kappa b^a_\lambda) C^{-1}_{\mu\nu ab}(\epsilon_{\mu\rho\sigma}\partial_\rho b^b_\sigma) + \mathrm{i} b^a_\lambda J^a_\lambda,\end{aligned} \tag{2.10}$$

where in the second line we have defined the dislocation current J^a_λ after performing partial integration, with

$$J^a_\lambda = \epsilon_{\lambda\mu\nu}\partial_\mu\partial_\nu u^a_\mathrm{sing}, \tag{2.11}$$

analogous to the vortex density in the standard vortex-boson duality [41, 42]. From this action we see that dislocations J^a_λ can be viewed as charged particles and interact by exchanging gauge fields b^a_λ. For this reason the fields b^a_λ are referred to as stress photons in the stress-strain duality. Moreover, the dislocations can in turn lead to shear stress in the material and therefore source the stress gauge fields.

2.2.2 Quantum nematic as dual stress superconductor

As we start with a bosonic crystal, it is natural to expect that these dislocations are also bosonic. Therefore, at the melting transition to the nematic phase, these dislocation will proliferate and condense. Moreover, in the content of stress-strain duality, dislocations are charged particles and interact by electromagnetism-like stress gauge fields. Therefore, the

condensate of dislocations means BEC of charged particles and the nematic phase in this content can be viewed as a superconductor, a dual stress superconductor, as the disordered superfluid (Mott insulator) can be viewed as an superconductor of vortexes.

However, the dislocation condensate has a variety of complications, rendering the stress superconductor to be a much richer affair. First of all, instead of the simple scalar topological charge of the vortex (the winding number), dislocations carry the Burgers vector charge B^a. For a lattice in two spatial dimensions, B^a is quantized in terms of two orthogonal vectors. This translates to stress gauge fields b^a_μ coming in two 'Burgers flavors'. Comparing to the vortex condensate characterized by a single $U(1)$-condensate field, this implies that we have to cope with two independent disorder fields taking care of the restoration of translational symmetry in the two orthogonal space directions. We therefore need two complex scalar Higgs fields $\Phi^a = |\Phi^a| \mathrm{e}^{\mathrm{i}\phi^a}$ with $a = x, y$ to represent the dislocation condensate. Therefore, the amplitude of dislocation condensate can be regarded as that of a two-component Bose–Einstein condensate,

$$\begin{aligned}\mathcal{L}_{|\Phi|} &= V(|\Phi^x|, |\Phi^y|) \\ &= \tfrac{\alpha_x}{2}|\Phi^x|^2 + \tfrac{\alpha_y}{2}|\Phi^y|^2 + \tfrac{\beta_x}{4}|\Phi^x|^4 + \tfrac{\beta_y}{4}|\Phi^y|^4 + \tfrac{\gamma}{2}|\Phi^x|^2|\Phi^y|^2, \end{aligned} \tag{2.12}$$

where γ describes the interaction between the two condensates, $\alpha_{x,y}$ and $\beta_{x,y}$ affect symmetries.

Furthermore, to incorporate the condensate phase fluctuations and the dual stress gauge fields, we can rest on a general principle: the coupling between gauge fields and an isolated charged particle $\mathrm{i}A_\mu J_\mu$ turns into the minimal gauge coupling of the condensate field formed from these particles, enumerated by the covariant derivative $\partial_\mu - \mathrm{i}A_\mu$ acting on the condensate field. Dealing with stress photons, the flavored sourcing term $\mathrm{i}b^a_\mu J^a_\mu$ suggests that the disorder field theory should contain the covariant derivative terms $\sim |(\mathbf{e}^a\partial_\mu - \mathrm{i}b^a_\mu)\Phi^a|^2$ for all flavors, where $\mathbf{e}^a$ denotes the basis vectors.

Moreover, there is one more ingredient that has to be dealt with: the glide constraint, $\epsilon_{\mathfrak{t}\mu a} J^a_\mu = 0$, which restricts the dislocations to only move along their Burgers vectors, when interstitial excitations are absent [43]. This can be imposed by a Lagrange multiplier field $\lambda(x)$ [14, 39, 43],

$$\mathcal{L}_{\text{glide}} = \mathrm{i}\lambda\epsilon_{\mathfrak{t}\mu a} J^a_\mu. \tag{2.13}$$

Then at any stage of the calculation, integrating out λ will impose the

glide constraint. The source term involving the dislocation current correspondingly becomes [14],

$$\mathcal{L}_{\text{source}} = \mathrm{i}\left(b^a_\mu + \lambda\epsilon_{\mathfrak{t}\mu a}\right) J^a_\mu. \tag{2.14}$$

The recipe is now to replace b^a_μ with $b^a_\mu + \lambda\epsilon_{\mathfrak{t}\mu a}$ when coupling to dislocations, which works equally well for single dislocations as for dislocation condensates.

Concluding, in the path integral, the dislocation source term including the glide constraint Eq. (2.14) is just a gauge covariant derivative "dressed with the glide constraint" acting on the $\Phi^{x,y}$ disorder fields. This implies that we are dealing with gradient terms in the effective action,

$$\mathcal{L}_{\text{kin}} = \frac{1}{2}\sum_{a=x,y} |\left(\partial_\mu - \mathrm{i}b^a_\mu - \mathrm{i}\lambda\epsilon_{\mathfrak{t}\mu a}\right)\Phi^a|^2. \tag{2.15}$$

We have now completed the formulation of the disorder field theory describing the dual stress superconductors. In full it is given by the Lagrangian,

$$\mathcal{L}_{\text{stress SC}} = \mathcal{L}_{\text{kin}} + \mathcal{L}_{|\Phi|} + \mathcal{L}_{\text{stress}} \tag{2.16}$$

where the minimal coupling term $\mathcal{L}_{\text{kin}}$ takes care of the interactions between the stress gauge fields and the dual disorder parameters, the condensation of the disorder fields is governed by the potential $\mathcal{L}_{|\Phi|}$, Eq. (2.12), and

$$\mathcal{L}_{\text{stress}} = \tfrac{1}{2}(\epsilon_{\mu\kappa\lambda}\partial_\kappa b^a_\lambda)C^{-1}_{\mu\nu ab}(\epsilon_{\nu\rho\sigma}\partial_\rho b^b_\sigma) \tag{2.17}$$

given by Eq. (2.10), describing the stress gauge fields of the crystal.

2.2.3 Collective modes of quantum nematics

We have discussed the filed theory description of the topological melting of crystals in $2+1$ d. With the Lagrangian Eq. (2.16), we can compute the spectrum of the collective modes of quantum nematics. Remarkably, besides two modes inherited from propagating phonons of a crystal, there are in additional a rotational Goldstone mode due to the $O(2)$ rotational symmetry breaking and phase fluctuations of the flavored dislocation condensate [31]. This richer spectrum is not that obvious without the strain-stress duality.

Massive transversal phonon

In the duality language, dislocations are charged particles coupled to the dual stress gauge fields and quantum nematics can be regarded as stress superconductors. Much like the $U(1)$ gauge field obtains a Higgs mass in a real superconductor, a component of stress photon fields b^a_μ will acquire a mass set by the magnitude of the dislocation condensate. The massive components of stress photon fields propagate shear stress and duals from the transversal phonon in a solid. Moreover, in analogy with the Meissner effect of a real superconductor, external shear stresses are expelled from the dual stress superconductor. This just reflects the fact that, nematic liquid crystals do not carry the shear modulus, thus can not propagate shear stress.

Zero sound of the nematic superfluid

Though nematic liquid crystals do not have response to shear force, they response to compressional force and can propagate sound. In the stress-strain duality, under proper coordinate framework and gauge fixing, one can show that dislocations decouple from the component of stress gauge fields propagating compressional stress [31]. To this component of the stress gauge field, dislocations are neutral particles whose condensate is a superfluid, instead a superconductor. Moreover, the dislocation superfluid will liberate the constituent bosons from the crystal lattice to form a real superfluid. Therefore, the compressional sound, inherited from the longitudinal phonon of a crystal, is actually the zero sound of a superfluid.

Rotational Goldstone mode

The nematic superfluid just discussed, however, is different to a normal superfluid, since though the translational symmetry is restored, the rotational symmetry remains broken. Followed from the Goldstone theorem [44], there is a rotational Goldstone mode from the $O(2)$ rotational symmetry breaking. One further finds that, the velocity of this mode is propotional to the magnitute of the dislocation condensate[45]. This is consistent with the fact that the rotational Goldstone mode is missing in solids. At a more fundamental level, this mode is confined in solids similar to the confinement in QCD. The rotational Goldstone mode is a perturbation to the orientational order sourced by external torque force or individual disclinations. In a solid, the energy cost for propagating the torque stress

or for separating a disclination-anti-disclination pair grows with distance r as r^2. Therefore, single disclinations are confined, and by perturbing a solid with an external torque source will excite massless phonons, instead of rotational Goldstone modes. In quantum nematics, however, dislocations are free and disclinations are deconfined defects in the background of dislocation condensates. The force of separating a disclination and an anti-disclination decays logarithmically, as separating a vortex-anti-vortex pair, and rotational Goldstone modes are thus propagating.

On the other hand, this mode is overdamped in a thermal classical nematic liquid crystal. In a thermal nematic, which mechanically is a fluid, the rotational Goldstone mode couples to the circulation of the fluid and, therefore, is subjected to viscous damping. Dealing with quantum nematics, which is a superfluid, circulations are massive and can only enter in form of quantized vortices. Therefore the rotational Goldstone mode is protected against the circulation and can propagate as an undamped mode.

Massive phase modes of dislocation condensate

There are also phase fluctuations of dislocation condensates. These modes are massive and reveal the short range structure of the system. That is, the translational symmetry has been restored in quantum nematics by the dislocation condensate, however, at the energy scale larger than the Higgs mass of dislocation condensates (the length scale smaller than the distance between dislocations), the system will discover its short-range crystal nature.

2.3 Order parameter theory for $2+1$ d quantum nematics

In the melting process to quantum nematics discussed in the previous chapter, the translational symmetry has been restored by dislocation condensate. What remains of the crystalline order is the discrete rotational symmetry, for which the corresponding topological defects are disclinations. The next step is to develop a theory describing phases with these discrete rotational symmetries and their transitions to the isotropic liquid. The rotational symmetries of nematics melt from $2+1$ d crystals are classified by two dimensional crystallographic point groups. However, in

full generality, nematics in two spatial dimensions are classified by all the two dimensional point groups, i.e., C_N and D_N, not necessarily restricted by the crystalline symmetry. Therefore, in the rest of this chapter, we will lift us from crystallographic point groups, and for simplicity we will focus on the cyclic groups C_N which are Abelian.

2.3.1 $SO(2)/Z_N$ Gauge theory and C_N quantum nematics

The proper order parameter theory of C_N nematics need correctly incorporating the N-fold rotational symmetry. In case $N = 1$, the rotational symmetry is trivial and the effective theory is simply the XY model with a two dimensional vector order parameter, $\phi = (\cos\theta, \sin\theta)$ or a complex scalar order parameter, $\phi = e^{i\theta}$. For C_N nematics in general, however, the order parameters are tensors of rank N [46]. An example is the two-dimensional director order parameter $Q^{ab} = n^a n^b - \frac{1}{2}\delta^{ab}$ for C_2 nematics. Follow the conventional Landau paradigm, one may like to write down a generalized Landau-de Gennes free energy or to construct a lattice model with regard to these tensors. However, this is not convenient when N is large where one needs to deal with theories of high rank tensors.

One notice that, for C_N nematics, the N-fold symmetry means that the angle θ defines the $O(2)$ rotor $(\cos\theta, \sin\theta)$ or $e^{i\theta}$ should be identified as

$$\theta \equiv \theta + 2\pi k/N, \quad k = 1, 2, \ldots, N. \tag{2.18}$$

This is a local, discrete symmetry enforcing the point group symmetries on the rotor θ. In contrast to global symmetries that imply degeneracies of states, such local symmetries imply that two states related by the local symmetries are physically the same or indistinguishable. In effect, the rotor ceases to be a physical variable due to the local symmetry, similarly to the uniaxial nematic vector $\mathbf{n} \cong -\mathbf{n}$ giving rise to the director.

Such local symmetries are ubiquitous in physics and are usually referred to as gauge symmetries. They do not, however, represent symmetries in the traditional sense but instead redundancies in the degrees of freedom and in this sense can be introduced whenever convenient [47, 48]. All physical observables are gauge invariant and the disappearance of the gauge degrees of freedom can be made explicit by imposing a suitable gauge fix.

The gauge formulation for nematic liquid crystals was first applied in Refs. [25, 26], where a Z_2 gauge theory [49, 50] is coupled to $O(3)$ vector

fields in order to implement the head-to-tail symmetry of director fields. Following the same logic, the effective theory of $2+1$ d C_N nematics can be formulated by Z_N gauged XY rotors [30], leading to a $SO(2)/Z_N$ theory, by the isomorphism $C_N \simeq Z_N$,

$$\begin{aligned} S &= S_I + S_G, \\ S_I &= -\frac{J}{2}\sum_{\langle ij\rangle} \phi_i^* U_{ij}\phi_j + \text{ c.c.} = -J\sum_{\langle ij\rangle}\cos(\theta_i - \theta_j - a_{ij}), \\ S_G &= -\frac{K}{2}\sum_{\square}\prod_{\langle ij\rangle} U_{ij} + \text{ c.c.} = -K\sum_{\square}\cos(\sum_{\langle ij\rangle\in\square} a_{ij}). \end{aligned} \tag{2.19}$$

Here the invariance of S under the local symmetry Eq. (2.18) necessitates the introduction of the C_N gauge field $U_{ij} = \mathrm{e}^{-\mathrm{i}a_{ij}}$ acting on the rotors $\phi_i = \mathrm{e}^{\mathrm{i}\theta_i}$, where $a_{ij} = \frac{2\pi}{N}k_{ij}$ and $k_{ij} = 0, 1, \ldots, N-1$ are Z_N valued fields on the links $\langle ij\rangle$ of the lattice. Consistency requires $U_{ji} = U_{ij}^*$ and all sums and products over the plaquettes $\square$ are taken in a counterclockwise manner along their boundary. Moreover, the the local symmetry Eq. (2.18) is now realized by the local gauge transformation

$$\begin{aligned} \theta_i &\to \theta_i + \frac{2\pi k_i}{N}, \\ a_{ij} &\to a_{ij} + \frac{2\pi(k_i - k_j)}{N}. \end{aligned} \tag{2.20}$$

Let us now briefly describe the interpretation of the $SO(2)/Z_N$ gauge theory in the context of nematics [25, 26, 30]. The meaning of the term S_I is as usual: it favors the ordering of the orientational degrees of freedom but now modulo the N-fold symmetries. On the other hand, the term S_G represents the simplest gauge invariant term for the gauge fields $\{U_{ij}\}$. This term describes the dynamics of disclinations. In terms of the Volterra construction (Sec. 2.1.1), disclinations for C_N nematics are classified by elements of the group C_N. The presence of a disclination leads to a rotation to the vector encircling it. These defect are now encoded by frustrated plaquette of the Z_N gauge theory with K defining the defect core energy. As depicted in Fig. 2.3, parallel transporting a vector abound a frustrated plaquette is just as encircling a disclination core.

2.3.2 Phase diagram of the $SO(2)/Z_N$ model

Having defined the gauge model of nematics, we now analyze its phase diagram. The possible phases and transitions can be sketched by discussing

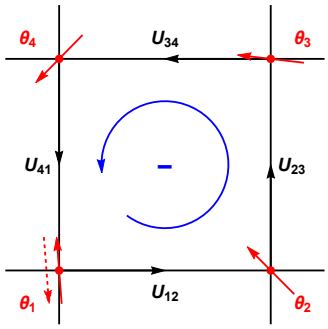

Figure 2.3. The lattice model has rotors $\{\theta_i\}$ (red) defined on sites and gauge fields $\{U_{ij}\}$ on the links (black arrows). In the simplest case of $SO(2)/Z_2$, a disclination is given by a $e^{i\pi} = -1$ gauge flux over a plaquette and leads to a π-rotation ambiguity (dashed) at the site 1 when encircling clockwise.

the various limiting behaviors of the gauge model Eq. (2.19), leading to a phase diagram given in Fig. 2.4.

$J \to 0$ limit

In the limit $J \to 0$, the theory Eq. (2.19) is just pure Z_N-gauge theory in three dimensions and there is a confinement–deconfinement phase transition at $K = K_c$ [51–53]. Z_N gauge fluxes are condensed in the confined regime at $K < K_c$. In the deconfined regime at $K > K_c$, however, the gauge fields have a gap and the Z_N gauge fluxes remain well defined excitations over the vacuum. At finite but small J, we expect that the behavior of the gauge fields remain similar to that in a pure gauge theory. This phase is actually topological [48, 26, 54, 30] given that this is the deconfined phase of Z_N gauge theory.

$J \to \infty$ limit

In this limit, the S_I term in Eq. (2.19) will suppresses all non-gauge fluctuations of rotor fields, since $\cos(\theta_i - \theta_j - a_{ij}) = 0$ is favored. Thus the rotor and gauge fields are ordered, independent of K. Even for $K = 0$, excitations of the gauge theory are still gapped via the S_I term and the spectrum contains Coulomb-confined neutral pairs of gauge excitations with finite energy. Hence, there is no phase transition in the gauge theory as a function of K for large enough J. We identify this phase with ordered rotor fields and no free Z_N gauge flux excitations as the C_N nematic phase.

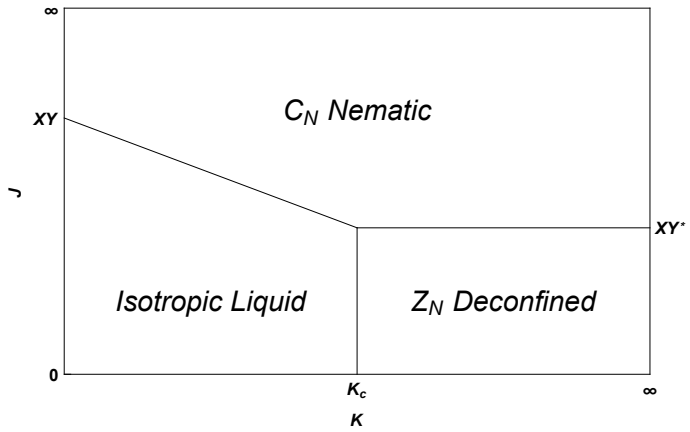

Figure 2.4. The schematic phase diagram of the $SO(2)/Z_N$ gauge theory. The C_N nematic phase has long range orientational order and Z_N disclinations. In the isotropic liquid phase at small J and K, the Z_N disclinations are condensed and the orientational order is destroyed. In the $Z_{N\geq 2}$ deconfined phase only N-tuples of $Z_{N\geq 2}$ vortices are condensed, leading to a phase with free Z_N disclinations but no long range orientational order.

$K \to 0$ limit

Here the theory Eq. (2.19) reduces to S_I and the gauge fields do not have independent dynamics. The nematic coupling J will drive a phase transition between the C_N nematic phase and a completely disordered phase which is identified as the isotropic liquid phase.

Moreover, in this limit, gauge fields on different links are decoupled and we can trace them out to obtain an effective action for pure matter fields. It is convenient to do so under the Villain approximation [55–57],

$$\begin{aligned} e^{-S_I} &= \prod_{\langle ij \rangle} e^{J\cos(\theta_i - \theta_j - a_{ij})} \\ &\to \sum_{\{l_{ij}\}\in\mathbb{Z}} \prod_{\langle ij \rangle} N_V(J) e^{-\frac{J_V}{2}(\theta_i - \theta_j - a_{ij} + 2\pi l_{ij})^2}, \end{aligned} \tag{2.21}$$

Here l_{ij}'s are integer valued auxiliary fields on the link $\langle ij \rangle$, $J_V(J)$ is the effective Villain coupling and $N_V(J)$ is an unimportant analytical normalization factor. Note that $a_{ij} = \frac{2\pi k_{ij}}{N}$ is Z_N valued. We can rewrite

the above equation as

$$\sum_{\{l_{ij}\}\in\mathbb{Z}} \prod_{\langle ij\rangle} N_V(J) e^{-\frac{J_V}{2N^2}[N(\theta_i-\theta_j)-Na_{ij}+2N\pi l_{ij}]^2}$$

$$\to \sum_{\{m_{ij}\}\in\mathbb{Z}} \prod_{\langle ij\rangle} N_V(J) e^{-\frac{J'_V}{2}[N(\theta_i-\theta_j)-2\pi m_{ij}]^2}, \tag{2.22}$$

where $m_{ij} = Nl_{ij} + k_{ij}$ and $J'_V = \frac{J_V}{N^2}$.

One recognizes that, Eq. (2.22) just corresponds to the Villain form of a cosine model with the periodicity $\frac{2\pi}{N}$,

$$S_{\text{eff}} = -J_{\text{eff}} \sum_{\langle ij\rangle} \cos N(\theta_i - \theta_j). \tag{2.23}$$

In Eq. (2.23), the gauge fields have disappeared and the matter fields appear in a a form $\Phi_N = e^{iN\theta}$, compared to the original rotor $\phi = e^{i\theta}$. This is to be expected, since gauge symmetries cannot broke [28], the matter fields have to appear in gauge invariant combinations. $\Phi_N = e^{iN\theta}$ correctly encodes the symmetry of the original theory Eq. (2.19) and thus a valid order parameter for C_N nematics.

Furthermore, the Villain form Eq. (2.22) also reveals the N-dependence of the C_N nematic-liquid transition at the $K \to 0$ limit. The Villain model has a critical value at $J'_{V,c} \sim 0.33$ in three dimensions [55]. It follows that Eq. (2.22) is critical at $J_{V,c} = N^2 J'_{V,c}$. Via the relation between the coupling in the original consine model and the coupling in the Villain model [55],

$$e^{-\frac{1}{2J'_V}} \simeq \frac{I_1(J)}{I_0(J)}, \tag{2.24}$$

we numerically evaluate the critical coupling J_c of the $SO(2)/Z_N$ model in the limit $K \to 0$, where $I_n(x)$ is the modified Bessel function of the first kind. These values agree rather well with the critical coupling from our Monte Carlo simulations, as shown in Fig. 2.5.

$K \to \infty$ limit

In this limit, excitations in the gauge fields will be completely suppressed. We can fix a gauge $a_{ij} \equiv 0$ by which the $SO(2)/Z_N$ theory formally reduces to a XY model. As a result, there is a phase transition driven

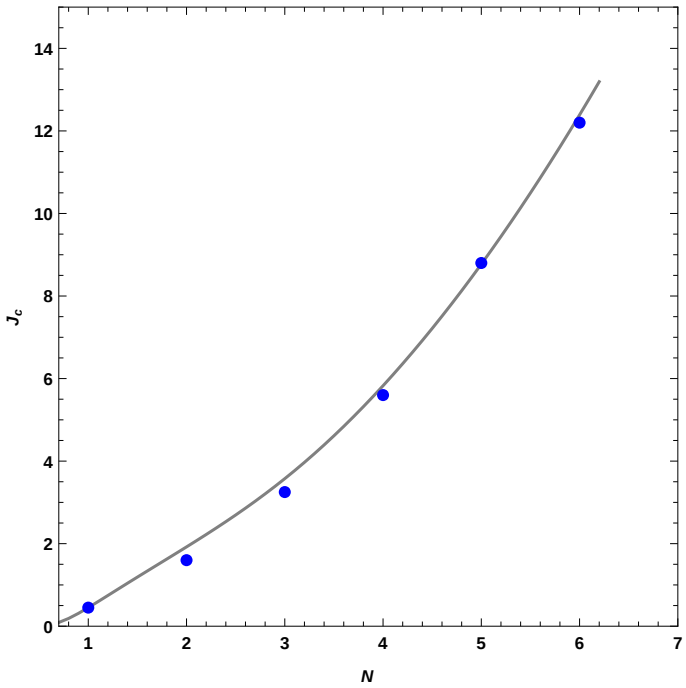

Figure 2.5. The critical value J_c of the nematic-to-isotropic transition as a function of N at $K = 0$ of Eq. (2.19) from Monte Carlo data (blue dots) comparing to the Villain estimate Eq. (2.24) (the line).

by the condensate of 2π vortices. However, these vortices are not those in a normal XY model. Since the fundamental defects of C_N nematics are $\frac{2\pi}{N}$ disclinations, which are embodied by the Z_N flux in the gauge theory, the 2π vortices in this transition are combinations of Z_N fluxes. The condensate of these vortices will destroy the long range orientational order. However, single Z_N fluxes are still gapped and the gauge theory is in its deconfinement phase. Therefore, this transition will result in a topological phase. It has been argued that such a phase has a microscopic identification in the context of spin nematics [58, 59, 16] and systems with electron fractionalizations [60, 61]. However, dealing with the 'molecular' microscopy of the quantum liquid crystals discussed here, such an identification remains obscure. Moreover, since all physical quantities should be gauge invariant, this phase transition is characterized by the Z_N invariant composite field $e^{iN\theta}$ rather than the XY variable $e^{i\theta}$. In the case $N = 2$ this has been studied by various authors [62, 63] and was referred to as the XY^* universality class.

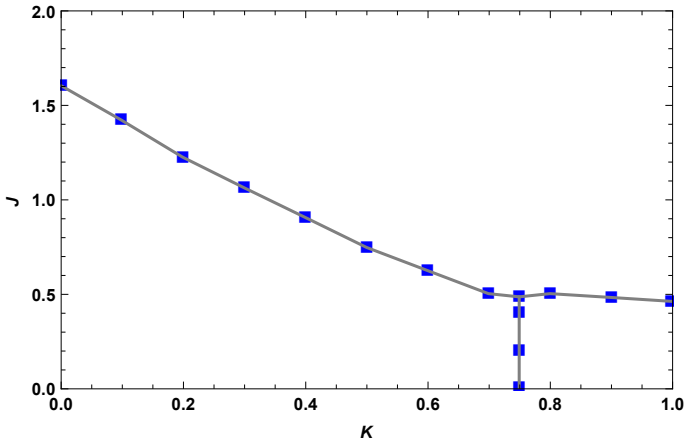

Figure 2.6. The phase diagram of the $SO(2)/Z_2$ theory as determined by Monte-Carlo calculations.

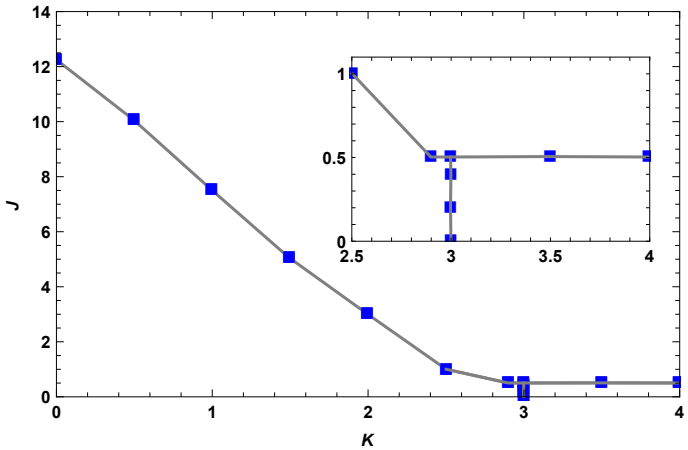

Figure 2.7. The phase diagram of the $SO(2)/Z_6$ theory as determined by Monte-Carlo calculations. Note the larger J_c at $K = 0$ and the shrinking of the deconfined region to larger K as compared to $SO(2)/Z_2$ case.

Numerical phase diagrams

To verify the phase diagram Fig. 2.4 we just discussed, we simulated the $SO(2)/Z_N$ theory Eq. (2.19) with the Metropolis Monte Carlo on systems size $L^3 = 8^3, 10^3, 12^3$, by computing the susceptibility of the C_N nematic order parameter $e^{iN\theta}$. Our results for the cases $N = 2$ and $N = 6$ are shown in Figs. 2.6 and 2.7. As expected, the critical value of $J_c(N)$ at $K = 0$ grows with N. Indeed, the $SO(2)/Z_N$ theory Eq. (2.19) tends to a $SO(2)/SO(2)$ theory when $N \to \infty$, which is known to exhibit no phase transition for the $K = 0$ line [27]. On the other hand, $K_c(N)$ for the pure Z_N gauge theory also grows with N [52]. This result to the fact that the size of the deconfined phase will shrink for larger N, as it is evident from Figs. 2.6 and 2.7.

2.4 Concluding remarks

We have discussed the dislocation-mediated quantum melting of two spatial dimensional bosonic crystals in terms of the stress-strain duality. Within this duality, dislocations are charged particles coupled to dual stress photon fields, and their condensate, the quantum nematics, can be viewed as stress superconductors. We also discussed the relation of the collective modes of this dual superconductor with the modes in the original system. Moreover, we showed that the finite rotational symmetry of quantum nematics can be realized by discrete gauge symmetries, and construct a $SO(2)/Z_N$ gauge theory being the order parameter theory of the Abelian C_N nematics. We analyzed the general topology of the phase diagram of this theory and the nature of the associated phase transitions.

Chapter 3

Generalized $3D$ nematics and discrete non-Abelian gauge theory

The subject of "vestigial"or "mesophase" (intermediate temperature) order was born in the theater of classical molecular matter in the form of nematic, cholesteric and smectic liquid crystals [21, 22, 11]. Although this is a very mature field, it has been suffering from the limitation that mesophases are experimentally only easily formed departing from "rod-like" degrees of freedom, giving rise to uniaxial nematics [11, 64–66]. In addition, a substantial literature is devoted to biaxial nematics with D_{2h} symmetry, associated with plate-like constituents or "mesogens" [67–75]. However, departing from the Landau-de Gennes symmetry paradigm, these represent only two examples of a vast family of potential phases: in principle matter can break the $O(3)$ rotational symmetry of three-dimensional ($3D$) space down to any of its subgroups, i.e., 3D point groups. Chemistry has not proven to be very flexible in this regard, but new opportunities open up with the advances in the manufacturing of nanoparticles and colloids [76–79] that can be given particular shapes, while there is potentially quite a bit of control over their mutual interactions [80–83, 79].

As a further impetus for this pursuit, we construct a general framework in terms of a lattice model that can incorporate all three dimensional point group symmetries and therefore is ideal to study generalized nematics. Concretely, we achieve this by a generic lattice formulation of discrete non-Abelian gauge theory. The model allows us to expose some spectacular, generic traits of the statistical physics arising for the most symmetric point groups. We demonstrate that their order parameters are subjected to thermal fluctuations of unprecedented intensity. This is illustrated in Fig. 3.2 where we show the transition temperatures (T_c's) of the various

nematics relative to a common reference — their mean field temperatures would be identical. The actual T_c's of the highly symmetric I, O and T are nonetheless extremely reduced by thermal fluctuations, as compared to the transition temperatures of less symmetric nematics. In addition, we uncover that chiral symmetry plays a very special role. This associates to the breaking of $O(3)$ to its subgroup of proper rotations $SO(3)$ and refers to the familiar property that molecules can be left- or right handed, as in e.g. sugar water formed exclusively from left-handed glucose molecules, leading to well-known optical activity. However, we now depart from chiral point groups describing mixtures of equal number of left- and right handed species which are subjected to spontaneous symmetry breaking, resulting in the formation of chiral nematics and chiral liquids, reminiscent of the recently pointed out domains of well-defined broken chirality in liquid phases of systems of C_{2v} symmetric "bent-core" mesogens [84] and chiral liquids melted from cubic crystalline phases [85]. Moreover, we show that, even under the most adverse conditions for vestigial order to occur, a chiral liquid still splits the isotropic liquid from the full nematic order for the most symmetric I, O and T chiral point groups, as consequence of the extreme thermal fluctuations of the full orientational order.

Why has this spectacular statistical physics not been discovered a long time ago? After all, constructing the theory of three-dimensional orientational order should be a well-defined exercise in the Landau paradigm of spontaneous symmetry breaking. However, the Landau-de Gennes order parameter theory of more symmetric nematics generically involves a complicated high-rank tensor order parameter theory [18, 86–93], making the physical ramifications are basically unexplored, in spite of the identification of the general structure of point group invariants [94, 95]. In this sense the problem represents one of the remaining frontiers of the Landau paradigm. Indeed, dealing with more complicated point groups, one has to generalize the familiar uniaxial order parameter: $\mathbb{Q}_{ab} = \frac{3}{2} n_a n_b - \frac{1}{2}\delta_{ab}$, in terms of a vector $\mathbf{n} = (n_x, n_y, n_z)$, to complicated higher rank tensors (up to rank 6 for I_h, the symmetry of a regular icosahedron, cf. Appendix 3.A). Notwithstanding, we find that a mathematical edifice borrowed from high-energy physics is remarkably efficient in computing universal and generic features of the associated statistical physics: 3D $O(3)/G$ lattice gauge theory, where the gauge group G describes the discrete point groups associated with the nematic ordering. This has been inspired by the seminal observation in Refs. [25, 26] that a particularly simple $O(3)$-vector Z_2

gauge incarnation encodes for the uniaxial nematic order parameter in 3D and our extension of this idea to the 2D proper point groups $(SO(2)/Z_p)$, encapsulating the full family of 2D Abelian nematic orders [30]. From a theoretical perspective, the surprises of the statistical physics of generalized nematics are thus a manifestation of the richness of discrete gauge theories involving the in general non-Abelian three dimensional point groups.

3.1 Gauge theory description of generalized nematic phases

The symmetry breaking framework of orientational order is straightforward to address in the context of the subgroups structure in Fig. 1.1. The associated physics of the nematic phases can then be studied in terms of Landau-de Gennes theory, where an order parameter tensor is needed for each subgroup of $O(3)$ [18, 86–93]. Instead of the Landau-de Gennes free energy, we can consider a lattice model for the coarse grained order parameter tensors. The lattice model should offer a realization of the phase transition(s) associated with the Landau classification [65–67, 72–75, 96, 97, 71]. However, the construction of the order parameters is a non-trivial problem in itself, and there is the additional task of enumerating the parameters in the free energy or lattice model that classify the phases. In most cases, these goals have been achieved only to a degree by improvising in specific simplified cases and the resulting generic classification of three-dimensional nematic phases remains therefore quite unexplored.

It goes therefore without mentioning that a uniform framework to explore this rich landscape of generalized nematics in a systemic fashion would be a value asset to the active research fields concerned with generalized nematic order. This should have also direct bearing on the experimental side in the long term. Indeed, although it has been pointed out a long time ago that nematics phases formed out of "platelets", i.e. mesogens having D_{2h} symmetry, can in principle give rise to generalized biaxial nematics [72], only recently the stabilization has been quantified in terms of anisotropy in the constituents and interactions [68, 69, 98], see also [99] for a review. Furthermore, the $C_6(N+6)$ phase of DNA comprises an experimentally observed example of a nematic phase having another symmetry than the familiar uniaxial one [100, 101]. Finally, to the best of our knowledge, the only other specific mesogenic systems that have

received considerable attention are those carrying C_{2v} symmetry. These "banana" shaped constituents have most importantly also been studied in the context of experiment [102] as well as in theoretical setups [91]. We do point out that in these instances the mesogens appear to organize into more complicated aggregates in the observed liquid crystal, columnar and smectic phases. Nonetheless, they motivate the relevance of the pursuit of generalized nematics that are captured within our comprehensive gauge theoretical description.

As first observed in Refs. [25, 26], see also [92], the uniaxial nematic point group symmetry can be incorporated as gauge symmetry on coarse grained local degrees of freedom of a lattice model, instead of the director order parameter tensor $\mathbb{Q}_{ab}$. Moreover, the gauge symmetries give rise to an explicit way of incorporating the topological defects in to the model and an effective way to generate the order parameters. This approach can be generalized to all three dimensional point groups. However, before turning to the problem of nematics with general point group symmetries that highlight the intricacies of the non-Abelian nature, let us first review the gauge theoretical description for uniaxial nematics.

3.1.1 Uniaxial nematics and Z_2 gauge theory

The $D_{\infty h}$-uniaxial order can be captured by an $O(3)$-vector model coupled to a Z_2 gauge theory, turning the order parameter vector $\mathbf{n}$ into a director (the rod) with a head-to-tail symmetry. The simplicity in the gauge formulation is rooted in the Abelian Z_2 nature of the uniaxial $D_{\infty h}$ symmetry acting on $\mathbf{n}$. More specifically, to describe the coarse grained order parameter theory, one departs from an auxiliary cubic lattice regulating the short-distance cut-off of the theory. The theory has variables $\sigma^z_{ij} = \pm 1$ living on the bonds $\langle ij \rangle$ of the lattice, that interact by a plaquette term $-K \sum_{i}^{l} \square_{j}^{k} \sigma^z_{ij}\sigma^z_{jk}\sigma^z_{kl}\sigma^z_{li}$ thereby defining Wegner's Ising gauge theory [50]. To describe nematics, the gauge fields are minimally coupled to nearest-neighbor $O(3)$ vectors $\mathbf{n}_i$ on the sites of the lattice via a Higgs term $-J \sum_{\langle ij \rangle} \sigma^z_{ij} \mathbf{n}_i \cdot \mathbf{n}_j$.

Despite its simplicity, the Ising lattice gauge theory is actually enough to elucidate the nature of non-perturbative discrete gauge theories in general [27]. For large J the matter and gauge fields are ordered via the Higgs mechanism. The coupling K controls the gauge fields and for small K,J the gauge fields are confined, effectively "gluing" the matter fields to gauge invariant singlets not unlike quark confinement in hadrons. For large K

and small J, matter is disordered while the gauge fields are "ordered" forming a deconfining phase with topological gauge fluxes as excitations. Although realizations of such "topological nematic phases" [26] have been identified in strongly interacting electron systems [60, 61, 58, 16], deconfinement seems unphysical dealing with "molecular" matter. Therefore the regime of interest is strong gauge coupling $K \to 0$, where one finds the fully ordered "Higgs phase" and a fully disordered confining phase. These encode for the uniaxial nematic phase and the isotropic liquid, respectively. The gauge symmetry identifies $\mathbf{n}_i \simeq -\mathbf{n}_i$ and as a result, the physical gauge invariant observables correspond with the directors $\mathbb{Q}_{ab}$. Consequently, upon integrating out the fluctuating gauge fields at $K \to 0$, one obtains an effective theory of the de-Gennes kind [66]: $H \sim \sum_{\langle i,j \rangle} \mathrm{Tr}\, \mathbb{Q}_i \cdot \mathbb{Q}_j$, with the $\mathbb{Q}_i$ being the uniaxial tensor order parameter [11].

3.1.2 Generalized nematics and non-Abelian gauge theory

For the uniaxial case only a single "nematic" vector along the $D_{\infty h}$ axis is required and the Z_2 gauge symmetry then simply turns the vector into the director. However, in case of a general 3D nematic "mesogen", one has to introduce a discrete lattice gauge theory that can cope with any of the non-abelian point group symmetries $G \subset O(3)$. Accordingly, one should depart from 3D matrix rotor fields R_i defined in terms of an orthonormal triad as

$$R_i = (\mathbf{l}_i \quad \mathbf{m}_i \quad \mathbf{n}_i)^T \in O(3), \tag{3.1}$$

instead of a single vector. The $O(3)$ constraints make the vectors $\mathbf{n}_i^\alpha = \{\mathbf{l}_i, \mathbf{m}_i, \mathbf{n}_i\}_{\alpha=1,2,3}$ to an orthonormal triad that is right or left handed pending on

$$\sigma_i = \det(R_i) = \mathbf{l}_i \cdot (\mathbf{m}_i \times \mathbf{n})_i = \pm 1. \tag{3.2}$$

The generalized nematic symmetry implies identifications of the triad as

$$R_i \simeq \Lambda_i R_i, \quad \mathbf{n}_i^\alpha \simeq \Lambda_i^{\alpha\beta} \mathbf{n}_i^\beta, \quad \forall \Lambda_i \in G, \tag{3.3}$$

generalizing the Z_2 director symmetry of the single vector $\mathbf{n}_i$. In very concrete terms, the gauge symmetries on the $O(3)$-triad R_i thus encode for the physical degrees of freedoms of "mesogens" with the symmetry G in their "body-fixed" frame. See Fig. 3.1 for an illustration. On the other hand, global rotations $\Omega \in O(3)$ defined by a space-fixed frame and

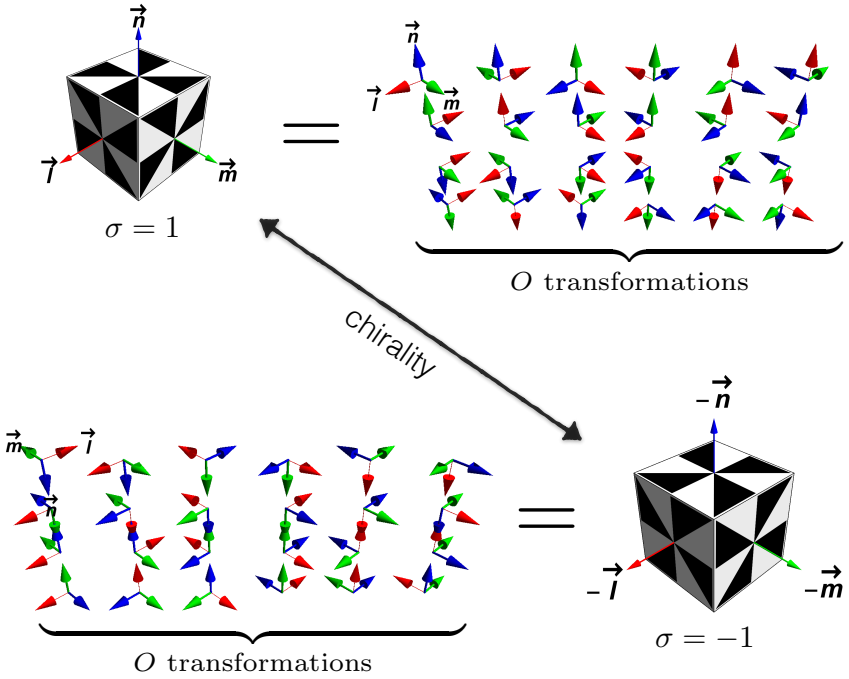

Figure 3.1. The correspondence between the shapes of "mesogens" and the gauge symmetries acting on the rotors (triads). Here O-symmetric "mesogens" (cubes) are considered as an example [103]. Top: The orientations of the "mesogen" correspond to triads R_i. Acting with O gauge transformations on the triads shows orientations that leave the mesogens invariant, and are realized as gauge symmetries in the model Eq. (3.5). Bottom: When the symmetry group of the mesogen is a proper point group, there are two mesogens that have the same symmetry but opposite chirality. Chirality is indicated by the black-white "propeller" scheme of the cube or left- and right-handed triads. Imposing the chirality $\sigma \to -\sigma$ as a symmetry leads to O_h symmetry.

distinguished from the local body-fixed rotations of the mesogens, act on the triads as

$$R_i \to R_i \Omega^{\mathrm{T}}, \quad \mathbf{n}_i^\alpha \to \Omega \cdot \mathbf{n}_i^\alpha, \quad \Omega \in O(3). \tag{3.4}$$

where the $\cdot$ denotes ordinary matrix multiplication of the vector $\mathbf{n}_i^\alpha$.

The so-called $O(3)/G$ lattice gauge theory can be formulated by introducing such degrees on an auxiliary cubic lattice with $O(3)$ triads R_i defined on sites and gauge fields $U_{ij} \in G$ defined on links,

$$\beta H = -\sum_{\langle ij \rangle} \mathrm{Tr}\left[R_i^T \mathbb{J} U_{ij} R_j\right] - \sum_{\square} \sum_{\mathcal{C}_\mu} K_{\mathcal{C}_\mu} \delta_{\mathcal{C}_\mu}(U_\square) \mathrm{Tr}\Big[U_\square\Big], \tag{3.5}$$

where the invariance of a point-group-symmetric "mesogen", which leads to the identification $R_i \simeq \Lambda_i R_i$, is realized by the gauge transformation

$$R_i \to \Lambda_i R_i, \quad U_{ij} \to \Lambda_i U_{ij} \Lambda_j^T, \quad \forall \Lambda_i \in G. \tag{3.6}$$

In addition the model has the global $O(3)$-rotation symmetry Eq. (3.4).

The first term in Eq. (3.5) models the orientational interaction between G-symmetric "mesogens", where $\mathbb{J}$ is a symmetric coupling matrix encoding the nematic "exchange" terms, which is invariant under G: $\Lambda \mathbb{J} \Lambda^{\mathrm{T}} = \mathbb{J}$, $\forall \Lambda \in G$. In standard gauge theory language, this term is nothing but a Higgs term [27] for the matter fields R_i. In the current context, however, the central importance lies in the fact that it favors alignment of G-symmetric "mesogens" and thus can realize spontaneous symmetry breaking from an isotropic $O(3)$ liquid phase to a nematic phase having point group symmetry.

The second term in Eq. (3.5) is a defect suppression term, generalizing the K term of the Z_2 case. It involves oriented products of gauge fields $U_\square = \prod_{\langle ij \rangle \in \square} U_{ij}$ around plaquettes $\square$ of the lattice. Plaquettes with non-zero gauge flux or field strength, $U_\square \neq \mathbb{1}$, represent topological defects in the nematic. Under a gauge transformation Λ_i, $U_\square \to \Lambda_i U_\square \Lambda_i^T$ and therefore is defined only up to conjugation. Correspondingly, $K_{\mathcal{C}_\mu}$ denotes the core energy of the defects with the flux $U_\square \in G$ and is a function of the conjugacy classes $\mathcal{C}_\mu$ of the group G since defects in the same conjugacy class are physically equivalent. These gauge defects do not directly classify topological defects in nematics, but they are closely related via the so-called Volterra construction [104, 33]. The nematic defects are usually classified by homotopy groups of the manifold $O(3)/G$ [19, 20]

which is the order parameter space of the G-nematic and as well the low-energy manifold of the model Eq. (3.5) in the Higgs phase. Disordered configurations in the Higgs term can be suppressed by assigning a finite core-energy to the gauge defects. Thus, $K_{\mathcal{C}_\mu}$ can effectively be regarded as tuning the fugacity of the nematic defects. As we are however interested in the ordinary nematic to isotropic transitions, we will not consider the gauge field dynamics associated with finite $K_{\mathcal{C}_\mu}$ and set these parameters to zero in the remainder.

3.1.3 Realization of the generalized nematic orders

All physics in the model Eq. (3.5) follows from gauge invariant quantities, as by Elitzur's theorem [28] correlation functions of gauge non-invariant quantities vanish. This is in direct analogy to the Z_2 or $D_{\infty h}$-case, where one describes the physics in terms of gauge invariant tensor which is director order parameter $\mathbb{Q}_{ab}$. In the general case, the relevant order parameters are high-rank tensors that are linear combinations of tensor constructed from the rotors $(R_i)^\alpha_a = (\mathbf{n}^\alpha_i)_a$. Formally, they can be expressed as

$$\begin{aligned} \mathbb{O}^{(G)}_i &= \sum_{\{\lambda\}} c_\lambda \mathbb{O}^\lambda_i, \\ (\mathbb{O}^{\lambda=\alpha\beta\cdots\gamma}_i)_{ab\cdots c} &= (R_i)^\alpha_a (R_i)^\beta_b \cdots (R_i)^\gamma_c, \end{aligned} \tag{3.7}$$

where $\lambda = (\alpha, \beta, \ldots, \gamma)$ is a multi-index. The above tensors transform under the gauge group G on the indices α and as vectors under global $O(3)$-rotations on the indices a. The order parameters are obtained as the averages of $\langle \mathbb{O}^{(G)} \rangle$ and these tensors are specified by their rank and tensor-symmetries. We note that the tensors $\mathbb{O}^\lambda_i$ are not all independent due to the $O(3)$ constraints on the R_i.

The gauge theory realizes G-nematic ordering by guaranteeing that when the $O(3)$ symmetry spontaneously breaks, $\langle \mathbb{O}^G_i \rangle \neq 0$, but all non gauge-invariant combinations of $(R_i)^\alpha_a$ vanish. One observes that the theory Eq. (3.10) can in fact act as an order parameter generator, since gauge-invariant quantities can be constructed via e.g. integrating out gauge fields. This is one of the advantages of the gauge theoretical description over traditional methods such as Landau-de Gennes theories and lattice models for nematic ordering, as these methods rely the on the relevant order parameters tensors as input [65, 66, 72–74, 96, 97, 105, 71].

Moreover, though these traditional methods have been proven to be very fruitful for nematics with relatively simple symmetries such as $D_{\infty h}$ and D_{2h}, they are quite involved for general point groups. In this regard, one may consider the I_h-icosahedral nematic, whose order parameter is a rank-6 traceless tensor of the form (see Table 4.1 in Chapter 4):

$$\mathbb{O}^{I_h} = \sum_{\text{cyc}} \Big[\mathbf{l}^{\otimes 6} + \sum_{\{+,-\}} \Big(\frac{1}{2}\mathbf{l} \pm \frac{\tau}{2}\mathbf{m} \pm \frac{1}{2\tau}\mathbf{n} \Big)^{\otimes 6} \Big] - \frac{1}{7} \sum_{\text{perm}} \delta_{ab}\delta_{cd}\delta_{ef} \bigotimes_{\substack{\mu=a,b,c,\\ d,e,f}} \mathbf{e}_\mu, \tag{3.8}$$

where $^{\otimes n}$ denotes the tensor power, $\delta_{ab} \bigotimes_{\mu=a,b} \mathbf{e}_\mu = \delta_{ab}\mathbf{e}_a \otimes \mathbf{e}_b$, "cyclic" refers to all cyclic permutations of $\{\mathbf{l}, \mathbf{m}, \mathbf{n}\}$, $\sum_{\{+,-\}}$ sums over all four combinations of the two $\pm$ signs, $\tau = \frac{1+\sqrt{5}}{2}$ is the golden ratio, and $\sum_{\text{perm}}$ sums over all non-equivalent combinations of the indices of the tensor. An order parameter lattice model of the form $H \sim -\sum_{\langle ij \rangle} \text{Tr}\, \mathbb{O}_i^{I_h} \cdot \mathbb{O}_j^{I_h}$ can be obtained from the gauge theory Eq. (3.5) by integrating out the gauge fields in a high- or low-temperature expansion, generalizing the lattice models of the uni- and biaxial nematics. However, needless to say, $\mathbb{O}_i^{I_h}$ contains an abundant number of terms making the corresponding order parameter theory inevitably complicated (See Appendix 3.C).

On the other hand, the gauge theory Eq. (3.5) is convenient for nematics of arbitrary point group symmetries. It requires the symmetry of nematics only as input for fixing degrees of freedom of the gauge fields U_{ij} and fits all point groups in a universal framework. Therefore, it is a remarkably efficient device to study generalized nematic ordering.

Finally, returning to the subgroup structure in Fig. 1.1, we remark that, within the gauge model, a subset of intermediate phases in Fig. 1.1 can be realized by simply tunning temperature and the coupling matrix $\mathbb{J}$. These involve generalized biaxial-uniaxial-liquid transitions for axial groups $\{C_n, C_{nv}, S_n, C_{nh}, D_n, D_{nh}, D_{nd}\}$ where an anisotropic $\mathbb{J}$ is possible. We will discuss in a separate work the anisotropic couplings in Eq. (3.5) in order to bring the anisotropy-induced intermediate phases of the $O(3)$ subgroup hierarchy into play [32].

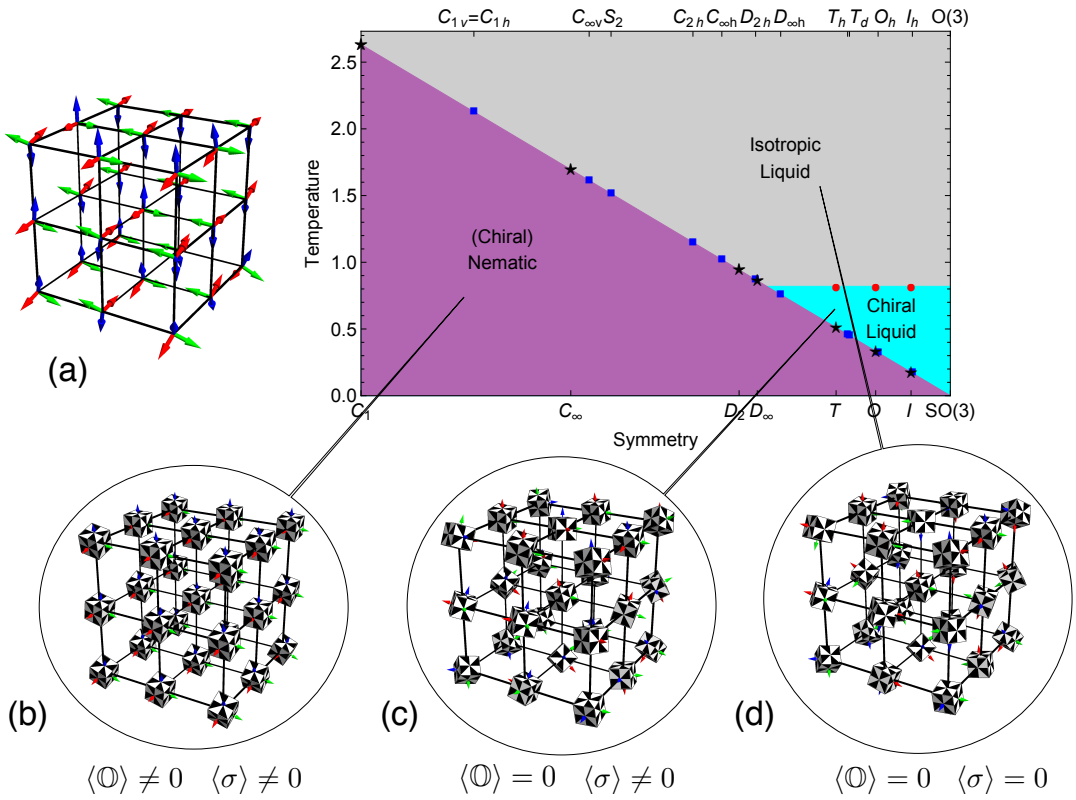

Figure 3.2. Phase diagram of different point-group-symmetric nematics. The vertical axis is the temperature in units of J, the bottom and top axis label proper and improper point groups, respectively, in the order of increasing symmetry. The nematic transition temperature, shown by stars for point groups and squares for improper point groups, is decreasing with increasing symmetry due to thermal fluctuations in the orientational order. These fluctuations become huge for highly symmetric groups, and lead to the emergence of a vestigial chiral liquid phase for the I, O and T nematics. The transition temperature, shown by filled circles, of the chiral liquid phase to the fully disordered isotropic liquid phase is identical in the gauge theory Eq. (3.5) because of a common orientationally disordered background. The results presented here are studied on a cubic lattice(**a**), where the triad matter fields reside on sites and the gauge fields are defined on links (black), and with isotropic coupling $\mathbb{J} = J\mathbb{1}$. The long range ordering associated with the three phases is shown in the insets by using the O-nematic as an example (Fig. 2): (**b**) nematic which is full ordered; (**c**) chiral liquid which has no orientation order but has a preferred chirality; and (**d**) isotropic liquid which is fully disordered. Note that cubes in (**c**) have a preferred black-and-white color scheme, while in (**d**) the two color schemes appear randomly. For details of the simulations, see Appendix 3.A.

3.2 Nematic transitions

As outlined in the previous section, the gauge theory Eq. (3.5) is an efficient and flexible framework for generalized nematics, and it is straightforward to simulate numerically using the standard Metropolis Monte-Carlo algorithm. As mentioned, in order to focus on nematic-isotropic liquid (Higgs-confinement) transitions, we have set $K_{\mathcal{C}} = 0$, i.e. the defects do not have an explicit core energy. Phase transitions can then be detected by monitoring the strength of the generalized nematic ordering, $q = \sqrt{\mathrm{Tr}[\langle \mathbb{O}^{\boldsymbol{\lambda}}_{ab\ldots c}\rangle]^2}$ and the specific heat (Appendix 3.A.1). We accordingly simulated all three dimensional crystallographic point groups, the icosahedral groups $\{I, I_h\}$ and the five infinite axial point groups $\{C_\infty$, $C_{\infty v}$, $C_{\infty h}$, D_∞, $D_{\infty h}\}$.

3.2.1 Giant thermal fluctuations of highly symmetric nematics

The results for a large number of representatives are collected in Fig. 3.2, where the vertical axis is the reduced temperature and the horizontal axes arbitrarily accommodate point groups in increasing order of symmetry. In Fig. 3.2 the isotropic coupling $\mathbb{J} = J\mathbb{1}$ has been chosen for simplicity. A remarkable observation here is the huge thermal fluctuations for nematics of highly symmetric point groups as evidenced by the extremely low transition temperatures. The trivial C_1 nematic sitting in the bottom of Fig.1.1 has the highest transition temperature T_c which consistently decreases towards $T = 0$ as one ascends the subgroup hierachy towards $O(3)$. This is surprising because with the isotropic coupling matrix $\mathbb{J} = J\mathbb{1}$, a naive mean field theory would predict all nematics to have the same T_c, whereas thermal fluctuations in three dimensional systems typically reduce T_c by a modest $\sim 20\%$ [106]. However, dealing with the most symmetric icosahedral $\{I, I_h\}$ nematics, this reduction is more than an order of magnitude! One thus immediately notices the symmetry hierarchy in Fig.1.1.

To understand the physics better, let us first zoom in on the C_1 "nematic" having the highest transition temperature. This incarnates triads having no symmetry and describes a non-linear $O(3)$ matrix model maximally breaking the rotational symmetry [18]. Moving to $\{C_\infty, C_{\infty v}\}$, $\{D_2, D_{2h}\}$ and $\{D_\infty, D_{\infty h}\}$ cases, the geometric interpretation of the mesogens become cones, cuboids and cylinders, respectively. Climbing further up the hierarchy of Fig. 1.1, the triads turn into tetrahedrons $\{T, T_d, T_h\}$,

cubes $\{O, O_h\}$ and icosahedra $\{I, I_h\}$. It is intuitively clear that towards spheres $\{SO(3), O(3)\}$ sitting in the top of the symmetry hierarchy, the differences between the ordered state and isotropic space are increasingly harder to discern and the thermal fluctuations associated with the order will increase in severity.

We emphasize that in Fig. 3.2 the isotropic coupling $\mathbb{J}$ is taken, so that thermal fluctuations are roughly equal for all three axes defined by the triads. This is important for the axial point groups $\{C_n, C_{nv}, S_n, C_{nh}, D_n, D_{nh}, D_{nd}\}$, whose geometric interpretation as mesogens is in terms of (colored) n-gonal prisms [103]. These nematics are characterized by a primary order parameter for the main axis and a secondary order parameter in the perpendicular plane (Chapter 4.2.2). When n increases, the n-gonal prisms become more cone- or cylinder-like, and the in-plane fluctuations hence are more severe and tend to restore the in-plane $O(2)$ symmetry, while ordering is easy along the main axis just as in the $n = \infty$ case. Thus we cannot simply incorporate these cases into Fig. 3.2, since to properly quantify the influence of these in-plane fluctuations, we need coupling matrices $\mathbb{J}$ with anisotropic entries (Chapter 5). However, we can already conclude that the same trend is also true for in-plane fluctuations of the axial nematics. Consequently, the remarkable power of the gauge theory Eq. (3.5) allows for a common microscopic reference for all different point groups, making it always possible to compare the orientational fluctuations in absolute terms.

Finally, though in Fig. 3.2 the gauge theory Eq. (3.5) has been studied in the $K_{\mathcal{C}} = 0$ limit, we have preliminarily checked by our simulations that until sufficiently large $K_{\mathcal{C}}$, the results remain qualitatively similar to those in the $K_{\mathcal{C}} = 0$ limit. Therefore the features that have been discussed are stable against finite $K_{\mathcal{C}}$. A large $K_{\mathcal{C}}$ will suppress the defects and therefore the disordering, leading to the phase transitions moving to higher temperatures. For large enough $K_{\mathcal{C}}$ and small enough Higgs couplings, the theory will feature a confinement-deconfinement phase transition of the gauge fields [50]. With deconfined gauge fields and disordered rotors, the physics is quite different and entails a regime of (non-Abelian) topological excitations and topological order. Although such deconfinement phenomena have been identified in strongly correlated electron systems [60, 61, 58, 16], there are no identified analogues in thermal liquid crystal systems.

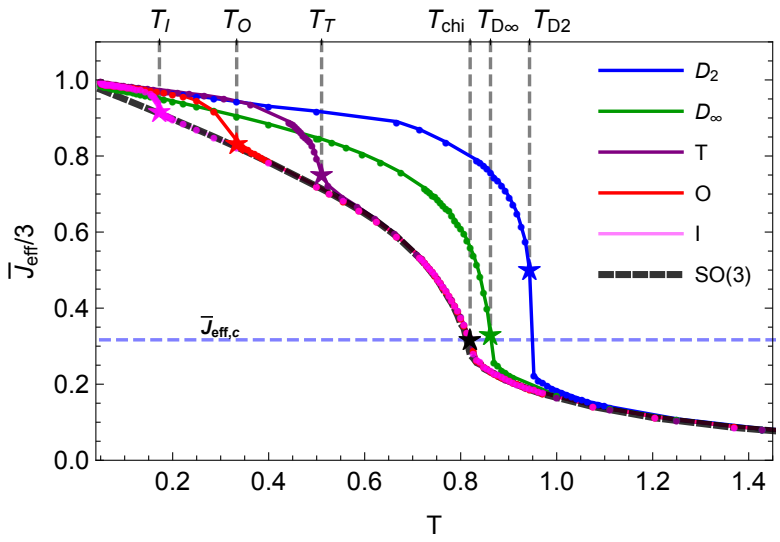

Figure 3.3. The mean-field coupling, $\overline{J}_{\rm eff}$ defined by Eq. (3.10), measuring the short range nematic correlations, as a function of the temperature (in units of J). Transition temperatures of the chiral and nematic transitions are indicated by stars and the group $SO(3)$ (black) is shown as a reference. The dashed blue line shows a critical mean-field coupling $\overline{J}_{{\rm eff},c} \simeq 0.95$ where the chiral order sets in. Due to huge fluctuations in the nematic order, $\overline{J}_{\rm eff}$ exceeds the critical value at the chiral transition at $T_{\rm chi} \simeq 0.82$ for the highly symmetric groups I, O and T, which is well above the transition to the nematic phase. In contrast, for the less symmetric D_∞ and D_2 groups, $\overline{J}_{\rm eff}$ only exceeds the critical value at the nematic transition by a sudden jump.

3.2.2 The chiral liquid as fluctuation driven vestigial phase

Another remarkable result of the gauge theory Eq. (3.5) at $K_{\mathcal{C}} = 0$ (and small but finite $K_{\mathcal{C}}$) limit is the emergence of a chiral liquid phase (the light blue region in Fig. 3.2) for T, O and I nematics. This phase spontaneously breaks the $O(3)$ symmetry of the isotropic liquid to $SO(3)$ and is characterized by chiral order and the absence of any orientational order. From the symmetry point of view, this phase is in principle possible for all proper point groups $\{C_n, D_n, T, O, I\}$, i.e., subgroups of $SO(3)$. However, according to our simulations, it only occurs as "vestigial" phase for highly symmetric T, O and I nematics before the nematic full order sets in. Furthermore, the chiral transition temperatures are identical within the accuracy of our simulations.

The mechanism at work for the chiral liquid is an elegant mixture of intricacies of the point group symmetries and fluctuation physics: the chiral phase arises in essence via order-out-of-disorder.

The chiral symmetry is related to the central (or commuting) group of inversions $Z_2 = \{\mathbb{1}, -\mathbb{1}\}$ in $O(3) = SO(3) \times Z_2$. Due to the Abelian nature of the inversions, the pseudoscalar chirality $\sigma_i = \det R_i = \pm 1$ can be always factored out. The rotors can be parametrized with composite fields as $R_i = \sigma_i \widetilde{R}_i$, where $\widetilde{R}_i \in SO(3)$ is a rotation matrix of pseudovectors. In the context of our gauge model, the fields $\{\sigma_i\}$ are well-defined and physical (gauge-invariant) for gauge groups composed of only proper rotations. The Hamiltonian Eq. (3.5) at $K_{\mathcal{C}} = 0$ thus can be rewritten as

$$\beta H_{K_{\mathcal{C}}=0} = -\sum_{\langle ij \rangle} \sigma_i \sigma_j \mathrm{Tr}\Big(\widetilde{R}_i^T \mathbb{J} U_{ij} \widetilde{R}_j\Big), \tag{3.9}$$

featuring explicit global $O(3) = SO(3) \times Z_2$ symmetry that can be broken separately.

One notices that the $SO(3)$ part, $\widetilde{q}_{ij} = \mathrm{Tr}[\widetilde{R}_i^T U_{ij} \widetilde{R}_j]$, in the Hamiltonian Eq. (3.9) provides an effective coupling for the chiral Ising fields and vice versa. $\widetilde{q}_{ij}$ measures the short range correlations of the orientational order. As discussed in Section 3.2.1, depending on the underlying symmetry, fluctuations in the orientational order can be relatively mild or extremely severe. In contrast, the Ising order σ_i in three dimensions is subjected to rather benign fluctuations. Hence, when fluctuations in the orientational order are severe, the effective short-range coupling for the chiral Ising fields induced by $\widetilde{q}_{ij}$ can be very strong before the full nematic order sets in, and cause the chiral Ising fields to order.

To verify the the validity of the above scenario, we can take a mean-field approximation by defining an average Ising coupling $\overline{J}_{\text{eff}}$ of short-range correlations as

$$\overline{J}_{\text{eff}} = \frac{1}{N_{\text{bonds}}} \sum_{\langle ij \rangle} \langle \text{Tr}(\tilde{R}_i^T \mathbb{J} U_{ij} \tilde{R}_j) \rangle, \tag{3.10}$$

and measure it in our simulation. In Fig. 3.3 we show $\overline{J}_{\text{eff}}$ for various point group symmetries. As expected, in the case of highly symmetric T, O, I nematics, $\overline{J}_{\text{eff}}$ builds up smoothly and becomes strong enough for the chiral Ising order well above the nematic transition temperature, whereas for the less symmetric cases (e.g. D_2, D_∞) $\overline{J}_{\text{eff}}$ is small before the chiral order sets in, then changes abruptly when a direct isotropic-nematic transition taking place (see Appendix 3.B for more details).

Fig. 3.3 also reveals a peculiarity of the "microscopic physics" hard wired in the gauge model, that should surely not be taken literally dealing with physical nematic systems. One observes that at temperatures well above the nematic transitions, the $\overline{J}_{\text{eff}}$'s for the various point groups coincide. This includes the "baseline" of the $SO(3)$ point group featuring only the chiral phase. However, rather than just having a temperature independent chiral coupling, there is still quite some action going on in the orientational sector. The remaining orientational fields $\widetilde{q}_{ij}$ are then described by $SO(3)/SO(3)$ gauge theory, albeit coupled to the chiral degrees of freedom. The temperature dependence is set by a famous gauge theory contraption [27]: when the matter fields are in the fundamental representation of the gauge group, for small $K_{\mathcal{C}}$ the theory is described by weakly interacting fields on the links and the Higgs phase (at large J) becomes indistinguishable from confinement (small J). The details are of interest to gauge theorists, and what matters in the present context is that it adds a temperature dependence of independent $SO(3)$ bond-fields to the effective chiral coupling which has no relationship to the microscopic physics of the condensed matter system. For a mean-field calculation of the chiral transition for the Ising-$SO(3)/SO(3)$ theory, see Appendix 3.B.

Nevertheless, again the benefit of the gauge formulation is a common reference frame to compare the fluctuations in absolute terms. One infers from Fig. 3.3 that only rather close to the nematic transitions, when the ordering sets in, the $\overline{J}_{\text{eff}}$'s "peel off" the $SO(3)/SO(3)$ reference line. The tendency towards chiral order is hard wired in the gauge model to be the same for all chiral point groups but is controlled by the orientational

fluctuations. The extra correlations associated with the full point group symmetry are of importance only close to the full ordering. In the I, O and T cases this happens at much lower temperatures than the chiral transition and therefore their chiral transition temperatures are very nearly identical (within the accuracy of our simulations). However, referring to the same "common gauge", the intrinsic fluctuations of the less symmetric nematics (e.g. D_∞, D_2) are just too weak to disorder the orientational fields and leave room for the chiral vestigial phase.

The mechanism discussed above has actually quite a history in the context of the magnetism of iron-based superconductors [107, 108], featuring "stripe antiferromagnets" breaking not only internal spin symmetry, but also spatial rotational symmetry. Departing from a square lattice (C_4 symmetry) in two dimensions, the x and y directions become inequivalent ("nematic" C_2 symmetry) in the striped antiferromagnet, involving an Ising-type symmetry breaking. Generically one finds that either first the "nematic" order sets in followed by the full magnetic order at a somewhat lower temperature, or both occur in a single merged first order transition [107]. A qualitatively similar mechanism is invoked to explain these observations (see, e.g., Refs. [108, 107]), with the lattice symmetry taking the role of chiral symmetry with the antiferromagnet replacing the $O(3)$-rotations breaking phase. However, in terms of a classical unfrustrated spin model featuring the symmetries of the striped antiferromaget, it is impossible to stabilize the vestigial "C_2-nematic" phase in three dimensions [108]. This is because the thermal fluctuations of the classical $O(3)$ spins are falling short in this regard as compared to highly symmetric nematics and one has to resort to microscopic frustration physics of the iron-based materials to boost the thermal fluctuations.

3.3 Concluding remarks

There is a rich landscape of "generalized nematics", formed and fully classified in terms of the 3D point group symmetries. Still waiting to be fully explored, they represent a remaining frontier of the Ginzburg-Landau order parameter paradigm involving order parameters of unprecedented complexity.

In this chapter, we have introduced a lattice gauge theory model that realizes generalized nematic ordering in three dimensions and incorporates all point groups. We further mobilized the machinery of discrete

non-Abelian gauge theory, discovering that it is remarkably powerful in addressing generic features of the statistical physics of such systems. In addition to the generalized nematics phases, we identified a vestigial chiral liquid phase that arises for nematics systems with high point group symmetries.

Compared to the intricacies facing the experimentalists in the soft matter laboratories, the gauge model has somewhat of a status of a "spherical cow". However, when it comes to isolating the physical principle at work under a single framework, one can also view it as the limit of Platonic perfection.

To realize these in the laboratory, one needs preferably building blocks with T, O or I symmetry. As a case in point of the strange traits of chemistry, such molecules are extremely rare and we have only found a few examples for each. An example of a T-symmetric molecule is the $[Ga_4L_6]^{12-}$ tetrahedral metal-ligand cluster [109]. Very recently nano-sized "giant" tetrahedra have been fabricated by placing different polyhedral oligomeric silsesquioxane (POSS) molecular nanoparticles at the vertices of a rigid tetrahedral framework. These tetrahedra have in addition tunable hydrophilic interactions and have been observed in self-assembled crystalline and alloyed supramolecular quasicrystalline phases induced by entropic packing [79]. The even more exuberant O representative is the transporting protein Ferritine that stores and releases iron in organisms [110]. Finally, the chiral icosahedral symmetry is found in the form of viruses [111] including the common rhinovirus [112]. We note, however, that all these cases in fact involve very complex molecules in the nano-scale. Nevertheless, it appears that there is a realistic potential to overcome the experimental challenges of the control over the shapes and interactions of nano-particles and colloids. We hope that our theoretical insights might act as a source of inspiration for the experimental community to build systems with such intricate spatial symmetries and find out whether for instance the vestigial chiral order can be realized in the laboratory.

Viewed from a fundamental theoretical perspective, the non-Abelian gauge theories associated with point groups are highly interesting by themselves, and arriving at a timely moment. We have only explored a small corner (large gauge coupling, minimal extra structure) of the full portfolio of these theories. Dealing with the Higgs (generalized nematic) phases there is interesting work to do, such as further exploring the nature of

the topological defects occurring in the high symmetry point groups [34]. Moreover, upon increasing the gauge coupling $K_{\mathcal{C}}$ a landscape of deconfining phases will appear [50, 27] that remains to be charted. This has its merit in yet a quite different field of physics. Deconfining states of discrete gauge theories play a crucial role in the subject of topological order and topological quantum computation [113–116], often limited to two-spatial dimensions or Abelian symmetries. The point group symmetries form natural building blocks to extent this to the non-Abelian realms in three dimensions.

3.A Details of simulations and generalized nematic order parameters

The phase diagram in Fig. 3.2 was determined by simulating the lattice gauge theory Eq. (3.5) by the Metropolis Monte-Carlo on lattices of sizes $L^3 = 8^3, \ldots, 24^3$. To ensure the thermalization of our ensembles, we monitored the results for both cooling from a random initial state as well as heating from a uniform ordered initial state.

Using our gauge theory formulation, we have calculated the associated nematic tensor order parameters in Table 4.1, and the the pseudo-scalar chiral order parameter $\sigma_i = \mathbf{l}_i \cdot (\mathbf{m}_i \times \mathbf{n}_i)$. Phases in the phase diagram are defined as

$$\begin{cases} \langle \mathbb{O}^G_{ab\ldots c} \rangle \neq 0 & \text{nematic} \\ \langle \mathbb{O}^G_{ab\ldots c} \rangle = 0, \langle \sigma \rangle \neq 0 & \text{chiral} \\ \langle \mathbb{O}^G_{ab\ldots c} \rangle = 0, \langle \sigma \rangle = 0 & \text{isotropic,} \end{cases} \tag{3.11}$$

where $\mathbb{O}^G$ is the order parameter tensor with G rotational symmetry, $\langle \cdots \rangle$ denotes the thermal average, $\mathbb{O} = L^{-3} \sum_i \mathbb{O}_i$ and $\sigma = L^{-3} \sum_i \sigma_i$.

3.A.1 Strength of the nematic ordering

The nematic interaction in Eq. (3.5) prefers homogeneous alignment of triads so that the components of the nematic order parameter with G rotational symmetry $\mathbb{O}^G_{abc\ldots,i}$ develop an expectation value. This will lead to the two point correlation function behaving as (repeated indices are summed over)

$$\lim_{|i-j|\to\infty} \langle \mathbb{O}^G_{abc\ldots,i} \mathbb{O}^G_{abc\ldots,j} \rangle = \begin{cases} \langle \mathbb{O}^G_{abc\ldots} \rangle^2 > 0, & \text{nematic} \\ 0, & \text{otherwise.} \end{cases} \tag{3.12}$$

The order parameter tensor has G rotational symmetry. This allows us to define a strength of the nematic ordering as $q = \sqrt{\langle \mathbb{O}^G_{ab\ldots c} \rangle^2}$, by which phases defined in Eq. (3.11) can be equivalently defined as

$$\begin{cases} q \neq 0,\ \sigma \neq 0 & \text{nematic} \\ q = 0,\ \sigma \neq 0 & \text{chiral} \\ q = 0,\ \sigma = 0 & \text{isotropic,} \end{cases} \tag{3.13}$$

where $\sigma = \langle \sigma_i \rangle$ measures the strength of the long range chiral order.

The phase transitions can be located by the peak of the susceptibility of the nematic order and the chiral order, $\chi(q)$ and $\chi(\sigma)$, defined as

$$\chi(q) = \frac{L^3}{T}\Big(\langle q^2 \rangle - \langle q \rangle^2\Big), \tag{3.14}$$

$$\chi(\sigma) = \frac{L^3}{T}\Big(\langle \sigma^2 \rangle - \langle \sigma \rangle^2\Big), \tag{3.15}$$

As summarized in Fig.3.2, for the T-, O- and I-nematic $\chi(q)$ and $\chi(\sigma)$ peak at different temperatures indicating two phase transitions respect to the nematic order and the chiral order, while for others $\chi(q)$ and $\chi(\sigma)$ peaks coincide.

To corroborate of the strength of the nematic ordering q as a probe of the phase transition, we also compute the heat capacity defined as

$$c_v = \frac{1}{T^2 L^3}\Big(\langle E^2 \rangle - \langle E \rangle^2\Big), \tag{3.16}$$

where E is the internal energy. Consistent with the results by computing $\chi(q)$ and $\chi(\sigma)$, c_v exhibits two well separated peaks for the T-, O- and I-nematics coincided with the peak of $\chi(q)$ and $\chi(\sigma)$, while one peak for others which do not support the chiral phase.

3.B Detailed analysis of the fluctuation induced chiral phase

With the mean field approximation Eq. (3.10), the Hamiltonian Eq. (3.9) can be rewritten as

$$\begin{aligned} \beta H_{K_{\mathcal{C}}=0} &= -\sum_{\langle ij \rangle} J_{\text{eff},ij}(\beta)\sigma_i\sigma_j, \\ J_{\text{eff},ij} &= \beta \overline{J}_{\text{eff}} + \delta J_{\text{eff},ij}. \end{aligned} \tag{3.17}$$

$J_{\text{eff},ij}(\beta)$ can be viewed as an effective coupling for the Ising fields, and can be computed analytically under a further mean field approximation (Appendix 3.B.1) in the degenerate limit of gauge group $G = SO(3)$. In this case the matter-gauge variables are independent fields $W_{ij} = \widetilde{R}_i U_{ij} \widetilde{R}_j^T \in SO(3)$ interacting only via the coupling to the chiral Ising variables. By performing a partial integration over the $SO(3)$ fields we determine $J_{\text{eff},ij}(\beta)$ as a power series, and by solving $J_{\text{eff},ij}(\beta_{\text{chi}}) = \beta_{c,\text{3DIsing}}$

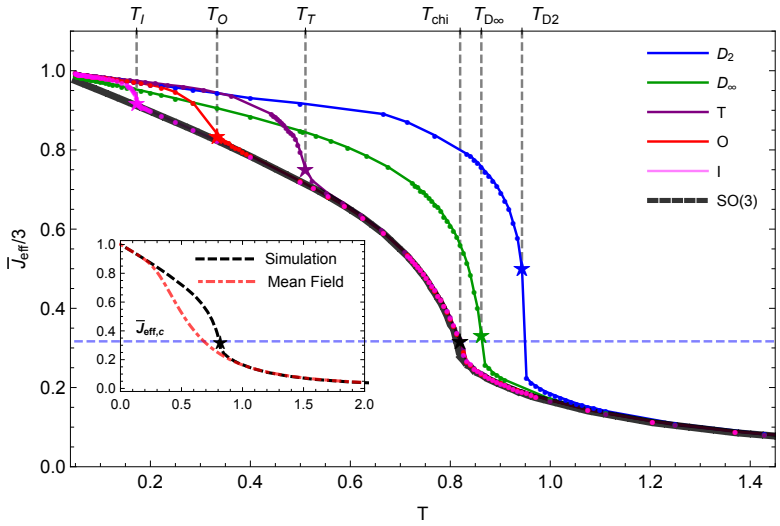

Figure 3.4. Comparison of $\overline{J}_{\rm eff}$ for $G = SO(3)$ case computed by the mean-field approximation Eq. (3.19) and by Monte Carlo simulations. Data in Fig. 3.3 are reproduced here for convenience.

to high order we obtain the chiral temperature $\beta_{\rm chi} \simeq 1.2064$ in perfect agreement with our Monte-Carlo value. Similarly, $\overline{J}_{\rm eff}(\beta)$ can be calculated in a mean-field approximation for the Ising fields, and the curve $\overline{J}_{\rm eff,MF}$ is shown in Fig. 3.4 (inset) in comparison to the $G = SO(3)$ Monte-Carlo data. As expected the mean-field result $\overline{J}_{\rm eff,MF}$ is correct in the high and low temperature regions. We clearly see the correlations of the chiral Ising and orientational degrees of freedom amplifying the $SO(3)$ ordering very close to the chiral transition where the curves start to deviate. One also observes from Fig. 3.4 that below the chiral transition the system indeed finally realizes that the orientational symmetries are actually different with the effect that the transition temperatures to the full nematic order are quite different. This is to be expected based on the different fluctuations of the nematic order parameters, as discussed above.

3.B.1 Calculations for $G = SO(3)$

In order to quantify the interdependence of the orientational and Ising degrees of freedom, we can compute the coupling $J_{\rm eff}(\beta)$, as well as $\overline{J}_{\rm eff}$ in a mean-field approximation for the Ising fields in the case of gauge group $G = SO(3)$. There is no phase transition in the orientational degrees of freedom [27] and the effective action with the coupling $J_{{\rm eff},ij}(\beta)$ for the Ising fields is always well-defined. Specifically, the partition function takes

the form

$$\begin{aligned} Z_{SO(3)} &= \sum_{\{\sigma_i\}} \int \mathcal{D}\{\widetilde{R}_i, U_{ij}\} \prod_{\langle ij\rangle} e^{\beta \mathrm{Tr}[\widetilde{R}_i U_{ij} \widetilde{R}_j]\sigma_i\sigma_j} \\ &= \sum_{\{\sigma_i\}} \prod_{\langle ij\rangle} \int_{SO(3)} \mathrm{d}W_{ij}\ e^{\beta \mathrm{Tr}[W_{ij}]\sigma_i\sigma_j} \\ &= \sum_{\{\sigma_i\}} e^{-\sum_{\langle ij\rangle} J_{\mathrm{eff},ij}(\beta)\sigma_i\sigma_j}, \end{aligned}$$

where in the second line, due to the $SO(3)$ gauge symmetry, we can always pick a gauge where $\widetilde{R}_i = \mathbb{1}$ for all i and a new $SO(3)$ link variable $W_{ij} = \widetilde{R}_i U_{ij} \widetilde{R}_j^T$ and trivially integrate over the matter fields $\{\widetilde{R}_i\}$ and $U_{ij} \in SO(3)$ with the Haar measure $\frac{1}{8\pi^2}\int_{SO(3)} \mathrm{d}g = 1$, see [117]. We determine $J_{\mathrm{eff}}(\beta)$ from the odd-power series expansion of $\log f(x)$ with

$$\begin{aligned} f(x) &= \frac{1}{8\pi^2} \int_{SO(3)} \mathrm{d}W e^{x\mathrm{Tr}[W]} \\ &= \frac{1}{8\pi^2} \int_{S^2} \mathrm{d}\Omega \int_0^\pi \mathrm{d}\varphi\ 2(1-\cos\varphi) e^{x(1+2\cos\varphi)} \\ &= e^x \Big(I_0(2x) - I_1(2x) \Big), \end{aligned} \tag{3.18}$$

where S^2 is the two-sphere with volume element $\mathrm{d}\Omega$ and $I_n(x)$ is the modified Bessel function of the first kind. Here we used that $\mathrm{Tr}[W(\widehat{n},\varphi)] = 1 + 2\cos\varphi$, where $\varphi \in [0,\pi)$ is the angle of rotation and $\widehat{n}$ the axis of rotation of the element $W \in SO(3)$. The angle φ also determines the conjugacy classes of $SO(3) \simeq \mathbb{RP}^3$. The measure $\mathrm{d}\Omega\mathrm{d}\varphi(1-\cos\varphi)$ satisfies $\mathrm{d}g = \mathrm{d}(hg) = \mathrm{d}(gh'^{-1})$ for all $h, h' \in SO(3)$ [117]. We have evaluted $J_{\mathrm{eff}}(\beta)$ to high order and equating $J_{\mathrm{eff}}(\beta_{\mathrm{chi}}) = \beta_{c,\mathrm{3DIsing}} \simeq 0.2215$ converges and gives $\beta_{\mathrm{chi}} = 1.2064$ in excellent agreement with our Monte-Carlo value.

Similarly, we can compute effective mean-field value of $\overline{J}_{\mathrm{eff}}(\beta)$ with the Ising variables $\sigma_{\mathrm{MF}} \sim \sigma_i\sigma_j$ from

$$\begin{aligned} \overline{J}_{\mathrm{eff,MF}}(\beta) &= \langle \mathrm{Tr}[W_{ij}] \rangle(\beta) \\ &= \frac{1}{Z_{\mathrm{MF}}} \sum_{\sigma_{\mathrm{MF}}=\pm 1} \prod_{\langle ij\rangle} \int_{SO(3)} \mathrm{d}W_{ij}\ \mathrm{Tr}[W_{ij}] e^{\beta \mathrm{Tr}[W_{ij}]\sigma_{\mathrm{MF}}} \\ &= \frac{\Big[\beta\sinh(\beta) + \cosh(\beta)\Big]\, {}_0F_1\left(2;\beta^2\right) - \cosh(\beta) I_0(2\beta)}{\cosh(\beta) I_0(2\beta) - \sinh(\beta) I_1(2\beta)}, \end{aligned} \tag{3.19}$$

where ${}_0F_1(a;x)$ is the regularized confluent hypergeometric function. The correlator $\langle \mathrm{Tr}[W_{ij}]\rangle$ leading to $\overline{J}_{\mathrm{eff,MF}}$ is again independent of i,j since the link variables W_{ij} are free in the mean-field approximation for the Ising variables. The theoretical line of $J_{\mathrm{eff,MF}}(\beta)$ for $SO(3)$ is shown in Fig. 3.4 for comparison with the Monte-Carlo results. We see, as expected, that the low and high temperature correlations of $SO(3)$ agree with the MF result and this in fact applies to all point groups. For $SO(3)$ and T, I, O realizing the vestigial chiral phase, closer to the transition temperature β_{chi}, the fluctuations of the Ising fields reinforce the orientational short-range order significantly from the mean-field result. What is surprising is that the fluctuations continue to be identical to $G = SO(3)$ for T, O and I, close until to the regime of the nematic transition.

3.C The I_h tensor order parameter

In Eq. (3.8) we presented the order parameter tensor, $\mathbb{O}^{I_h}$, of an icosahedral phase in a compact form. Due to the high rank and the five-fold rotation, $\mathbb{O}^{I_h}$ is in fact highly complex. This complexity is avoided in the gauge theory Eq. (3.5), however, it will show up in traditional Landau theories. To highlight the advantage of our gauge theory, here we present the full expanded form of $\mathbb{O}^{I_h}$.

$$
\begin{aligned}
\mathbb{O}^{I_h} =& \sum_{\mathrm{cyc}} \Big[\mathbf{l}^{\otimes 6} + \sum_{\{+,-\}} \Big(\frac{1}{2}\mathbf{l} \pm \frac{\tau}{2}\mathbf{m} \pm \frac{1}{2\tau}\mathbf{n} \Big)^{\otimes 6} \Big] - \frac{1}{7} \sum_{\mathrm{perm}} \delta_{ab}\delta_{cd}\delta_{ef} \bigotimes_{\substack{\mu=a,b,c,\\ d,e,f}} \mathbf{e}_\mu \\
=& \frac{35}{16} l\otimes l\otimes l\otimes l\otimes l\otimes l - \frac{1}{32}\sqrt{5} l\otimes l\otimes l\otimes l\otimes m\otimes m + \\
& \frac{13}{32} l\otimes l\otimes l\otimes l\otimes m\otimes m + \frac{1}{32}\sqrt{5} l\otimes l\otimes l\otimes l\otimes n\otimes n + \\
& \frac{13}{32} l\otimes l\otimes l\otimes l\otimes n\otimes n - \frac{1}{32}\sqrt{5} l\otimes l\otimes l\otimes m\otimes l\otimes m + \\
& \frac{13}{32} l\otimes l\otimes l\otimes m\otimes l\otimes m - \frac{1}{32}\sqrt{5} l\otimes l\otimes l\otimes m\otimes m\otimes l + \\
& \frac{13}{32} l\otimes l\otimes l\otimes m\otimes m\otimes l + \frac{1}{32}\sqrt{5} l\otimes l\otimes l\otimes n\otimes l\otimes n + \\
& \frac{13}{32} l\otimes l\otimes l\otimes n\otimes l\otimes n + \frac{1}{32}\sqrt{5} l\otimes l\otimes l\otimes n\otimes n\otimes l + \\
& \frac{13}{32} l\otimes l\otimes l\otimes n\otimes n\otimes l - \frac{1}{32}\sqrt{5} l\otimes l\otimes m\otimes l\otimes l\otimes m + \\
\end{aligned}
$$

$$\frac{13}{32}l\otimes l\otimes m\otimes l\otimes l\otimes m-\frac{1}{32}\sqrt{5}l\otimes l\otimes m\otimes l\otimes m\otimes l+$$
$$\frac{13}{32}l\otimes l\otimes m\otimes l\otimes m\otimes l-\frac{1}{32}\sqrt{5}l\otimes l\otimes m\otimes m\otimes l\otimes l+$$
$$\frac{13}{32}l\otimes l\otimes m\otimes m\otimes l\otimes l+\frac{1}{32}\sqrt{5}l\otimes l\otimes m\otimes m\otimes m\otimes m+$$
$$\frac{13}{32}l\otimes l\otimes m\otimes m\otimes m\otimes m+\frac{3}{16}l\otimes l\otimes m\otimes m\otimes n\otimes n+$$
$$\frac{3}{16}l\otimes l\otimes m\otimes n\otimes m\otimes n+\frac{3}{16}l\otimes l\otimes m\otimes n\otimes n\otimes m+$$
$$\frac{1}{32}\sqrt{5}l\otimes l\otimes n\otimes l\otimes l\otimes n+\frac{13}{32}l\otimes l\otimes n\otimes l\otimes l\otimes n+$$
$$\frac{1}{32}\sqrt{5}l\otimes l\otimes n\otimes l\otimes n\otimes l+\frac{13}{32}l\otimes l\otimes n\otimes l\otimes n\otimes l+$$
$$\frac{3}{16}l\otimes l\otimes n\otimes m\otimes m\otimes n+\frac{3}{16}l\otimes l\otimes n\otimes m\otimes n\otimes m+$$
$$\frac{1}{32}\sqrt{5}l\otimes l\otimes n\otimes n\otimes l\otimes l+\frac{13}{32}l\otimes l\otimes n\otimes n\otimes l\otimes l+$$
$$\frac{3}{16}l\otimes l\otimes n\otimes n\otimes m\otimes m-\frac{1}{32}\sqrt{5}l\otimes l\otimes n\otimes n\otimes n\otimes n+$$
$$\frac{13}{32}l\otimes l\otimes n\otimes n\otimes n\otimes n-\frac{1}{32}\sqrt{5}l\otimes m\otimes l\otimes l\otimes l\otimes m+$$
$$\frac{13}{32}l\otimes m\otimes l\otimes l\otimes l\otimes m-\frac{1}{32}\sqrt{5}l\otimes m\otimes l\otimes l\otimes m\otimes l+$$
$$\frac{13}{32}l\otimes m\otimes l\otimes l\otimes m\otimes l-\frac{1}{32}\sqrt{5}l\otimes m\otimes l\otimes m\otimes l\otimes l+$$
$$\frac{13}{32}l\otimes m\otimes l\otimes m\otimes l\otimes l+\frac{1}{32}\sqrt{5}l\otimes m\otimes l\otimes m\otimes m\otimes m+$$
$$\frac{13}{32}l\otimes m\otimes l\otimes m\otimes m\otimes m+\frac{3}{16}l\otimes m\otimes l\otimes m\otimes n\otimes n+$$
$$\frac{3}{16}l\otimes m\otimes l\otimes n\otimes m\otimes n+\frac{3}{16}l\otimes m\otimes l\otimes n\otimes n\otimes m-$$
$$\frac{1}{32}\sqrt{5}l\otimes m\otimes m\otimes l\otimes l\otimes l+\frac{13}{32}l\otimes m\otimes m\otimes l\otimes l\otimes l+$$
$$\frac{1}{32}\sqrt{5}l\otimes m\otimes m\otimes l\otimes m\otimes m+\frac{13}{32}l\otimes m\otimes m\otimes l\otimes m\otimes m+$$
$$\frac{3}{16}l\otimes m\otimes m\otimes l\otimes n\otimes n+\frac{1}{32}\sqrt{5}l\otimes m\otimes m\otimes m\otimes l\otimes m+$$
$$\frac{13}{32}l\otimes m\otimes m\otimes m\otimes l\otimes m+\frac{1}{32}\sqrt{5}l\otimes m\otimes m\otimes m\otimes m\otimes l+$$

$$\frac{13}{32}l\otimes m\otimes m\otimes m\otimes m\otimes l+\frac{3}{16}l\otimes m\otimes m\otimes n\otimes l\otimes n+$$
$$\frac{3}{16}l\otimes m\otimes m\otimes n\otimes n\otimes l+\frac{3}{16}l\otimes m\otimes n\otimes l\otimes m\otimes n+$$
$$\frac{3}{16}l\otimes m\otimes n\otimes l\otimes n\otimes m+\frac{3}{16}l\otimes m\otimes n\otimes m\otimes l\otimes n+$$
$$\frac{3}{16}l\otimes m\otimes n\otimes m\otimes n\otimes l+\frac{3}{16}l\otimes m\otimes n\otimes n\otimes l\otimes m+$$
$$\frac{3}{16}l\otimes m\otimes n\otimes n\otimes m\otimes l+\frac{1}{32}\sqrt{5}l\otimes n\otimes l\otimes l\otimes l\otimes n+$$
$$\frac{13}{32}l\otimes n\otimes l\otimes l\otimes l\otimes n+\frac{1}{32}\sqrt{5}l\otimes n\otimes l\otimes l\otimes n\otimes l+$$
$$\frac{13}{32}l\otimes n\otimes l\otimes l\otimes n\otimes l+\frac{3}{16}l\otimes n\otimes l\otimes m\otimes m\otimes n+$$
$$\frac{3}{16}l\otimes n\otimes l\otimes m\otimes n\otimes m+\frac{1}{32}\sqrt{5}l\otimes n\otimes l\otimes n\otimes l\otimes l+$$
$$\frac{13}{32}l\otimes n\otimes l\otimes n\otimes l\otimes l+\frac{3}{16}l\otimes n\otimes l\otimes n\otimes m\otimes m-$$
$$\frac{1}{32}\sqrt{5}l\otimes n\otimes l\otimes n\otimes n\otimes n+\frac{13}{32}l\otimes n\otimes l\otimes n\otimes n\otimes n+$$
$$\frac{3}{16}l\otimes n\otimes m\otimes l\otimes m\otimes n+\frac{3}{16}l\otimes n\otimes m\otimes l\otimes n\otimes m+$$
$$\frac{3}{16}l\otimes n\otimes m\otimes m\otimes l\otimes n+\frac{3}{16}l\otimes n\otimes m\otimes m\otimes n\otimes l+$$
$$\frac{3}{16}l\otimes n\otimes m\otimes n\otimes l\otimes m+\frac{3}{16}l\otimes n\otimes m\otimes n\otimes m\otimes l+$$
$$\frac{1}{32}\sqrt{5}l\otimes n\otimes n\otimes l\otimes l\otimes l+\frac{13}{32}l\otimes n\otimes n\otimes l\otimes l\otimes l+$$
$$\frac{3}{16}l\otimes n\otimes n\otimes l\otimes m\otimes m-\frac{1}{32}\sqrt{5}l\otimes n\otimes n\otimes l\otimes n\otimes n+$$
$$\frac{13}{32}l\otimes n\otimes n\otimes l\otimes n\otimes n+\frac{3}{16}l\otimes n\otimes n\otimes m\otimes l\otimes m+$$
$$\frac{3}{16}l\otimes n\otimes n\otimes m\otimes m\otimes l-\frac{1}{32}\sqrt{5}l\otimes n\otimes n\otimes n\otimes l\otimes n+$$
$$\frac{13}{32}l\otimes n\otimes n\otimes n\otimes l\otimes n-\frac{1}{32}\sqrt{5}l\otimes n\otimes n\otimes n\otimes n\otimes l+$$
$$\frac{13}{32}l\otimes n\otimes n\otimes n\otimes n\otimes l-\frac{1}{32}\sqrt{5}m\otimes l\otimes l\otimes l\otimes l\otimes m+$$
$$\frac{13}{32}m\otimes l\otimes l\otimes l\otimes l\otimes m-\frac{1}{32}\sqrt{5}m\otimes l\otimes l\otimes l\otimes m\otimes l+$$

$$\frac{13}{32}m\otimes l\otimes l\otimes l\otimes m\otimes l-\frac{1}{32}\sqrt{5}m\otimes l\otimes l\otimes m\otimes l\otimes l+$$
$$\frac{13}{32}m\otimes l\otimes l\otimes m\otimes l\otimes l+\frac{1}{32}\sqrt{5}m\otimes l\otimes l\otimes m\otimes m\otimes m+$$
$$\frac{13}{32}m\otimes l\otimes l\otimes m\otimes m\otimes m+\frac{3}{16}m\otimes l\otimes l\otimes m\otimes n\otimes n+$$
$$\frac{3}{16}m\otimes l\otimes l\otimes n\otimes m\otimes n+\frac{3}{16}m\otimes l\otimes l\otimes n\otimes n\otimes m-$$
$$\frac{1}{32}\sqrt{5}m\otimes l\otimes m\otimes l\otimes l\otimes l+\frac{13}{32}m\otimes l\otimes m\otimes l\otimes l\otimes l+$$
$$\frac{1}{32}\sqrt{5}m\otimes l\otimes m\otimes l\otimes m\otimes m+\frac{13}{32}m\otimes l\otimes m\otimes l\otimes m\otimes m+$$
$$\frac{3}{16}m\otimes l\otimes m\otimes l\otimes n\otimes n+\frac{1}{32}\sqrt{5}m\otimes l\otimes m\otimes m\otimes l\otimes m+$$
$$\frac{13}{32}m\otimes l\otimes m\otimes m\otimes l\otimes m+\frac{1}{32}\sqrt{5}m\otimes l\otimes m\otimes m\otimes m\otimes l+$$
$$\frac{13}{32}m\otimes l\otimes m\otimes m\otimes m\otimes l+\frac{3}{16}m\otimes l\otimes m\otimes n\otimes l\otimes n+$$
$$\frac{3}{16}m\otimes l\otimes m\otimes n\otimes n\otimes l+\frac{3}{16}m\otimes l\otimes n\otimes l\otimes m\otimes n+$$
$$\frac{3}{16}m\otimes l\otimes n\otimes l\otimes n\otimes m+\frac{3}{16}m\otimes l\otimes n\otimes m\otimes l\otimes n+$$
$$\frac{3}{16}m\otimes l\otimes n\otimes m\otimes n\otimes l+\frac{3}{16}m\otimes l\otimes n\otimes n\otimes l\otimes m+$$
$$\frac{3}{16}m\otimes l\otimes n\otimes n\otimes m\otimes l-\frac{1}{32}\sqrt{5}m\otimes m\otimes l\otimes l\otimes l\otimes l+$$
$$\frac{13}{32}m\otimes m\otimes l\otimes l\otimes l\otimes l+\frac{1}{32}\sqrt{5}m\otimes m\otimes l\otimes l\otimes m\otimes m+$$
$$\frac{13}{32}m\otimes m\otimes l\otimes l\otimes m\otimes m+\frac{3}{16}m\otimes m\otimes l\otimes l\otimes n\otimes n+$$
$$\frac{1}{32}\sqrt{5}m\otimes m\otimes l\otimes m\otimes l\otimes m+\frac{13}{32}m\otimes m\otimes l\otimes m\otimes l\otimes m+$$
$$\frac{1}{32}\sqrt{5}m\otimes m\otimes l\otimes m\otimes m\otimes l+\frac{13}{32}m\otimes m\otimes l\otimes m\otimes m\otimes l+$$
$$\frac{3}{16}m\otimes m\otimes l\otimes n\otimes l\otimes n+\frac{3}{16}m\otimes m\otimes l\otimes n\otimes n\otimes l+$$
$$\frac{1}{32}\sqrt{5}m\otimes m\otimes m\otimes l\otimes l\otimes m+\frac{13}{32}m\otimes m\otimes m\otimes l\otimes l\otimes m+$$
$$\frac{1}{32}\sqrt{5}m\otimes m\otimes m\otimes l\otimes m\otimes l+\frac{13}{32}m\otimes m\otimes m\otimes l\otimes m\otimes l+$$

$$\frac{1}{32}\sqrt{5}m\otimes m\otimes m\otimes m\otimes l\otimes l+\frac{13}{32}m\otimes m\otimes m\otimes m\otimes l\otimes l+$$
$$\frac{35}{16}m\otimes m\otimes m\otimes m\otimes m\otimes m-\frac{1}{32}\sqrt{5}m\otimes m\otimes m\otimes m\otimes n\otimes n+$$
$$\frac{13}{32}m\otimes m\otimes m\otimes m\otimes n\otimes n-\frac{1}{32}\sqrt{5}m\otimes m\otimes m\otimes n\otimes m\otimes n+$$
$$\frac{13}{32}m\otimes m\otimes m\otimes n\otimes m\otimes n-\frac{1}{32}\sqrt{5}m\otimes m\otimes m\otimes n\otimes n\otimes m+$$
$$\frac{13}{32}m\otimes m\otimes m\otimes n\otimes n\otimes m+\frac{3}{16}m\otimes m\otimes n\otimes l\otimes l\otimes n+$$
$$\frac{3}{16}m\otimes m\otimes n\otimes l\otimes n\otimes l-\frac{1}{32}\sqrt{5}m\otimes m\otimes n\otimes m\otimes m\otimes n+$$
$$\frac{13}{32}m\otimes m\otimes n\otimes m\otimes m\otimes n-\frac{1}{32}\sqrt{5}m\otimes m\otimes n\otimes m\otimes n\otimes m+$$
$$\frac{13}{32}m\otimes m\otimes n\otimes m\otimes n\otimes m+\frac{3}{16}m\otimes m\otimes n\otimes n\otimes l\otimes l-$$
$$\frac{1}{32}\sqrt{5}m\otimes m\otimes n\otimes n\otimes m\otimes m+\frac{13}{32}m\otimes m\otimes n\otimes n\otimes m\otimes m+$$
$$\frac{1}{32}\sqrt{5}m\otimes m\otimes n\otimes n\otimes n\otimes n+\frac{13}{32}m\otimes m\otimes n\otimes n\otimes n\otimes n+$$
$$\frac{3}{16}m\otimes n\otimes l\otimes l\otimes m\otimes n+\frac{3}{16}m\otimes n\otimes l\otimes l\otimes n\otimes m+$$
$$\frac{3}{16}m\otimes n\otimes l\otimes m\otimes l\otimes n+\frac{3}{16}m\otimes n\otimes l\otimes m\otimes n\otimes l+$$
$$\frac{3}{16}m\otimes n\otimes l\otimes n\otimes l\otimes m+\frac{3}{16}m\otimes n\otimes l\otimes n\otimes m\otimes l+$$
$$\frac{3}{16}m\otimes n\otimes m\otimes l\otimes l\otimes n+\frac{3}{16}m\otimes n\otimes m\otimes l\otimes n\otimes l-$$
$$\frac{1}{32}\sqrt{5}m\otimes n\otimes m\otimes m\otimes m\otimes n+\frac{13}{32}m\otimes n\otimes m\otimes m\otimes m\otimes n-$$
$$\frac{1}{32}\sqrt{5}m\otimes n\otimes m\otimes m\otimes n\otimes m+\frac{13}{32}m\otimes n\otimes m\otimes m\otimes n\otimes m+$$
$$\frac{3}{16}m\otimes n\otimes m\otimes n\otimes l\otimes l-\frac{1}{32}\sqrt{5}m\otimes n\otimes m\otimes n\otimes m\otimes m+$$
$$\frac{13}{32}m\otimes n\otimes m\otimes n\otimes m\otimes m+\frac{1}{32}\sqrt{5}m\otimes n\otimes m\otimes n\otimes n\otimes n+$$
$$\frac{13}{32}m\otimes n\otimes m\otimes n\otimes n\otimes n+\frac{3}{16}m\otimes n\otimes n\otimes l\otimes l\otimes m+$$
$$\frac{3}{16}m\otimes n\otimes n\otimes l\otimes m\otimes l+\frac{3}{16}m\otimes n\otimes n\otimes m\otimes l\otimes l-$$

$$\frac{1}{32}\sqrt{5}m\otimes n\otimes n\otimes m\otimes m\otimes m+\frac{13}{32}m\otimes n\otimes n\otimes m\otimes m\otimes m+$$
$$\frac{1}{32}\sqrt{5}m\otimes n\otimes n\otimes m\otimes n\otimes n+\frac{13}{32}m\otimes n\otimes n\otimes m\otimes n\otimes n+$$
$$\frac{1}{32}\sqrt{5}m\otimes n\otimes n\otimes n\otimes m\otimes n+\frac{13}{32}m\otimes n\otimes n\otimes n\otimes m\otimes n+$$
$$\frac{1}{32}\sqrt{5}m\otimes n\otimes n\otimes n\otimes n\otimes m+\frac{13}{32}m\otimes n\otimes n\otimes n\otimes n\otimes m+$$
$$\frac{1}{32}\sqrt{5}n\otimes l\otimes l\otimes l\otimes l\otimes n+\frac{13}{32}n\otimes l\otimes l\otimes l\otimes l\otimes n+$$
$$\frac{1}{32}\sqrt{5}n\otimes l\otimes l\otimes l\otimes n\otimes l+\frac{13}{32}n\otimes l\otimes l\otimes l\otimes n\otimes l+$$
$$\frac{3}{16}n\otimes l\otimes l\otimes m\otimes m\otimes n+\frac{3}{16}n\otimes l\otimes l\otimes m\otimes n\otimes m+$$
$$\frac{1}{32}\sqrt{5}n\otimes l\otimes l\otimes n\otimes l\otimes l+\frac{13}{32}n\otimes l\otimes l\otimes n\otimes l\otimes l+$$
$$\frac{3}{16}n\otimes l\otimes l\otimes n\otimes m\otimes m-\frac{1}{32}\sqrt{5}n\otimes l\otimes l\otimes n\otimes n\otimes n+$$
$$\frac{13}{32}n\otimes l\otimes l\otimes n\otimes n\otimes n+\frac{3}{16}n\otimes l\otimes m\otimes l\otimes m\otimes n+$$
$$\frac{3}{16}n\otimes l\otimes m\otimes l\otimes n\otimes m+\frac{3}{16}n\otimes l\otimes m\otimes m\otimes l\otimes n+$$
$$\frac{3}{16}n\otimes l\otimes m\otimes m\otimes n\otimes l+\frac{3}{16}n\otimes l\otimes m\otimes n\otimes l\otimes m+$$
$$\frac{3}{16}n\otimes l\otimes m\otimes n\otimes m\otimes l+\frac{1}{32}\sqrt{5}n\otimes l\otimes n\otimes l\otimes l\otimes l+$$
$$\frac{13}{32}n\otimes l\otimes n\otimes l\otimes l\otimes l+\frac{3}{16}n\otimes l\otimes n\otimes l\otimes m\otimes m-$$
$$\frac{1}{32}\sqrt{5}n\otimes l\otimes n\otimes l\otimes n\otimes n+\frac{13}{32}n\otimes l\otimes n\otimes l\otimes n\otimes n+$$
$$\frac{3}{16}n\otimes l\otimes n\otimes m\otimes l\otimes m+\frac{3}{16}n\otimes l\otimes n\otimes m\otimes m\otimes l-$$
$$\frac{1}{32}\sqrt{5}n\otimes l\otimes n\otimes n\otimes l\otimes n+\frac{13}{32}n\otimes l\otimes n\otimes n\otimes l\otimes n-$$
$$\frac{1}{32}\sqrt{5}n\otimes l\otimes n\otimes n\otimes n\otimes l+\frac{13}{32}n\otimes l\otimes n\otimes n\otimes n\otimes l+$$
$$\frac{3}{16}n\otimes m\otimes l\otimes l\otimes m\otimes n+\frac{3}{16}n\otimes m\otimes l\otimes l\otimes n\otimes m+$$
$$\frac{3}{16}n\otimes m\otimes l\otimes m\otimes l\otimes n+\frac{3}{16}n\otimes m\otimes l\otimes m\otimes n\otimes l+$$

$$\frac{3}{16}n\otimes m\otimes l\otimes n\otimes l\otimes m+\frac{3}{16}n\otimes m\otimes l\otimes n\otimes m\otimes l+$$
$$\frac{3}{16}n\otimes m\otimes m\otimes l\otimes l\otimes n+\frac{3}{16}n\otimes m\otimes m\otimes l\otimes n\otimes l-$$
$$\frac{1}{32}\sqrt{5}n\otimes m\otimes m\otimes m\otimes m\otimes n+\frac{13}{32}n\otimes m\otimes m\otimes m\otimes m\otimes n-$$
$$\frac{1}{32}\sqrt{5}n\otimes m\otimes m\otimes m\otimes n\otimes m+\frac{13}{32}n\otimes m\otimes m\otimes m\otimes n\otimes m+$$
$$\frac{3}{16}n\otimes m\otimes m\otimes n\otimes l\otimes l-\frac{1}{32}\sqrt{5}n\otimes m\otimes m\otimes n\otimes m\otimes m+$$
$$\frac{13}{32}n\otimes m\otimes m\otimes n\otimes m\otimes m+\frac{1}{32}\sqrt{5}n\otimes m\otimes m\otimes n\otimes n\otimes n+$$
$$\frac{13}{32}n\otimes m\otimes m\otimes n\otimes n\otimes n+\frac{3}{16}n\otimes m\otimes n\otimes l\otimes l\otimes m+$$
$$\frac{3}{16}n\otimes m\otimes n\otimes l\otimes m\otimes l+\frac{3}{16}n\otimes m\otimes n\otimes m\otimes l\otimes l-$$
$$\frac{1}{32}\sqrt{5}n\otimes m\otimes n\otimes m\otimes m\otimes m+\frac{13}{32}n\otimes m\otimes n\otimes m\otimes m\otimes m+$$
$$\frac{1}{32}\sqrt{5}n\otimes m\otimes n\otimes m\otimes n\otimes n+\frac{13}{32}n\otimes m\otimes n\otimes m\otimes n\otimes n+$$
$$\frac{1}{32}\sqrt{5}n\otimes m\otimes n\otimes n\otimes m\otimes n+\frac{13}{32}n\otimes m\otimes n\otimes n\otimes m\otimes n+$$
$$\frac{1}{32}\sqrt{5}n\otimes m\otimes n\otimes n\otimes n\otimes m+\frac{13}{32}n\otimes m\otimes n\otimes n\otimes n\otimes m+$$
$$\frac{1}{32}\sqrt{5}n\otimes n\otimes l\otimes l\otimes l\otimes l+\frac{13}{32}n\otimes n\otimes l\otimes l\otimes l\otimes l+$$
$$\frac{3}{16}n\otimes n\otimes l\otimes l\otimes m\otimes m-\frac{1}{32}\sqrt{5}n\otimes n\otimes l\otimes l\otimes n\otimes n+$$
$$\frac{13}{32}n\otimes n\otimes l\otimes l\otimes n\otimes n+\frac{3}{16}n\otimes n\otimes l\otimes m\otimes l\otimes m+$$
$$\frac{3}{16}n\otimes n\otimes l\otimes m\otimes m\otimes l-\frac{1}{32}\sqrt{5}n\otimes n\otimes l\otimes n\otimes l\otimes n+$$
$$\frac{13}{32}n\otimes n\otimes l\otimes n\otimes l\otimes n-\frac{1}{32}\sqrt{5}n\otimes n\otimes l\otimes n\otimes n\otimes l+$$
$$\frac{13}{32}n\otimes n\otimes l\otimes n\otimes n\otimes l+\frac{3}{16}n\otimes n\otimes m\otimes l\otimes l\otimes m+$$
$$\frac{3}{16}n\otimes n\otimes m\otimes l\otimes m\otimes l+\frac{3}{16}n\otimes n\otimes m\otimes m\otimes l\otimes l-$$
$$\frac{1}{32}\sqrt{5}n\otimes n\otimes m\otimes m\otimes m\otimes m+\frac{13}{32}n\otimes n\otimes m\otimes m\otimes m\otimes m+$$

$$\frac{1}{32}\sqrt{5}n\otimes n\otimes m\otimes m\otimes n\otimes n+\frac{13}{32}n\otimes n\otimes m\otimes m\otimes n\otimes n+$$
$$\frac{1}{32}\sqrt{5}n\otimes n\otimes m\otimes n\otimes m\otimes n+\frac{13}{32}n\otimes n\otimes m\otimes n\otimes m\otimes n+$$
$$\frac{1}{32}\sqrt{5}n\otimes n\otimes m\otimes n\otimes n\otimes m+\frac{13}{32}n\otimes n\otimes m\otimes n\otimes n\otimes m-$$
$$\frac{1}{32}\sqrt{5}n\otimes n\otimes n\otimes l\otimes l\otimes n+\frac{13}{32}n\otimes n\otimes n\otimes l\otimes l\otimes n-$$
$$\frac{1}{32}\sqrt{5}n\otimes n\otimes n\otimes l\otimes n\otimes l+\frac{13}{32}n\otimes n\otimes n\otimes l\otimes n\otimes l+$$
$$\frac{1}{32}\sqrt{5}n\otimes n\otimes n\otimes m\otimes m\otimes n+\frac{13}{32}n\otimes n\otimes n\otimes m\otimes m\otimes n+$$
$$\frac{1}{32}\sqrt{5}n\otimes n\otimes n\otimes m\otimes n\otimes m+\frac{13}{32}n\otimes n\otimes n\otimes m\otimes n\otimes m-$$
$$\frac{1}{32}\sqrt{5}n\otimes n\otimes n\otimes n\otimes l\otimes l+\frac{13}{32}n\otimes n\otimes n\otimes n\otimes l\otimes l+$$
$$\frac{1}{32}\sqrt{5}n\otimes n\otimes n\otimes n\otimes m\otimes m+\frac{13}{32}n\otimes n\otimes n\otimes n\otimes m\otimes m+$$
$$\frac{35}{16}n\otimes n\otimes n\otimes n\otimes n\otimes n-\frac{1}{7}\delta_{ab}\delta_{cd}\delta_{ef}\bigotimes_{\substack{\mu=a,b,c,\\d,e,f}}\mathbf{e}_\mu-\frac{1}{7}\delta_{ab}\delta_{ce}\delta_{df}\bigotimes_{\substack{\mu=a,b,c,\\e,d,f}}\mathbf{e}_\mu$$
$$-\frac{1}{7}\delta_{ab}\delta_{cf}\delta_{de}\bigotimes_{\substack{\mu=a,b,c,\\f,d,e}}\mathbf{e}_\mu-\frac{1}{7}\delta_{ac}\delta_{bd}\delta_{ef}\bigotimes_{\substack{\mu=a,c,b,\\d,e,f}}\mathbf{e}_\mu-\frac{1}{7}\delta_{ac}\delta_{be}\delta_{df}\bigotimes_{\substack{\mu=a,c,b,\\e,d,f}}\mathbf{e}_\mu$$
$$-\frac{1}{7}\delta_{ac}\delta_{bf}\delta_{de}\bigotimes_{\substack{\mu=a,c,b,\\f,d,e}}\mathbf{e}_\mu-\frac{1}{7}\delta_{ad}\delta_{bc}\delta_{ef}\bigotimes_{\substack{\mu=a,d,b,\\c,e,f}}\mathbf{e}_\mu-\frac{1}{7}\delta_{ad}\delta_{be}\delta_{cf}\bigotimes_{\substack{\mu=a,d,b,\\e,c,f}}\mathbf{e}_\mu$$
$$-\frac{1}{7}\delta_{ad}\delta_{bf}\delta_{ce}\bigotimes_{\substack{\mu=a,d,b,\\f,c,e}}\mathbf{e}_\mu-\frac{1}{7}\delta_{ae}\delta_{bc}\delta_{df}\bigotimes_{\substack{\mu=a,e,b,\\c,d,f}}\mathbf{e}_\mu-\frac{1}{7}\delta_{ae}\delta_{bd}\delta_{cf}\bigotimes_{\substack{\mu=a,e,b,\\d,c,f}}\mathbf{e}_\mu$$
$$-\frac{1}{7}\delta_{ae}\delta_{bf}\delta_{cd}\bigotimes_{\substack{\mu=a,e,b,\\f,c,d}}\mathbf{e}_\mu-\frac{1}{7}\delta_{af}\delta_{bc}\delta_{de}\bigotimes_{\substack{\mu=a,f,b,\\c,d,e}}\mathbf{e}_\mu-\frac{1}{7}\delta_{af}\delta_{bd}\delta_{ce}\bigotimes_{\substack{\mu=a,f,b,\\d,c,e}}\mathbf{e}_\mu$$
$$-\frac{1}{7}\delta_{af}\delta_{be}\delta_{cd}\bigotimes_{\substack{\mu=a,f,b,\\e,c,d}}\mathbf{e}_\mu. \tag{3.20}$$

Chapter 4

Classification of $3D$ point-group-symmetric order parameter tensors

Rotational symmetry breaking of the three dimensional (3D) orthogonal group $O(3)$ plays an important role in many condensed matters systems, from classical and quantum spins to molecular and strongly correlated electronic nematic liquids [17, 11, 118, 119]. In familiar instances, like the Heisenberg ferromagnet and the uniaxial nematic, the full rotational group $O(3)$ is broken to $O(2)$ and $D_{\infty h}$, respectively. However these are in fact only two special cases of the rich landscape of $O(3)$ symmetry breaking. Indeed, as a matter of principle, matter can break the rotational symmetries of isotropic space $O(3)$ to any of its subgroups, leading to long range orientational order characterized by complicated tensors order parameters.

The subgroups of $O(3)$ have been mathematically identified for a long time, however, it appears that the zoo of point-group orientational orders has never been explored in full generality. Needless to say, the classification of rotational order parameters for some non-broken symmetries has been gradually accumulating since the past century due to various motives. Firstly, in the soft matter literature the unixial ($D_{\infty h}$) and biaxial (D_{2h}) order parameter have been shown to be characterized by second-rank tensors [11], which have been intensively studied in various theories [72–74, 71, 86, 75, 120, 93]. In addition, higher rank ordering tensors for the T_d-tetrahedral [89–91, 97], O_h-cubic [18, 88, 96] and I_h-icosahedral [121–123, 88, 89, 124] orders have been discussed by many authors e.g. in the context of Landau theories and nematic lattice models. Nonetheless, these cover still only a small subset of all 3D point group symmetries and, to the best of our knowledge, the order parameters for most instances are not known explicitly nor have they appeared within a single unified classifi-

cation scheme. These general order parameters, however, are becoming of more practical interest. New exotic orientational orders may be realized in ensembles of anisotropic constituents, especially nano- and colloidal particles of different shapes [81, 82]. In particular, the increasing experimental ability to control such degrees of freedom [80, 125, 126, 78] is especially promising in this regard. Secondly, many unconventional orientational orders have also been proposed for quantum magnets [127, 128, 116] and spinor condensates [129, 130]. In all these cases, the order parameters associated with each symmetry are indispensable to eventually verify the symmetry of these phases and the associated physics.

Now we will use the gauge theory we introduced in Chapter 3.1 to develop a systematic way of deriving the tensor order parameter with arbitrary point groups. In particular, we will highlight the order parameters for physically interesting symmetries including all the crystallographic point groups, the icosahedral groups arising in the context of quasi-crystalline ordering, and the five infinite axial groups $\{C_\infty \simeq SO(2), C_{\infty v} \simeq O(2), C_{\infty h}, D_\infty, D_{\infty h}\}$ exhibiting a continuous rotational $SO(2)$-axis. We show that in order to uniquely characterize a point-group-symmetric orientational order of a phase, at most two order parameter tensors and a pseudoscalar are needed: the second ordering tensor is required by the finite axial groups $\{C_n, C_{nv}, S_{2n}, C_{nh}, D_n, D_{nh}, D_{nd}\}$, whereas the pseudoscalar chiral order parameter is a requisite associated with the handedness or chirality of the proper point groups $\{C_n, D_n, T, O, I\}$ that are subgroups of the group of proper three-dimensional rotations $SO(3)$.

4.1 Construction of orientational ordering tensor

4.1.1 Warm up: Heisenberg ferromagnetic order and uniaxial nematic order

Let us begin by recalling the characterization of rotational ordering in the familiar context of the Heisenberg ferromagnet and the conventional uniaxial nematic.

In the ferromagnetic phase of a classical Heisenberg magnet, the rotational $O(3)$ symmetry of the Hamiltonian breaks down to the point group $C_{\infty v} \simeq O(2)$ defined by the axis of magnetization $\mathbf{M}$. The order parameter $\mathbf{M} = \langle \mathbf{n}_i \rangle$ is given by the macroscopic averaging of local spins $\mathbf{n}_i$ and is a 3D vector with an orientational order parameter space $O(3)/O(2) \simeq S^2$.

On the other hand, for uniaxial liquid crystals or spin nematics, where

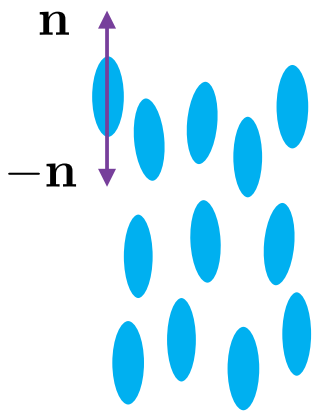

Figure 4.1. Sketch of $D_{\infty h}$ uniaxial molecules. The orientation of a molecule can be defined by a single axis.

the $O(3)$ symmetry is broken to the point group $D_{\infty h}$ in the ordered phase, the system exhibits a macroscopic ordering along an axis $\mathbf{n}$. The uniaxial symmetry $D_{\infty h}$ acts on the order parameter as $\mathbf{n} \to -\mathbf{n}$ and these describe the same macroscopic ordering. Often depicted as being formed of explicitly rod-like "molecules" (Fig. 4.1), a coarse-grained order parameter can be formulated in terms of a local vector $\mathbf{n}_i$ along the "long" axis of each "molecule", with the identification of $\mathbf{n}_i$ with $-\mathbf{n}_i$. To define the uniaxial orientational order, one therefore needs a second rank tensor, $\mathbb{Q}[\mathbf{n}] = \mathbf{n} \otimes \mathbf{n} - \frac{\mathbb{1}}{3}$, which is characterized by its invariance under $\mathbf{n} \to -\mathbf{n}$. Accordingly, the global order parameter is defined as $\mathbb{Q}[\mathbf{n}] = \langle \mathbb{Q}[\mathbf{n}_i] \rangle$ in the coarse-grained order parameter theory and formally relates to the uniaxial order parameter space $O(3)/D_{\infty h} \simeq S^2/Z_2 \simeq \mathbb{RP}^2$, the real projective plane.

4.1.2 General $3D$ orientational order

The above familiar examples share the key feature of having an $O(2)$ symmetry in the plane perpendicular to the ordering vector, which is why the underlying physics is so apparent: the order parameter is defined by one axis and the rotations in the perpendicular plane are trivial, and the degrees of freedom effectively reduce to 1D objects (the spins and the rods in the above examples).

Nonetheless, for general 3D point-group-symmetric ordering, the order parameter and the coarse grained degrees of freedom form intrinsic 3D objects (Fig. 4.2). To define the 3D orientation one therefore has to depart

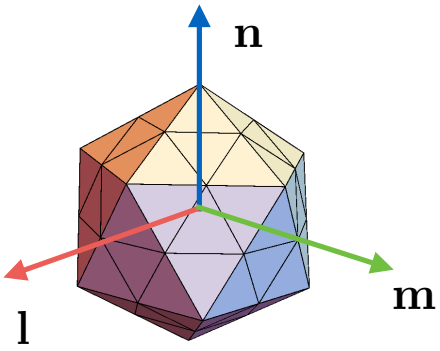

Figure 4.2. To define the orientation of a $3D$ object in general, one need an $O(3)$ triad. Here an icosahedron is used for instance.

from a full $O(3)$ rotation matrix R,

$$R = \begin{pmatrix} \mathbf{l} & \mathbf{m} & \mathbf{n} \end{pmatrix}^T. \tag{4.1}$$

The rows $\{\mathbf{l}, \mathbf{m}, \mathbf{n}\}$ of R form an orthonormal triad $\mathbf{n}^\alpha = \{\mathbf{l}, \mathbf{m}, \mathbf{n}\}$. In other words, R is a rotation that brings the triad $\mathbf{n}^\alpha = \{\mathbf{l}, \mathbf{m}, \mathbf{n}\}$ into coincidence with a fixed "laboratory" frame $\mathbf{e}_a = \{\mathbf{e}_1, \mathbf{e}_2, \mathbf{e}_3\}$ and can be defined by three Euler angles with respect to the unit vectors $\mathbf{e}_a$. The determinant of R defines the handedness or chirality of the triad,

$$\sigma = \det R = \epsilon_{abc}(\mathbf{l} \otimes \mathbf{m} \otimes \mathbf{n})_{abc} = \mathbf{l} \cdot (\mathbf{m} \times \mathbf{n}) = \pm 1, \tag{4.2}$$

which is a pseudoscalar and invariant under the proper rotations $SO(3)$. Moreover, due to $O(3) = SO(3) \times \{\mathbb{1}, -\mathbb{1}\}$, we have the decomposition

$$R = \sigma \widetilde{R} = \sigma \begin{pmatrix} \widetilde{\mathbf{l}} & \widetilde{\mathbf{m}} & \widetilde{\mathbf{n}} \end{pmatrix}^T \tag{4.3}$$

where $\widetilde{R} \in SO(3)$ and its rows $\tilde{\mathbf{n}}^\alpha = \{\tilde{\mathbf{l}}, \tilde{\mathbf{m}}, \tilde{\mathbf{n}}\}$ are pseudovectors. The $O(3)$ constraints $R^T R = R R^T = \mathbb{1}$ and $\det R = \pm 1$ of course reduce the free parameters to the three Euler angles $\Omega = (\theta, \phi, \varphi)$ and chirality in the frame $\mathbf{e}_a$ but we will find the vector notation with the $O(3)$-constraints understood very useful in the following.

The order parameter has to be invariant under all unbroken point-group transformations. As a result, an orientational order parameter with a point group symmetry G is defined by G-invariant tensors constructed from the triad R or $\mathbf{n}^\alpha = \{\mathbf{l}, \mathbf{m}, \mathbf{n}\}$. These tensors are equivalent to higher order multipoles or (three-dimensional) spherical harmonics. We will denote these order parameters tensors composed of the triads generically

as $\mathbb{O}^G$, where the additional label specifies the symmetry group G when appropriate. Concretely, in the two examples in Section 4.1.1, the order parameter tensor is the magnetization vector $\mathbb{O}^{C_{\infty v}}[\mathbf{n}] = \mathbf{n}$ and the second rank tensor or director $\mathbb{O}^{D_{\infty h}}[\mathbf{n}] = \mathbb{Q}[\mathbf{n}]$, respectively. Finally, we note that besides the orientational order, the composite chiral order parameter σ defined in Eq. (4.2) is needed for proper point-group symmetries such as $\{C_n, D_n, T, O, I\}$ due to the breaking of the chiral symmetry of $O(3)$.

As $\mathbb{O}^G$ needs to be uniquely invariant under a given symmetry G, it is in general highly non-trivial to construct its explicit form, even though the polynomial invariants of 3D points groups have been computed a long time ago [94, 95] and the representation theory of $SO(3)$ is known.

4.1.3 Deriving the ordering tensors from the gauge theory

Let us now establish the relation of the ordering tensors with the gauge theory introduced in Chapter 3.1. The goal is to construct a coarse-grained order parameter with certain point group symmetry.

As it has been briefly discussed in Chapter 3.1.3, theunderlying principle of deriving the order parameters is the fundamental gauge theoretical result: all physical observables have to be gauge invariant, since gauge symmetries cannot break spontaneously [28]. By construction, the model Eq. (3.5),

$$H = -\sum_{\langle ij \rangle} \mathrm{Tr}\,\Big[R_i^T \mathbb{J} U_{ij} R_j\Big] - \sum_{\square} \sum_{\mathcal{C}_\mu} K_{\mathcal{C}_\mu} \delta_{\mathcal{C}_\mu}(U_\square) \mathrm{Tr}\Big[U_\square\Big], \tag{4.4}$$

embodies the symmetry of the order parameter tensors by the gauge symmetry. In particular, if we integrate out the gauge fields in the Hamiltonian, the terms that survive are gauge invariant local combinations of the matter fields, corresponding to the order parameter tensors. This can be most easily accomplished in the strong coupling limit of the gauge theory $K_{\mathcal{C}} = 0$. In this limit, the gauge theory Eq. (3.5) reduces to

$$H = -\sum_{\langle ij \rangle} \mathrm{Tr}\,\Big[R_i^T \mathbb{J} U_{ij} R_j\Big], \tag{4.5}$$

and the gauge fields have no independent dynamics. The result is essentially the effective Hamiltonian of the orientational probability density $\rho(\{R_i\}) \sim \frac{1}{Z} \sum_{\{U_{ij}\}} e^{-\beta H[\{R_i\},\{U_{ij}\}]}$, but in order to find the order parameter tensors we do not need the effective Hamiltonian in closed form and

can simply utilize the high-temperature expansion for small β. The couplings $\mathbb{J}$ do not affect the general form of the expansion and we set them to be isotropic $\mathbb{J} = J\mathbb{1}$ for simplicity and measure the temperature in the units $\beta J \equiv \beta$.

The partition function of the model Eq. (4.5) is defined in the usual way,

$$\begin{aligned} Z &= \sum_{\{R_i\}} \sum_{\{U_{ij}\}} e^{-\beta H[R_i, U_{ij}]} \\ &= \sum_{\{\tilde{R}_i\}} \sum_{\{\sigma_i\}} \sum_{\{U_{ij}\}} e^{-\beta H[\tilde{R}_i, \sigma_i, U_{ij}]}, \end{aligned} \tag{4.6}$$

where the summations are naturally discrete over the lattice and discrete or continuous over the groups G and $O(3)$. In the second line we used made the handedness field explicit by Eq. (4.2), $R_i = \sigma_i \widetilde{R}_i$. In order to integrate over the gauge fields, the partition function is Taylor expanded in the high temperature limit $\beta \ll 1$,

$$Z = \sum_{\{\tilde{R}_i\}} \sum_{\{\sigma_i\}} \sum_{\{U_{ij}\}} \prod_{\langle ij \rangle} \sum_{n=0}^{\infty} \frac{1}{n!} (-\beta H_{ij})^n. \tag{4.7}$$

The integration over the gauge fields can be explicitly performed on the lattice order by order in the expansion. By construction, the terms appearing must be local terms that are composed of contractions of gauge invariant tensors. The result is therefore an expression starting with contractions $\sim \mathrm{Tr}\,[\mathbb{O}_i^G \cdot \mathbb{O}_j^G]$ coming from the lowest order non-zero terms $n_{\min} \sim \mathrm{rank}\, \mathbb{O}^G$ in the expansions. In other words, the lowest order non-trivial terms are composed of the lowest order invariant tensors that can be found from Table 4.1. We emphasize that by construction these tensors are the minimal and simplest possible set of invariant tensors allowed by the symmetries.

4.2 Minimal invariant tensors

4.2.1 Order parameter table

In Table 4.1 we show the lowest order invariant tensors for all the 32 crystallographic point groups, the 2 icosahedral groups and the 5 infinite axial groups.

The standard Schönflies notation [131, 95] is used in Table 4.1. The point groups are defined in the coordinate system spanned by the unit triad vectors $\mathbf{n}^\alpha = \{\mathbf{l}, \mathbf{m}, \mathbf{n}\}$ set up in the following way. All point groups have the origin as their fixed point. The rotational axis of cyclic rotation groups C_n of is chosen to be $\mathbf{n}$. The dihedral group D_n has an additional generator in terms of a π-rotation along the vector $\mathbf{l}$ or $\mathbf{m}$. The group C_{nv} is augmented with a "vertical" reflection in the plane $(\mathbf{l}, \mathbf{n})$. The groups C_{nh} and D_{nh} have an additional "horizontal" reflection plane $(\mathbf{l}, \mathbf{m})$. The group D_{nd} has vertical reflection planes in terms of bisectors of the dihedral π-rotation axes. The groups S_{2n} are composed of n-fold rotations in the plane $\mathbf{l}, \mathbf{m}$. The polyhedral groups T, T_d, T_h and O, O_h are defined in terms of a (tetrahedron embedded) in a cube with face normals $\mathbf{n}^\alpha = \{\mathbf{l}, \mathbf{m}, \mathbf{n}\}$. The group I_h is the symmetry group of an icosahedron with vertices at cyclic permutations of the coordinates $\pm\tau\mathbf{l} \pm \mathbf{m} \pm 0 \cdot \mathbf{n}$ and I its proper subgroup, following the conventions in [132].

Accordingly, $\mathbb{O}^G = \mathbb{O}^G[\mathbf{l}, \mathbf{m}, \mathbf{n}]$ and $\mathbb{O}^G = \{\mathbb{A}^G, \mathbb{B}^G\}$ denote the ordering tensor for polyhedral groups and for axial groups, respectively, where $\mathbb{A}^G = \mathbb{A}^G[\mathbf{n}]$ is the order parameter for the main axis $\mathbf{n}$ and $\mathbb{B}^G = \mathbb{B}^G[\mathbf{l}, \mathbf{m}]$ or $\mathbb{B}^G[\mathbf{l}, \mathbf{m}, \mathbf{n}]$ for the in-plane structure for the finite axial groups. Together with the handedness fields σ, they can uniquely define the order parameter for the symmetries mentioned above.

Amongst the ordering tensors in Table 4.1, the C_1 order parameters $\mathbb{O}^{C_1}[\mathbf{l}, \mathbf{m}, \mathbf{n}] = \{\mathbb{A}^{C_{\infty v}}[\mathbf{n}], \mathbb{B}^{C_1}[\mathbf{l}, \mathbf{m}]\} = \{\mathbf{l}, \mathbf{m}, \mathbf{n}\}$ simply constitute the original $O(3)$-rotor order parameter R of a phase with no unbroken symmetry (C_1 is the trivial group); $\mathbb{O}^{D_{2h}} = \{\mathbb{O}^{D_{\infty h}}[\mathbf{n}], \mathbb{B}^{D_{2h}}[\mathbf{l}, \mathbf{m}]\}$ compose the well known order parameter tensors for D_{2h}-biaxial nematics; $\mathbb{O}^{C_{\infty v}}[\mathbf{n}]$ and $\mathbb{O}^{D_{\infty h}}[\mathbf{n}]$ are the classical Heisenberg spin $\mathbf{n}$ and uniaxial director $\mathbb{Q}[\mathbf{n}]$, respectively; $\mathbb{O}^{O_h}[\mathbf{l}, \mathbf{m}, \mathbf{n}]$ has been discussed in Ref. [18]; $\mathbb{O}^{T_d}[\mathbf{l}, \mathbf{m}, \mathbf{n}]$ and $\mathbb{O}^{I_h}[\mathbf{l}, \mathbf{m}, \mathbf{n}]$ appear in a different form in Ref. [89], where an incomplete classification of order parameters for subgroups of $SO(3)$ is also discussed. However, many of the order parameter tensors in Table 4.1 are new and have not been classified in the context of a single unified framework.

Table 4.1. Classification of order parameters for three dimensional point groups. The first column specifies the symmetries and the second column specifies the type $\{\mathbb{O}, \mathbb{A}, \mathbb{B}\}$ of the order constructed from the $O(3)$ triad $R = (\mathbf{l}, \mathbf{m}, \mathbf{n})^T$. The third column gives the explicit form of ordering tensors in the chosen coordinates. They are traceless and vanish in the isotropic phase. The infinite axial groups $\{C_\infty, C_{\infty v}, C_{\infty h}, D_\infty, D_{\infty h}\}$ require a single ordering tensor, $\mathbb{A}[\mathbf{n}]$, describing the orientation of their primary symmetry axis, chosen to be $\mathbf{n}$; the finite axial groups $\{C_n, C_{nv}, C_{nh}, S_{2n}, D_n, D_{nh}, D_{nd}\}$ require two ordering tensors, $\mathbb{A}[\mathbf{n}]$ and $\mathbb{B}[\mathbf{l}, \mathbf{m}]$ or $\mathbb{B}[\mathbf{l}, \mathbf{m}, \mathbf{n}]$, for their primary axis and perpendicular in-plane structure, respectively; the polyhedral groups $\{T, T_d, T_h, O, O_h, I, I_h\}$, which treat $\{\mathbf{l}, \mathbf{m}, \mathbf{n}\}$ symmetrically, require only one ordering tensor $\mathbb{O}[\mathbf{l}, \mathbf{m}, \mathbf{n}]$. Due to the symmetry hierarchy, many point groups share ordering tensors (see Section 4.2.3). Together with the chiral order parameter $\sigma = \det R = \pm 1$ arisen for proper point groups, these ordering tensors uniquely define the orientational ordering of three dimensional point groups. For example, the order parameters for finite proper axial groups are given by $\mathbb{O}^G = \{\mathbb{A}^G, \mathbb{B}^G, \sigma\}$. $^{\otimes n}$ denotes the tensor power, e.g., $\mathbf{n}^{\otimes 2} = \mathbf{n} \otimes \mathbf{n}$ and $\delta_{ab} \bigotimes_{\mu=a,b} \mathbf{e}_\mu = \delta_{ab} \mathbf{e}_a \otimes \mathbf{e}_b$. $\tau = (1 + \sqrt{5})/2$ is the golden ratio. $\sum_{\text{cyc}}$ runs over cyclic permutations of $\{\mathbf{l}, \mathbf{m}, \mathbf{n}\}$. $\sum_{\text{perm}}$ sums over all non-equivalent combinations of the indices of the tensor. $\sum_{\text{perm}''}$ in the $\{C_{6v}, D_6, D_{6h}\}$ cases sums over all the six permutations of the indices d, e and f, and $\sum_{\text{perm}'} = \sum_{\text{perm}} - \sum_{\text{perm}''}$. $\sum_{\{+,-\}}$ for the $\{I, I_h\}$ is a sum over the four combinations of the two $\pm$ signs.

Symmetry Groups	Type	Ordering Tensors	Tensor Rank
C_1, C_{1h}	$\mathbb{B}[\mathbf{l},\mathbf{m}]$	$\mathbf{l}$, $\mathbf{m}$	1
S_2	$\mathbb{B}[\mathbf{l},\mathbf{m},\mathbf{n}]$	$\mathbf{l}\otimes\mathbf{m}$, $\mathbf{m}\otimes\mathbf{l}$, $\mathbf{m}\otimes\mathbf{n}$, $\mathbf{n}\otimes\mathbf{m}$, $\mathbf{n}\otimes\mathbf{l}$, $\mathbf{l}\otimes\mathbf{n}$	2
C_2, C_{2h}	$\mathbb{B}[\mathbf{l},\mathbf{m}]$	$\mathbf{l}\otimes\mathbf{m}$, $\mathbf{m}\otimes\mathbf{l}$	2
C_{2v}, D_2, D_{2h}	$\mathbb{B}[\mathbf{l},\mathbf{m}]$	$\mathbf{l}\otimes\mathbf{l}-\frac{1}{3}\mathbb{1}$, $\mathbf{m}\otimes\mathbf{m}-\frac{1}{3}\mathbb{1}$	2
S_4	$\mathbb{B}[\mathbf{l},\mathbf{m},\mathbf{n}]$	$\Big(\mathbf{l}\otimes\mathbf{l}-\mathbf{m}\otimes\mathbf{m}\Big)\otimes\mathbf{n}$	3
D_{2d}	$\mathbb{B}[\mathbf{l},\mathbf{m},\mathbf{n}]$	$\Big(\mathbf{l}\otimes\mathbf{m}+\mathbf{m}\otimes\mathbf{l}\Big)\otimes\mathbf{n}$	3
C_3, C_{3h}	$\mathbb{B}[\mathbf{l},\mathbf{m}]$	$\Big(\mathbf{l}^{\otimes 3}-\mathbf{l}\otimes\mathbf{m}^{\otimes 2}-\mathbf{m}\otimes\mathbf{l}\otimes\mathbf{m}-\mathbf{m}^{\otimes 2}\otimes\mathbf{l}\Big)$, $\Big(\mathbf{m}^{\otimes 3}-\mathbf{m}\otimes\mathbf{l}^{\otimes 2}-\mathbf{l}\otimes\mathbf{m}\otimes\mathbf{l}-\mathbf{l}^{\otimes 2}\otimes\mathbf{m}\Big)$	3
C_{3v}, D_3, D_{3h}	$\mathbb{B}[\mathbf{l},\mathbf{m}]$	$\Big(\mathbf{l}^{\otimes 3}-\mathbf{l}\otimes\mathbf{m}^{\otimes 2}-\mathbf{m}\otimes\mathbf{l}\otimes\mathbf{m}-\mathbf{m}^{\otimes 2}\otimes\mathbf{l}\Big)$	3
S_6	$\mathbb{B}[\mathbf{l},\mathbf{m},\mathbf{n}]$	$\Big(\mathbf{l}^{\otimes 3}-\mathbf{l}\otimes\mathbf{m}^{\otimes 2}-\mathbf{m}\otimes\mathbf{l}\otimes\mathbf{m}-\mathbf{m}^{\otimes 2}\otimes\mathbf{l}\Big)\otimes\mathbf{n}$, $\Big(\mathbf{m}^{\otimes 3}-\mathbf{m}\otimes\mathbf{l}^{\otimes 2}-\mathbf{l}\otimes\mathbf{m}\otimes\mathbf{l}-\mathbf{l}^{\otimes 2}\otimes\mathbf{m}\Big)\otimes\mathbf{n}$	4
D_{3d}	$\mathbb{B}[\mathbf{l},\mathbf{m},\mathbf{n}]$	$\Big(\mathbf{m}^{\otimes 3}-\mathbf{m}\otimes\mathbf{l}^{\otimes 2}-\mathbf{l}\otimes\mathbf{m}\otimes\mathbf{l}-\mathbf{l}^{\otimes 2}\otimes\mathbf{m}\Big)\otimes\mathbf{n}$	4
C_4, C_{4h}	$\mathbb{B}[\mathbf{l},\mathbf{m}]$	$\mathbf{l}^{\otimes 3}\otimes\mathbf{m}-\mathbf{m}^{\otimes 3}\otimes\mathbf{l}$	4
C_{4v}, D_4, D_{4h}	$\mathbb{B}[\mathbf{l},\mathbf{m}]$	$\mathbf{l}^{\otimes 2}\otimes\mathbf{m}^{\otimes 2}+\mathbf{m}^{\otimes 2}\otimes\mathbf{l}^{\otimes 2}-\frac{4}{15}\delta_{ab}\delta_{cd}\bigotimes_{\mu=a,b,c,d}\mathbf{e}_\mu+\frac{1}{15}\Big(\delta_{ac}\delta_{bd}\bigotimes_{\mu=a,c,b,d}\mathbf{e}_\mu+\delta_{ad}\delta_{bc}\bigotimes_{\mu=a,d,b,c}\mathbf{e}_\mu\Big)$, $\mathbf{l}^{\otimes 4}+\mathbf{m}^{\otimes 4}-\frac{2}{15}\sum_{\text{perm}}\delta_{ab}\delta_{cd}\bigotimes_{\mu=a,b,c,d}\mathbf{e}_\mu$	4
C_6, C_{6h}	$\mathbb{B}[\mathbf{l},\mathbf{m}]$	$\Big(\mathbf{l}^{\otimes 3}-\mathbf{l}\otimes\mathbf{m}^{\otimes 2}-\mathbf{m}\otimes\mathbf{l}\otimes\mathbf{m}-\mathbf{m}^{\otimes 2}\otimes\mathbf{l}\Big)\otimes\Big(\mathbf{m}^{\otimes 3}-\mathbf{m}\otimes\mathbf{l}^{\otimes 2}-\mathbf{l}\otimes\mathbf{m}\otimes\mathbf{l}-\mathbf{l}^{\otimes 2}\otimes\mathbf{m}\Big)$, $\Big(\mathbf{m}^{\otimes 3}-\mathbf{m}\otimes\mathbf{l}^{\otimes 2}-\mathbf{l}\otimes\mathbf{m}\otimes\mathbf{l}-\mathbf{l}^{\otimes 2}\otimes\mathbf{m}\Big)\otimes\Big(\mathbf{l}^{\otimes 3}-\mathbf{l}\otimes\mathbf{m}^{\otimes 2}-\mathbf{m}\otimes\mathbf{l}\otimes\mathbf{m}-\mathbf{m}^{\otimes 2}\otimes\mathbf{l}\Big)$	6
C_{6v}, D_6, D_{6h}	$\mathbb{B}[\mathbf{l},\mathbf{m}]$	$\Big(\mathbf{l}^{\otimes 3}-\mathbf{l}\otimes\mathbf{m}^{\otimes 2}-\mathbf{m}\otimes\mathbf{l}\otimes\mathbf{m}-\mathbf{m}^{\otimes 2}\otimes\mathbf{l}\Big)^{\otimes 2}+\frac{4}{105}\sum_{\text{perm}'}\delta_{ab}\delta_{cd}\delta_{ef}\bigotimes_{\substack{\mu=a,b,c,\\ d,e,f}}\mathbf{e}_\mu-\frac{2}{21}\sum_{\text{perm}''}\delta_{ad}\delta_{be}\delta_{cf}\bigotimes_{\substack{\mu=a,d,b,\\ e,c,f}}\mathbf{e}_\mu$, $\Big(\mathbf{m}^{\otimes 3}-\mathbf{m}\otimes\mathbf{l}^{\otimes 2}-\mathbf{l}\otimes\mathbf{m}\otimes\mathbf{l}-\mathbf{l}^{\otimes 2}\otimes\mathbf{m}\Big)^{\otimes 2}+\frac{4}{105}\sum_{\text{perm}'}\delta_{ab}\delta_{cd}\delta_{ef}\bigotimes_{\substack{\mu=a,b,c,\\ d,e,f}}\mathbf{e}_\mu-\frac{2}{21}\sum_{\text{perm}''}\delta_{ad}\delta_{be}\delta_{cf}\bigotimes_{\substack{\mu=a,d,b,\\ e,c,f}}\mathbf{e}_\mu$	6
C_n, C_{nv}, $C_\infty, C_{\infty v}$	$\mathbb{A}[\mathbf{n}]$	$\mathbf{n}$	1
$C_{\infty h}$	$\mathbb{A}[\mathbf{n}]$	$\sigma\mathbf{n}$	1
S_{2n}, C_{nh}, D_n, D_{nh}, D_{nd}, D_∞, $D_{\infty h}$	$\mathbb{A}[\mathbf{n}]$	$\mathbf{n}\otimes\mathbf{n}-\frac{1}{3}\mathbb{1}$	2
T	$\mathbb{O}[\mathbf{l},\mathbf{m},\mathbf{n}]$	$\sum_{\text{cyc}}\mathbf{l}\otimes\mathbf{m}\otimes\mathbf{n}$	3
T_d	$\mathbb{O}[\mathbf{l},\mathbf{m},\mathbf{n}]$	$\sum_{\text{cyc}}\Big(\mathbf{l}\otimes\mathbf{m}+\mathbf{m}\otimes\mathbf{l}\Big)\otimes\mathbf{n}$	3
T_h	$\mathbb{O}[\mathbf{l},\mathbf{m},\mathbf{n}]$	$\mathbf{m}^{\otimes 2}\otimes\mathbf{l}^{\otimes 2}+\mathbf{l}^{\otimes 2}\otimes\mathbf{n}^{\otimes 2}+\mathbf{n}^{\otimes 2}\otimes\mathbf{m}^{\otimes 2}-\frac{2}{5}\delta_{ab}\delta_{cd}\bigotimes_{\mu=a,b,c,d}\mathbf{e}_\mu+\frac{1}{10}\Big(\delta_{ac}\delta_{bd}\bigotimes_{\mu=a,c,b,d}\mathbf{e}_\mu+\delta_{ad}\delta_{bc}\bigotimes_{\mu=a,d,b,c}\mathbf{e}_\mu\Big)$	4
O, O_h	$\mathbb{O}[\mathbf{l},\mathbf{m},\mathbf{n}]$	$\mathbf{l}^{\otimes 4}+\mathbf{m}^{\otimes 4}+\mathbf{n}^{\otimes 4}-\frac{1}{5}\sum_{\text{perm}}\delta_{ab}\delta_{cd}\bigotimes_{\mu=a,b,c,d}\mathbf{e}_\mu$	4
I, I_h	$\mathbb{O}[\mathbf{l},\mathbf{m},\mathbf{n}]$	$\sum_{\text{cyc}}\Big[\mathbf{l}^{\otimes 6}+\sum_{\{+,-\}}\Big(\frac{1}{2}\mathbf{l}\pm\frac{\tau}{2}\mathbf{m}\pm\frac{1}{2\tau}\mathbf{n}\Big)^{\otimes 6}\Big]-\frac{1}{7}\sum_{\text{perm}}\delta_{ab}\delta_{cd}\delta_{ef}\bigotimes_{\substack{\mu=a,b,c,\\ d,e,f}}\mathbf{e}_\mu$	6

4.2.2 Structure of the ordering tensors

Continuous axial groups

The five infinite axial groups $\{C_\infty, C_{\infty v}, C_{\infty h}, D_\infty, D_{\infty h}\}$ require only one tensor to define the associated orientational order. This is because these groups contain a plane perpendicular to the vector $\mathbf{n}$ with continuous $SO(2)$ or $O(2)$ rotations, hence their in-plane structure is trivial and the order parameter effectively reduces to a vector ($C_\infty, C_{\infty v}$), a pseudovector ($C_{\infty h}$) or a director ($D_\infty, D_{\infty h}$), up to an additional chiral order parameter σ for the proper point groups.

Finite axial groups

Finite axial groups $\{C_n, C_{nv}, S_{2n}, C_{nh}, D_n, D_{nh}, D_{nd}\}$ require two ordering tensors $\{\mathbb{A}, \mathbb{B}\}$: $\mathbb{A} = \mathbb{A}[\mathbf{n}]$ describes the orientation of the primary axis, which is always chosen as $\mathbf{n}$ in Table 4.1, and tensors $\mathbb{B} = \mathbb{B}[\mathbf{l}, \mathbf{m}]$ or $\mathbb{B}[\mathbf{l}, \mathbf{m}, \mathbf{n}]$ for the perpendicular in-plane order. This generalizes well-known structure of the order parameters of biaxial (D_{2h}) liquid crystals. Due to symmetry relations which will be discussed later, the primary ordering tensors $\mathbb{A}[\mathbf{n}]$ for $\{C_n, C_{nv},\}$ and $\{S_{2n}, C_{nh}, D_n, D_{nh}, D_{nd}\}$ are identical to the order parameters $\mathbb{O}^{C_{\infty v}}[\mathbf{n}]$ and $\mathbb{O}^{D_{\infty h}}[\mathbf{n}]$, respectively.

Polyhedral groups

The finite symmetry groups $\{T, T_d, T_h, O, O_h, I, I_h\}$ related to the regular tetrahedron, octahedron and icosahedron, respectively, require only one ordering tensor involving the whole triad $\mathbf{n}^\alpha$. These symmetries permute $\{\mathbf{l}, \mathbf{m}, \mathbf{n}\}$ "isotropically" amongst each other, so there is no primary axis and the three axes appear symmetrically in the order parameter tensor.

Proper point groups: chirality

Besides the orientational order parameters, the proper point group symmetries $\{C_n, D_n, T, O, I\}$ are chiral and have an additional chiral order parameter. The simplest chiral order parameter is just the pseudoscalar handedness or chirality σ of the triad defined in Eq. (4.2). By definition, proper point groups do not possess any inversions and reflections and therefore cannot change the chirality or handedness of the triad.

4.2.3 Point groups and ordering tensors

As one may have already noticed from the above discussion and Table 4.1, although a symmetry can be uniquely defined by the collection of order parameter tensors $\mathbb{O}^G$ and the handedness σ, owing to the group structure, many orientational ordering tensors are shared by different symmetries. We will now clarify this by discussing their group structures.

Firstly, the primary ordering tensor $\mathbb{A}^G[\mathbf{n}]$ for C_n and C_{nv} groups is just the order parameter tensor of the C_∞ and $C_{\infty v}$ groups, $\mathbb{A}^{C_n}[\mathbf{n}] = \mathbb{A}^{C_v}[\mathbf{n}] = \mathbb{O}^{C_\infty}[\mathbf{n}] = \mathbb{O}^{C_{\infty v}}[\mathbf{n}]$. This is due to the simple fact that C_n and C_{nv} groups do not transform $\mathbf{n}$, hence they differ from C_∞ and $C_{\infty v}$ only by their in-plane structure related to $\mathbb{B}^G[\mathbf{l},\mathbf{m}]$. Similarly, the groups $\{S_{2n}, C_{nh}, D_n, D_{nh}, D_{nd}\}$ have the same effect on $\mathbf{n}$, $\mathbf{n} \to -\mathbf{n}$. Therefore, neglecting the $\mathbf{l}$ and $\mathbf{m}$ components, these symmetries lead to the same primary ordering tensor $\mathbb{A}[\mathbf{n}] = \mathbb{Q}[\mathbf{n}]$, the uniaxial director.

Moreover, the groups $\{C_n, C_{nh}, C_{nv}, D_n, D_{nh}\}$ are closely related in terms of symmetries. C_n and $C_{nh} = C_n \times \{\mathbb{1}, \sigma_h\}$ only differ by a reflection $\sigma_h : \mathbf{n} \to -\mathbf{n}$ in the horizontal mirror $(\mathbf{l},\mathbf{m})$-plane perpendicular to $\mathbf{n}$. Thus C_n and C_{nh} have the same in-plane structure leading to the same secondary order parameter $\mathbb{B}^{C_n}[\mathbf{l},\mathbf{m}]$. For the point groups $\{C_{nv}, D_n, D_{nh}\}$, we have $D_{nh} = D_n \times \{\mathbb{1}, \sigma_h\}$ and C_{nv} and D_n can be represented as semi-direct products $C_{nv} = C_n \rtimes \{\mathbb{1}, \sigma_v\}$ and $D_n = C_n \rtimes \{\mathbb{1}, c_2(\mathbf{l})\}$, where σ_v is a reflection ($\mathbf{l}$,$\mathbf{n}$)-plane and $c_2(\mathbf{l})$ is a two-fold rotation around the axis $\mathbf{l}$,

$$\sigma_v = \sigma_{\mathbf{ln}} = \begin{pmatrix} 1 & 0 & 0 \\ 0 & -1 & 0 \\ 0 & 0 & 1 \end{pmatrix}, \quad c_2(\mathbf{l}) = \begin{pmatrix} 1 & 0 & 0 \\ 0 & -1 & 0 \\ 0 & 0 & -1 \end{pmatrix}. \tag{4.8}$$

It is immediately clear that, σ_v and $c_2(\mathbf{l})$ have the same action on the $\mathbf{l}$ and $\mathbf{m}$ components. Therefore, $\{C_{nv}, D_n, D_{nh}\}$ also have the same in-plane order parameter $\mathbb{B}[\mathbf{l},\mathbf{m}]$.

The common structures of the finite axial groups have a direct implication on the associated phase transitions. For a phase with the symmetry of a finite axial group, it is in principle possible to disorder the primary and secondary order separately before the transition to the isotropic phase. If we first disorder the secondary order in a plane, the following sequences

of phase transitions can happen

$$\begin{aligned} &C_n, C_{nv} \to C_{\infty v} \to O(3), \\ &S_{2n}, C_{nh}, D_n, D_{nh}, D_{nd} \to D_{\infty h} \to O(3), \end{aligned} \tag{4.9}$$

related to the restoration of the in-plane $O(2)$ symmetry followed by disordering of order along the principal axis $\mathbf{n}$. These transitions generalize the biaxial-uniaxial-isotropic liquid transition of biaxial liquid crystals [72, 71]. We have numerically verified the transition sequences in Eq. (4.9) for a large number of symmetries and will present the detailed analyses for their phase diagrams in the next chapter.

Finally, in the case of the polyhedral groups, $T_h = T \times \{\mathbb{1}, -\mathbb{1}\}$, $O_h = O \times \{\mathbb{1}, -\mathbb{1}\}$ and $I_h = I \times \{\mathbb{1}, -\mathbb{1}\}$ are generated from the proper subgroups T, O and I by adding the inversion $-\mathbb{1}$. Since the ordering tensors of I and O in Table 4.1 are of even rank, this difference is not reflected directly in the orientational order parameters. There exist higher order invariant tensors that can distinguish O (I) from O_h (I_h), nonetheless one needs to consider at least a rank-5 (rank-7) tensors and it is therefore more convenient to distinguish them by the chirality σ (see Section 4.3.3 for more details).

Improper groups possessing only reflections but not the inversions $-\mathbb{1}$, including all axial groups C_{nv} for all n, $\{S_{2n}, C_{nh}, D_{nh}\}$ for odd n, D_{nd} for even n and the regular tetrahedral group T_d, have non-vanishing odd-rank order parameters in general. In these order parameters, terms related with right and left handed triads appear equally, making the order parameter invariant under certain improper reflections but not inversions. This will be reflected in the structure of the associated order parameters. For instance, as can be seen from Table 4.1, the order parameter for the tetrahedral-T_d group, $\mathbb{O}^{T_d}$ consists of a left and right handed copy of that of the tetrahedral-T group (see Section 4.3.3 for more details).

4.2.4 Determining the symmetry of a phase and phase transitions with ordering tensors

The ordering tensors we show in Table 4.1 generalize the local director tensor $\mathbb{Q}_{ab}$ for uniaxial nematics. The macroscopic order parameters are defined as coarse grained averages over the system

$$\langle \mathbb{O}^G \rangle = \frac{1}{V} \sum_i \langle \mathbb{O}_i^G \rangle, \tag{4.10}$$

where V denotes the spatial averaging volume. To verify the symmetry of a phase, one need in principle consider all independent entries of the order parameter tensor. This is in general quite involved since the number of the entries grows exponentially with the rank of the tensor.

However, for interactions favoring homogeneous a nematic order, such as the interaction in the gauge model Eq. (4.5), the symmetry of the phase can be revealed by the scalar two point functions in the limit of large separation. Since $\langle \mathbb{O}_i^G \rangle$ will develop a finite value in the ordered phase, at long distances the scalar two point function of the order parameter tensor behaves as

$$\begin{aligned} &\lim_{|i-j|\to\infty} \langle (\mathbb{O}_i^G)_{abc\ldots} (\mathbb{O}_j^G)_{abc\ldots} \rangle \\ &= \begin{cases} \text{Tr } \langle \mathbb{O}_i^G \rangle^2 > 0 & \text{nematic} \\ 0 & \text{otherwise.} \end{cases} \end{aligned} \tag{4.11}$$

The contractions in Tr $(\bullet)$ are determined up to the tensor symmetries of the order parameter. This allows us to define a strength for the ordering tensors,

$$q = \sqrt{\langle (\mathbb{O}_i^G)_{abc\ldots} \rangle^2}, \tag{4.12}$$

and the symmetry of the phase can be defined by the lowest order tensor and "smallest" group G with $q \neq 0$. Accordingly, a phase transition associated with $\langle \mathbb{O}_i^G \rangle$ can be identified from the susceptibility $\chi(q)$ of the ordering strength,

$$\chi(q) = \beta V \Big(\langle q^2 \rangle - \langle q \rangle^2 \Big). \tag{4.13}$$

We have numerically computed q and $\chi(q)$ in the model Eq. (4.5) for large number of point group symmetries [23]. Our simulations showed that $\chi(q)$ will exhibit a clear peak at the temperature where the heat capacity peaks, indicating that q in combination of simple symmetry arguments is indeed sufficient to determine the symmetry of a nematic phase with homogeneous distribution of order parameters.

However, we note that, when non-homogeneous distributions of order parameters are preferred, the symmetry of a state can be compatible but not identical to G, as also discussed, e.g., in Ref. [92]. In these cases, a non-zero q is not sufficient to identify the symmetry of the state, and one in principle need consider all components of $\langle \mathbb{O}_i^G \rangle$. However, the symmetry of

a phase may be also determined by the "eigenvalues" and the distribution of non-zero entries of $\langle \mathbb{O}_i^G \rangle$ [133]. Studies with this regard so far mostly concentrate on the rank-2 $D_{\infty h}$ and D_{2h} ordering tensors [134–136, 120]; it would be interesting to consider the ordering of the tensors in Table 4.1 in full generality without assumptions on microscopic configurations of a particular model.

4.3 Examples and discussion

In this section we will discuss some concrete examples of deriving the order parameter tensors in Table 4.1. For all finite and discrete point groups, we can integrate over the gauge fields in the expansion Eq. (4.7). For the continuous axial groups, we can do the integrations in closed form. The results are by construction composed of local contractions of the simplest gauge invariant tensors allowed by the symmetries, i.e. the tensors in Table 4.1.

4.3.1 Continuous axial groups: unixial nematics

The integration over the gauge groups $\{C_\infty, C_{\infty v}, C_{\infty h}, D_\infty, D_{\infty h}\}$ will lead to the familiar results. We will use the D_∞-uniaxial nematic as an example of the general procedure of deriving uniaxial nematic order parameters, the others being similar. The key point is the elimination of the triad vectors $\mathbf{l}, \mathbf{m}$ in the plane where the $SO(2)$-symmetry acts from the Hamiltonian upon integrating out the $SO(2)$-gauge fields, since there can be no gauge invariant combinations of these components in any finite order.

The gauge fields $U_{ij} \in D_\infty$ can be generated by the transformations $\{c_\theta(\mathbf{n}), c_2(\mathbf{m})\}$, where

$$c_\theta(\mathbf{n}) = \begin{pmatrix} \cos\theta & -\sin\theta & 0 \\ \sin\theta & \cos\theta & 0 \\ 0 & 0 & 1 \end{pmatrix}, c_2(\mathbf{m}) = \begin{pmatrix} -1 & 0 & 0 \\ 0 & 1 & 0 \\ 0 & 0 & -1 \end{pmatrix} \tag{4.14}$$

are a rotation about $\mathbf{n}$ by an angle $\theta \in [0, 2\pi)$ and a π-rotation about $\mathbf{m}$, respectively. We note that the "usual" uniaxial symmetry is given by $D_{\infty h} = D_\infty \times \{\mathbb{1}, -\mathbb{1}\}$ and follows with minimal modifications. We focus on the terms in the $(\mathbf{l}, \mathbf{m})$-plane and parametrize the gauge transformation

as

$$U_{ij} = \begin{pmatrix} \sigma_{11}\cos\theta_{ij} & \sigma_{12}\sin\theta_{ij} & \\ -\sigma_{21}\sin\theta_{ij} & \sigma_{22}\cos\theta_{ij} & \\ & & \sigma_{33} \end{pmatrix} \in D_\infty, \tag{4.15}$$

where $\theta_{ij} \in [0, 2\pi)$ parametrizes the C_∞ rotation and the constrained signs $\sigma_{\alpha\beta} = \pm 1$ are determined by the presence of the π-rotation in the orthogonal $(\mathbf{l}, \mathbf{n})$-plane. This gives from Eq. (4.5), with $\mathbb{J} = J\mathbb{1}$,

$$\begin{aligned} &H[\mathbf{l}, \mathbf{m}, \mathbf{n}, \theta, \sigma_{\alpha\beta}] \\ &= \sum_{\langle ij \rangle} \Big[\cos\theta_{ij} \Big(\sigma_{11} \mathbf{l}_i \cdot \mathbf{l}_j + \sigma_{22} \mathbf{m}_i \cdot \mathbf{m}_j \Big) \\ &\quad + \sin\theta_{ij} \Big(\sigma_{12} \mathbf{l}_i \cdot \mathbf{m}_j - \sigma_{21} \mathbf{m}_i \cdot \mathbf{l}_j \Big) + \mathbf{n}_i U_{ij,33} \cdot \mathbf{n}_j \Big]. \end{aligned} \tag{4.16}$$

Now we proceed to integrate over the $SO(2)$ angle θ_{ij}

$$\begin{aligned} &e^{-\beta H_{\text{eff}}[\mathbf{l}_i, \mathbf{l}_j, \mathbf{m}_i, \mathbf{m}_j, \sigma_{\alpha\beta}]} \\ &= \prod_{\langle ij \rangle} \frac{1}{2\pi} \int_0^{2\pi} \mathrm{d}\theta_{ij} \; e^{-H[\mathbf{l}_i, \mathbf{l}_j, \mathbf{m}_i, \mathbf{m}_j, \theta_{ij}, \sigma_{\alpha\beta}]} \\ &= \prod_{\langle ij \rangle} I_0(J_1 \sqrt{A_{ij}^2 + B_{ij}^2}). \end{aligned} \tag{4.17}$$

where $I_0(z)$ is a Bessel function of the first kind with the argument

$$\begin{aligned} &A_{ij}^2 + B_{ij}^2 \\ &= \Big[\sigma_{11} \mathbf{l}(i) \cdot \mathbf{l}(j) + \sigma_{22} \mathbf{m}(i) \cdot \mathbf{m}(j) \Big]^2 + \Big[\sigma_{12} \mathbf{l}(i) \cdot \mathbf{m}(j) - \sigma_{21} \mathbf{m}(i) \cdot \mathbf{l}(j) \Big]^2 \\ &= (\mathbf{l}_i \cdot \mathbf{l}_j)^2 + (\mathbf{m}_i \cdot \mathbf{m}_j)^2 + (\mathbf{m}_i \cdot \mathbf{l}_j)^2 + (\mathbf{l}_i \cdot \mathbf{m}_j)^2 \\ &\qquad + 2\sigma_{11}\sigma_{22} (\mathbf{m}_i \cdot \mathbf{m}_j)(\mathbf{l}_i \cdot \mathbf{l}_j) - 2\sigma_{12}\sigma_{21} (\mathbf{l}_i \cdot \mathbf{m}_j)(\mathbf{m}_i \cdot \mathbf{l}_j). \end{aligned} \tag{4.18}$$

Now, since $\det_{2\times 2} U_{ij} = \sigma_{11}\sigma_{22}\cos^2\theta_{ij} + \sigma_{12}\sigma_{21}\sin^2\theta_{ij} = \pm 1 = \det U_{ij} \times$

$U_{33,ij}$, we can simplify

$$\begin{aligned}
&A_{ij}^2 + B_{ij}^2 \\
&= (\mathbf{l}_i \cdot \mathbf{l}_j)^2 + (\mathbf{m}_i \cdot \mathbf{m}_j)^2 + (\mathbf{m}_i \cdot \mathbf{l}_j)^2 + (\mathbf{l}_i \cdot \mathbf{m}_j)^2 \\
&\quad + 2 \det_{2\times 2} U_{ij} \Big[(\mathbf{m}_i \cdot \mathbf{m}_j)(\mathbf{l}_i \cdot \mathbf{l}_j) - (\mathbf{l}_i \cdot \mathbf{m}_j)(\mathbf{m}_i \cdot \mathbf{l}_j) \Big] \\
&= 1 + (\mathbf{n}_i \cdot \mathbf{n}_j)^2 + 2 \det_{2\times 2} U_{ij} \sigma_i \sigma_j \mathbf{n}_i \cdot \mathbf{n}_j \\
&= (\sigma_i \sigma_j \mathbf{n}_i \cdot \mathbf{n}_j + \det_{2\times 2} U_{ij})^2,
\end{aligned} \tag{4.19}$$

where on the second-to-last line we used the $O(3)$ relation $\mathbf{l}_i \times \mathbf{m}_i = \sigma_i \mathbf{n}_i$. Using $\det_{2\times 2} U_{ij} = U_{ij,33}$ gives the result

$$H_{\text{eff}}[\mathbf{n}_i, U_{ij}] = -\sum_{\langle ij \rangle} \beta \mathbf{n}_i \cdot U_{ij,33} \mathbf{n}_j + \log I_0 \Big(\beta |\sigma_i \sigma_j \mathbf{n}_i \cdot \mathbf{n}_j + U_{ij,33}| \Big), \tag{4.20}$$

where $U_{ij,33} = \pm 1 \in Z_2$ since for $U_{ij} \in D_\infty / C_\infty \simeq \{\mathbb{1}, c_2(\mathbf{m})\} = Z_2$ when acting on $\mathbf{n}_i$. We recall that

$$I_0(z) = \sum_{k=0}^{\infty} \frac{(z^2/4)^k}{(k!)^2}, \tag{4.21}$$

meaning that to lowest order in β, we generate the term

$$\begin{aligned}
&\delta H_{\text{eff}}[\mathbf{n}_i, U_{ij,33}] \\
&\sim \sum_{\langle ij \rangle} \frac{\beta^2}{4} \Big[1 + 2\sigma_i \sigma_j \mathbf{n}_i \cdot U_{ij,33} \mathbf{n}_j + (\mathbf{n}_i \cdot \mathbf{n}_j)^2 \Big] + O(\beta^4) \\
&\sim \sum_{\langle ij \rangle} \frac{\beta^2}{2} \widetilde{\mathbf{n}}_i U_{ij,33} \cdot \widetilde{\mathbf{n}}_j + \text{higher orders},
\end{aligned} \tag{4.22}$$

in addition to the original Hamiltonian in terms of $\mathbf{n}_i$. By integrating out $U_{ij,33} \in Z_2$ one will find that all odd powers of $\mathbf{n}_i \cdot \mathbf{n}_j$ vanish and the first non-trivial term is second order with D_∞-invariant scalar contractions

$$(\tilde{\mathbf{n}}_i \cdot \tilde{\mathbf{n}}_j)^2 = (\mathbf{n}_i \cdot \mathbf{n}_j)^2 = \text{Tr}[\mathbb{Q}_i \cdot \mathbb{Q}_j] + const., \tag{4.23}$$

due to the fact that a pseudovector and a vector are indistinguishable for even powers. At the same time, this is the minimal $D_{\infty h}$-invariant tensor

contraction $\mathrm{Tr}[\mathbb{Q}_i \cdot \mathbb{Q}_j]$. Higher order terms in Eq. (4.7) are high order even functions such as $[(\mathbf{n}_i \cdot \mathbf{n}_j)^2]^2$, $[(\mathbf{n}_i \cdot \mathbf{n}_j)^2]^3$ etc. that can be neglected as irrelevant. Note however, that the full expansion Eq. (4.7) for D_∞ contains odd powers of β with terms of the form $\beta^3 \sigma_i \sigma_j [(\mathbf{n}_i \cdot \mathbf{n}_j)^2 + \cdots]$ that feature the chiral order parameter σ_i. These chiral terms vanish identically for the case $D_{\infty h}$ when summing over the gauge fields $U_{ij} = \{\mathbb{1}, -\mathbb{1}\}$ in $D_{\infty h} = D_\infty \times \{\mathbb{1}, -\mathbb{1}\}$.

4.3.2 Biaxial nematics

The D_∞- and $D_{\infty h}$-uniaxial nematics we just discussed are a well-known and relatively simple case in the generalized nematic family. Since the symmetries $\{C_\infty, C_{\infty v}, C_{\infty h}, D_\infty, D_{\infty h}\}$ all contain a $SO(2)$ part in the plane perpendicular to the $\mathbf{n}$, the vectors $\mathbf{l}$ and $\mathbf{m}$ disappear from the order parameter, as we saw above. For the symmetries $\{C_n, C_{nv}, C_{nh}, S_{2n}, D_n, D_{nh}, D_{nd}\}$ with finite n, however, there will be in-plane rotational symmetry breaking and we need a secondary "biaxial" order parameter $\mathbb{B}[\mathbf{l}, \mathbf{m}]$ or $\mathbb{B}[\mathbf{l}, \mathbf{m}, \mathbf{n}]$ to capture these phase transitions.

D_{2h}-biaxial order parameter

As can be seen from Table 4.1, for some axial nematics, there exist more than one biaxial order parameters $\mathbb{B}$. A familiar example is the biaxial D_{2h}-nematic, where we have the order parameters $\{\mathbb{B}_1^{D_{2h}}, \mathbb{B}_2^{D_{2h}}\}$,

$$\mathbb{B}_1^{D_{2h}} = \mathbf{l} \otimes \mathbf{l} - \frac{\mathbb{1}}{3}, \tag{4.24a}$$

$$\mathbb{B}_2^{D_{2h}} = \mathbf{m} \otimes \mathbf{m} - \frac{\mathbb{1}}{3} \tag{4.24b}$$

which are both clearly invariant under D_2 generated by $\{c_2(\mathbf{n}), c_2(\mathbf{l})\}$ and as well as the inversion $-\mathbb{1}$. Correspondingly, when integrating over $U_{ij} \in D_{2h}$ in the expansion Eq. (4.7), in the first non-trivial order one will obtain the scalar contractions

$$\begin{aligned} &\sim (l_a l_b)_i (l_a l_b)_j + (m_a m_b)_i (m_a m_b)_j + (n_a n_b)_i (n_a n_b)_j \\ &= \mathrm{Tr}[\mathbb{Q} \cdot \mathbb{Q}] + \mathrm{Tr}[\mathbb{B}_1^{D_{2h}} \cdot \mathbb{B}_1^{D_{2h}}] + \mathrm{Tr}[\mathbb{B}_2^{D_{2h}} \cdot \mathbb{B}_2^{D_{2h}}] + const., \end{aligned} \tag{4.25}$$

which cannot be written as a contraction a single local quantity like in Eq. (4.23). However, due to the $O(3)$-constraint,

$$\mathbf{l} \otimes \mathbf{l} + \mathbf{m} \otimes \mathbf{m} + \mathbf{n} \otimes \mathbf{n} = \mathbb{1}, \tag{4.26}$$

the commonly used D_{2h} biaxial order parameter tensor $\mathbb{B} = \mathbf{l}\otimes\mathbf{l} - \mathbf{m}\otimes\mathbf{m}$ is just a linear combination of $\{\mathbb{B}_1^{D_{2h}}, \mathbb{B}_2^{D_{2h}}\}$ and Eq. (4.25) reduces to contractions of the two independent rank-2 tensors.

Generalized biaxial order parameters

To show how more complicated order parameters are derived using the gauge theory, we next discuss the derivation of the secondary in-plane order parameters $\mathbb{B}^G$ of higher rank using the the order parameters of D_{2d}, D_{4h} and C_{6h} symmetries as examples.

We take D_{2d} symmetry as an example of a nematic with a third-rank order parameter. The D_{2d} group is generated by $\{c_2(\mathbf{n}), c_2(\mathbf{m}), \sigma_d\}$, where

$$c_2(\mathbf{n}) = \begin{pmatrix} -1 & 0 & 0 \\ 0 & -1 & 0 \\ 0 & 0 & 1 \end{pmatrix}, \sigma_d = \begin{pmatrix} 0 & 1 & 0 \\ 1 & 0 & 0 \\ 0 & 0 & 1 \end{pmatrix} \tag{4.27}$$

are a 2-fold rotation about $\mathbf{n}$ and a reflection about the $(\mathbf{l}+\mathbf{m}, \mathbf{n})$ plane and $c_2(\mathbf{m})$ is as that in Eq. (4.14).

These lead to a 4-fold symmetry in the $(\mathbf{l}, \mathbf{m})$-plane. To obtain the order parameter describing this symmetry breaking, we follow the same procedure discussed in the previous section, but now the gauge fields U_{ij} in Eq. (4.7) are elements of D_{2d}. Integrating over $U_{ij} \in D_{2d}$, one will find that the first non-trivial order is the second order with a term $(\mathbf{n}_i \cdot \mathbf{n}_j)^2$, which indicates as expected that $\mathbb{Q}[\mathbf{n}]$ is as well an order parameter for D_{2d} nematics. The 4-fold rotational symmetry combined with the reflections starts showing up at the third order in Eq. (4.7), where one finds the following contractions up to a constant factor

$$\begin{aligned} &\sim \sigma_i\sigma_j\Big[(\tilde{\mathbf{l}}_i \cdot \tilde{\mathbf{m}}_j)(\tilde{\mathbf{m}}_i \cdot \tilde{\mathbf{l}}_j) + (\tilde{\mathbf{l}}_i \cdot \tilde{\mathbf{l}}_j)(\tilde{\mathbf{m}}_i \cdot \tilde{\mathbf{m}}_j)\Big](\tilde{\mathbf{n}}_i \cdot \tilde{\mathbf{n}}_j) \\ &= [(l_a m_b + m_a l_b)n_c]_i[(l_a m_b + m_a l_b)n_c]_j \\ &= \mathrm{Tr}\left[\Big[(\mathbf{l}\otimes\mathbf{m} + \mathbf{m}\otimes\mathbf{l})\otimes\mathbf{n}\Big]_i \cdot \Big[(\mathbf{l}\otimes\mathbf{m} + \mathbf{m}\otimes\mathbf{l})\otimes\mathbf{n}\Big]_j\right], \end{aligned} \tag{4.28}$$

where the third-rank contraction $\mathrm{Tr}(\bullet_{abc} \cdot \bullet_{abc})$ is determined up to the symmetries of the order parameter tensor (symmetric in the first two indices). By construction, the local quantity appeared in Eq. (4.28) is D_{2d} invariant, hence can be used to define a D_{2d}-biaxial order parameter,

$$\mathbb{B}^{D_{2d}} = (\mathbf{l}\otimes\mathbf{m} + \mathbf{m}\otimes\mathbf{l})\otimes\mathbf{n}. \tag{4.29}$$

The full order parameter of a D_{2d} nematic is therefore given by

$$\mathbb{O}^{D_{2d}}[\mathbf{l},\mathbf{m},\mathbf{n}] = \{\mathbb{A}^{D_{\infty h}}[\mathbf{n}], \mathbb{B}^{D_{2d}}[\mathbf{l},\mathbf{m},\mathbf{n}]\}. \tag{4.30}$$

Continuing to D_{4h} symmetry, after integrating out the gauge fields for D_{4h}, at the fourth order one will find the following contractions up to constant factors and terms solely depending on the axial axis $\mathbf{n}$,

$$\begin{aligned}\sim \mathrm{Tr}\Big[&(\mathbf{l}_i^{\otimes 4} + \mathbf{m}_i^{\otimes 4}) \cdot (\mathbf{l}_j^{\otimes 4} + \mathbf{m}_j^{\otimes 4}) + 3(\mathbf{l}_i^{\otimes 2} \otimes \mathbf{m}_i^{\otimes 2} \\ &+ \mathbf{m}_i^{\otimes 2} \otimes \mathbf{l}_i^{\otimes 2}) \cdot (\mathbf{l}_j^{\otimes 2} \otimes \mathbf{m}_j^{\otimes 2} + \mathbf{m}_j^{\otimes 2} \otimes \mathbf{l}_j^{\otimes 2})\Big].\end{aligned} \tag{4.31}$$

One can therefore recognize two D_{4h}-invariant local tensors,

$$\begin{aligned}\mathbb{B}_1^{D_{4h}} = {}& \mathbf{l}^{\otimes 2} \otimes \mathbf{m}^{\otimes 2} + \mathbf{m}^{\otimes 2} \otimes \mathbf{l}^{\otimes 2} - \frac{4}{15}\delta_{ab}\delta_{cd} \bigotimes_{\mu=a,b,c,d} \mathbf{e}_\mu \\ &+ \frac{1}{15}\Big(\delta_{ac}\delta_{bd} \bigotimes_{\mu=a,c,b,d} \mathbf{e}_\mu + \delta_{ad}\delta_{bc} \bigotimes_{\mu=a,d,b,c} \mathbf{e}_\mu\Big),\end{aligned} \tag{4.32}$$

$$\mathbb{B}_2^{D_{4h}} = \mathbf{l}^{\otimes 4} + \mathbf{m}^{\otimes 4} - \frac{2}{15}\sum_{\mathrm{perm}} \delta_{ab}\delta_{cd} \bigotimes_{\mu=a,b,c,d} \mathbf{e}_\mu, \tag{4.33}$$

where we have subtracted the isotropic trace-part for convenience ("perm" denotes the summation over all non-equivalent pairings of the indices of the Kronecker delta functions).

However, these two tensors are not independent. Due the $O(3)$ relations Eq. (4.26), they satisfy

$$\mathbb{B}_1^{D_{4h}} + \mathbb{B}_2^{D_{4h}} = (\mathbf{l}^{\otimes 2} + \mathbf{m}^{\otimes 2})^{\otimes 2} = (\mathbb{1} - \mathbf{n}^{\otimes 2})^{\otimes 2}. \tag{4.34}$$

This in turn means that both $\mathbb{B}_1^{D_{4h}}$ and $\mathbb{B}_2^{D_{4h}}$ have dependence on the axial axis $\mathbf{n}$. Therefore, similarly to the D_{2h} case, it is more convenient to use the linear combination $\mathbb{B}_1^{D_{4h}} - \mathbb{B}_2^{D_{4h}}$ to characterize a D_{4h} order.

In case of C_{6h} symmetry, the biaxial order parameters are rank-6 tensor and defined by the local contractions

$$\sim \mathrm{Tr}\Big[\mathbb{B}_{1,i}^{D_{6h}} \cdot \mathbb{B}_{1,j}^{D_{6h}} + \mathbb{B}_{2,i}^{D_{6h}} \cdot \mathbb{B}_{2,j}^{D_{6h}} + \mathbb{B}_{1,i}^{C_{6h}} \cdot \mathbb{B}_{1,j}^{C_{6h}} + \mathbb{B}_{2,i}^{C_{6h}} \cdot \mathbb{B}_{2,j}^{C_{6h}}\Big], \tag{4.35}$$

up to constant factors and terms depending on the axial axis $\mathbf{n}$, where the explicit form of these tensors are given in Table 4.1. The D_{6h} order parameters appear here since $D_{6h}/C_{6h} \simeq \{\mathbb{1}, c_2(\mathbf{l})\}$ is a multiplicative

group of order two acting trivially at even powers, leading to redundancy at even orders of the expansion Eq. (4.7). The same phenomenon of course occurs for the C_6 quotients of $\{C_{6v}, D_6, D_{6h}\}$, etc., and the sixth order expansions coincide for the groups with identical order parameters.

Again due to the $O(3)$ relation Eq. (4.26) and Eq. (4.2), these order parameters are not independent. $\mathbb{B}_1^{D_{6h}} + \mathbb{B}_2^{D_{6h}} = (\mathbf{l}^{\otimes 2} + \mathbf{m}^{\otimes 2})^{\otimes 3} = (\mathbb{1} - \mathbf{n}^{\otimes 2})^{\otimes 3}$ depends solely on $\mathbf{n}$, and $\mathbb{B}_1^{C_{6h}} - \mathbb{B}_2^{C_{6h}}$ can be expressed as a function of the pseudovector $\widetilde{\mathbf{n}}$. As a consequence, the linear combination $\mathbb{B}_1^{D_{6h}} - \mathbb{B}_2^{D_{6h}}$ and $\mathbb{B}_1^{C_{6h}} + \mathbb{B}_2^{C_{6h}}$ are the appropriate in-plane order parameters for these symmetries.

The above procedure of deriving the biaxial order parameter is valid for all axial nematics with finite n-fold rotational symmetries. Naturally, the rank of the biaxial order parameter tensor increases with n and becomes infinite when $n \to \infty$. This reflects the fact that a biaxial order parameter does not exist for phases with an in-plane $SO(2)$ symmetry, $\{C_\infty, C_{\infty v}, C_{\infty h}, D_\infty, D_{\infty h}\}$.

4.3.3 Polyhedral nematics

Let us finally discuss the order parameters for the polyhedral groups.

Tetrahedral symmetries T, T_d and T_h

The proper tetrahedral group T can be generated by a two-fold rotation $c_2(\mathbf{n})$, as that in Eq. (4.27), and a three-fold rotation acting as a cyclic permutation of $\{\mathbf{l}, \mathbf{m}, \mathbf{n}\}$ given by

$$c_3(\mathbf{l} + \mathbf{m} + \mathbf{n}) = \begin{pmatrix} 0 & 1 & 0 \\ 0 & 0 & 1 \\ 1 & 0 & 0 \end{pmatrix}. \tag{4.36}$$

These result in 12 proper rotations that leave a tetrahedron embedded in a cube with normals $\mathbf{l}, \mathbf{m}, \mathbf{n}$ invariant. After summing over gauge fields $U_{ij} \in T$ in the expansion Eq. (4.7), one finds in the third order the following local contractions,

$$\begin{aligned} &\sim \sigma_i \sigma_j \mathrm{Tr}\Big[\Big(\tilde{\mathbf{l}} \otimes \tilde{\mathbf{m}} \otimes \tilde{\mathbf{n}}\Big)_i \cdot \Big(\sum_{\mathrm{cyc}} \tilde{\mathbf{l}} \otimes \tilde{\mathbf{m}} \otimes \tilde{\mathbf{n}}\Big)_j\Big] \\ &= \frac{1}{3}\mathrm{Tr}\Big[\Big(\sum_{\mathrm{cyc}} \mathbf{l} \otimes \mathbf{m} \otimes \mathbf{n}\Big)_i \cdot \Big(\sum_{\mathrm{cyc}} \mathbf{l} \otimes \mathbf{m} \otimes \mathbf{n}\Big)_j\Big], \end{aligned} \tag{4.37}$$

where $\sum_{\rm cyc}$ runs over cyclic permutations of $\{\mathbf{l},\mathbf{m},\mathbf{n}\}$. Hence we can define the T-invariant local tensor,

$$\mathbb{O}^T = \mathbb{O}_1^T = \sum_{\rm cyc} \mathbf{l}\otimes\mathbf{m}\otimes\mathbf{n}. \tag{4.38}$$

$\mathbb{O}^T$ in Eq. (4.38) contains only cyclic permutations of the three local axes and carries a chirality, as there are no improper operations in the T group. By interchanging two of these axes corresponding to a reflection, we obtain an equivalent T-invariant tensor but with different handedness,

$$\mathbb{O}_2^T = \sum_{\rm cyc} \mathbf{m}\otimes\mathbf{l}\otimes\mathbf{n}. \tag{4.39}$$

One realizes that a linear combination of $\mathbb{O}_1^T$ and $\mathbb{O}_2^T$ will give an ordering tensor that is invariant under the symmetry group of a regular tetrahedron, T_d. Indeed, integrating out the gauge fields for the T_d group, where $T_d = T \rtimes \{\mathbb{1}, \sigma_d\}$ and σ_d defined in Eq. (4.27) generating the odd permutation, one will find in the third order of Eq. (4.7)

$$\begin{aligned}
&\sim \sigma_i\sigma_j \mathrm{Tr}\left[\left(\tilde{\mathbf{l}}\otimes\tilde{\mathbf{m}}\otimes\tilde{\mathbf{n}}\right)_i \cdot \Big[\sum_{\rm cyc}(\tilde{\mathbf{l}}\otimes\tilde{\mathbf{m}}+\tilde{\mathbf{m}}\otimes\tilde{\mathbf{l}})\otimes\tilde{\mathbf{n}}\Big]_j\right] \\
&= \frac{1}{6}\mathrm{Tr}\left[\Big[\sum_{\rm cyc}(\mathbf{l}\otimes\mathbf{m}+\mathbf{m}\otimes\mathbf{l})\otimes\mathbf{n}\Big]_i \cdot \Big[\sum_{\rm cyc}(\mathbf{l}\otimes\mathbf{m}+\mathbf{m}\otimes\mathbf{l})\otimes\mathbf{n}\Big]_j\right]
\end{aligned} \tag{4.40}$$

giving precisely the order parameter tensor

$$\mathbb{O}^{T_d} = \sum_{\rm cyc}(\mathbf{l}\otimes\mathbf{m}+\mathbf{m}\otimes\mathbf{l})\otimes\mathbf{n} \tag{4.41}$$

as expected.

There is yet another point group belonging to the tetrahedral group family, the group T_h. Interestingly, due to $T_h = T\times\{\mathbb{1},-\mathbb{1}\}$, all odd orders in the expansion Eq. (4.7) vanish and the first non-trivial terms appear in the fourth order with the contractions,

$$\begin{aligned}
\sim&\mathrm{Tr}\Big[\left(\mathbf{l}^{\otimes4}+\mathbf{m}^{\otimes4}+\mathbf{n}^{\otimes4}\right)_i\cdot\left(\mathbf{l}^{\otimes4}+\mathbf{m}^{\otimes4}+\mathbf{n}^{\otimes4}\right)_j\Big] \\
&+\mathrm{Tr}\Big[\left(\mathbf{l}^{\otimes2}\otimes\mathbf{m}^{\otimes2}+\mathbf{m}^{\otimes2}\otimes\mathbf{n}^{\otimes2}+\mathbf{n}^{\otimes2}\otimes\mathbf{l}^{\otimes2}\right)_i \\
&\cdot\left(\mathbf{l}^{\otimes2}\otimes\mathbf{m}^{\otimes2}+\mathbf{m}^{\otimes2}\otimes\mathbf{n}^{\otimes2}+\mathbf{n}^{\otimes2}\otimes\mathbf{l}^{\otimes2}\right)_j\Big].
\end{aligned} \tag{4.42}$$

The second term in the above expression gives the T_h invariant order parameter tensor

$$\begin{aligned}\mathbb{O}^{T_h} &= \mathbb{O}_1^{T_h} \\ &= \mathbf{l}^{\otimes 2}\otimes\mathbf{m}^{\otimes 2}+\mathbf{m}^{\otimes 2}\otimes\mathbf{n}^{\otimes 2}+\mathbf{n}^{\otimes 2}\otimes\mathbf{l}^{\otimes 2}-\frac{2}{5}\delta_{ab}\delta_{cd}\bigotimes_{\mu=a,b,c,d}\mathbf{e}_\mu \\ &\quad+\frac{1}{10}\Big(\delta_{ac}\delta_{bd}\bigotimes_{\mu=a,c,b,d}\mathbf{e}_\mu+\delta_{ad}\delta_{bc}\bigotimes_{\mu=a,d,b,c}\mathbf{e}_\mu\Big),\end{aligned} \tag{4.43}$$

where we have subtracted the trace. The first term in Eq. (4.42) actually coincides with the O_h ordering tensor $\mathbb{O}^{O_h}$. This is because $O_h/T_h \simeq \{\mathbb{1}, -\sigma_d\}$ is a group of order two that leads to some redundant information at even orders in the expansion. $\mathbb{O}^{T_h}$ in Eq. (4.43) is not invariant under interchanging $\mathbf{l}$ and $\mathbf{m}$, which corresponds to the four fold rotation in O_h. Therefore, we can define another T_h-invariant tensor,

$$\begin{aligned}\mathbb{O}_2^{T_h} &= \mathbf{m}^{\otimes 2}\otimes\mathbf{l}^{\otimes 2}+\mathbf{n}^{\otimes 2}\otimes\mathbf{m}^{\otimes 2}+\mathbf{l}^{\otimes 2}\otimes\mathbf{n}^{\otimes 2}-\frac{2}{5}\delta_{ab}\delta_{cd}\bigotimes_{\mu=a,b,c,d}\mathbf{e}_\mu \\ &\quad+\frac{1}{10}\Big(\delta_{ac}\delta_{bd}\bigotimes_{\mu=a,c,b,d}\mathbf{e}_\mu+\delta_{ad}\delta_{bc}\bigotimes_{\mu=a,d,b,c}\mathbf{e}_\mu\Big).\end{aligned} \tag{4.44}$$

Due to the $O(3)$ constraints, however, this and the two terms in Eq. (4.42) are not independent,

$$\begin{aligned}&\mathbb{O}^{O_h}+\mathbb{O}_1^{T_h}+\mathbb{O}_2^{T_h} \\ &=(\mathbf{l}\otimes\mathbf{l}+\mathbf{m}\otimes\mathbf{m}+\mathbf{n}\otimes\mathbf{n})^{\otimes 2}+const. \\ &=\mathbb{1}\otimes\mathbb{1}+const..\end{aligned} \tag{4.45}$$

Therefore, both $\mathbb{O}_1^{T_h}$ and $\mathbb{O}_2^{T_h}$ suffice to describe the T_h orientational order.

Cubic symmetries O and O_h

The O group consists of all 24 proper rotations leaving a cube invariant, and O_h in addition contains inversions, $O_h = O\times\{\mathbb{1}, -\mathbb{1}\}$, and thus in total has 48 elements. A set of generators for O_h is given by $\{c_4(\mathbf{n}), c_3(\mathbf{l}+\mathbf{m}+\mathbf{n}), c_2(\mathbf{m}+\mathbf{n}), -\mathbb{1}\}$, where $c_3(\mathbf{l}+\mathbf{m}+\mathbf{n})$ is defined in Eq. (4.36), and $c_4(\mathbf{n})$ and $c_2(\mathbf{m}+\mathbf{n})$ are given as

$$c_4(\mathbf{n})=\begin{pmatrix}0&-1&0\\1&0&0\\0&0&1\end{pmatrix},\ c_2(\mathbf{m}+\mathbf{n})=\begin{pmatrix}-1&0&0\\0&0&1\\0&1&0\end{pmatrix}. \tag{4.46}$$

Non-zero terms for O_h appear likewise in fourth order of the expansion Eq. (4.7) and now one will obviously find the same contraction as the first term in Eq. (4.42) up to some a constant factor, hence one can define the O_h order parameter tensor as

$$\mathbb{O}^{O_h} = \mathbf{l}^{\otimes 4} + \mathbf{m}^{\otimes 4} + \mathbf{n}^{\otimes 4} - \frac{1}{5} \sum_{\text{perm}} \delta_{ab}\delta_{cd} \bigotimes_{\mu=a,b,c,d} \mathbf{e}_\mu. \tag{4.47}$$

For the proper subgroup O, we have an additional non-trivial third order in the expansion, which is simply $\sim \sigma_i \sigma_j$ giving the chiral order parameter.

Icosahedral symmetries I and I_h

The icosahedral group I consists of all 60 proper rotations that leave a icosahedron invariant and $I_h = I \times \{\mathbb{1}, -\mathbb{1}\}$ contains additionally 60 improper rotations. An icosahedron centered at $(0, 0, 0)$ can be defined by its 12 vertexes at [132]

$$(\pm\frac{1}{2},\ 0,\ \pm\frac{\tau}{2}), (\pm\frac{\tau}{2},\ \pm\frac{1}{2},\ 0), (0,\ \pm\frac{\tau}{2},\ \pm\frac{1}{2}), \tag{4.48}$$

where $\tau = (\sqrt{5}+1)/2$ is the golden ratio. It is invariant under a five fold rotations about its six diagonals. The axis $\mathbf{l} + \tau\mathbf{n}$ is the diagonal passing trough vertices $(-\frac{1}{2}, 0, -\frac{\tau}{2})$ and $(\frac{1}{2}, 0, \frac{\tau}{2})$. A set of generators of I_h is given by $\{c_5(\mathbf{l}+\tau\mathbf{n}), c_3(\mathbf{l}+\mathbf{m}+\mathbf{n}), c_2(\mathbf{n}), -\mathbb{1}\}$, where $c_3(\mathbf{l}+\mathbf{m}+\mathbf{n})$ and $c_2(\mathbf{n})$ are defined in Eq. (4.36) and Eq. (4.27), respectively, $c_5(\mathbf{l}+\tau\mathbf{n})$ is given by

$$c_5(\mathbf{l}+\tau\mathbf{n}) = \begin{pmatrix} 1/2 & -\tau/2 & 1/(2\tau) \\ \tau/2 & 1/(2\tau) & -1/2 \\ 1/(2\tau) & 1/2 & \tau/2 \end{pmatrix}. \tag{4.49}$$

The minimal non-trivial I_h invariant tensor appears in the sixth order in the expansion Eq. (4.7), leading to a rank-6 tensor,

$$\begin{aligned} \mathbb{O}^{I_h} = &\sum_{\text{cyc}} \Big[\mathbf{l}^{\otimes 6} + \sum_{\{+,-\}} \Big(\frac{1}{2}\mathbf{l} \pm \frac{\tau}{2}\mathbf{m} \pm \frac{1}{2\tau}\mathbf{n} \Big)^{\otimes 6} \Big] \\ &- \frac{1}{7} \sum_{\text{perm}} \delta_{ab}\delta_{cd}\delta_{ef} \bigotimes_{\substack{\mu=a,b,c,\\ d,e,f}} \mathbf{e}_\mu. \end{aligned} \tag{4.50}$$

Moreover, similar to the O-nematic case, an I-invariant order parameter consists of an orientational part and a chiral part and is accordingly defined as $\mathbb{O}^I = \{\mathbb{O}^{I_h}, \sigma\}$.

4.4 Concluding remarks

The rotational symmetries of three dimensional isotropic space $O(3)$ can in principle break to any non-trivial point group. According to the Landau-de Gennes paradigm, each symmetry is accompanied by a order parameter and associated phase transitions. These order parameters are high-rank tensors and quite involved in general. In virtue of the gauge theory introduced in previous chapter, we have developed a systematic way of classifying these order parameter tensors and have presented the explicit form of these order parameters for an extensive selection of the physically most relevant symmetries. Although we arrived at these results utilizing a particular gauge theoretical lattice model, the results are of course independent of the gauge theoretical machinery. With these order parameters it is in principle possible to study the nematic phases via Landau-de Gennes theories by considering all symmetry allowed couplings of the order parameters, for example using the approach outlined in Ref. [91]. Given the universality of the applications of the orientational tensor order parameters our work is of general interest for many different fields; in particular we anticipate that our results can provide for a road map for the search of new nematic phases of matter.

Chapter 5

Generalized biaxial phase transitions

"Vestigial" or "mesophases" of matter are a well established part of the canon of spontaneous symmetry breaking. It might well happen that due to thermal [11] (or even quantum [12]) fluctuations a phase is stabilized at intermediate temperatures (or coupling constant at $T = 0$) characterized by a symmetry intermediate between the high temperature isotropic phase and the fully symmetry broken phase at low temperature (small coupling constant). Iconic examples are liquid crystals [11], occurring in between the high temperature liquids and the low temperature crystals, characterized by only the breaking of the rotational symmetry ("nematics"), followed potentially by a partial breaking of translations ("smectic" or "columnar" phases) before full solidification sets in.

In the general sense of phases of matter that break the isotropy of Euclidean three dimensional space, nematic liquid crystals are in principle classified in terms of all subgroups of $O(3)$: the family of three dimensional point groups. There are a total of seven infinite axial families and seven polyhedral groups of such symmetries, exhibiting a very rich subgroup hierarchy. Accordingly, in principle it is allowed by symmetry to realize a very rich hierarchy of rotational vestigial phases, where upon lowering temperature phases in this symmetry hierarchy would be realized one after the other.

In experimental reality this is not encountered. Nearly all of the vast empirical landscape of liquid crystals deals with one particular form of nematic order: the uniaxial nematic characterized by the $D_{\infty h}$ point-group with "rod-like" molecules or mesogens that line up in the nematic phase. Another well established form is the "biaxial nematic" formed from platelets with three inequivalent director axes, characterized by the D_{2h} point group symmetry [72, 74, 67, 70, 69, 98, 99, 71]. D_{2h} is a subgroup of $D_{\infty h}$ and it is well understood that the uniaxial nematic can be

a vestigial mesophase that can occur in between the isotropic and biaxial phase. In order for such vestigial rotational sequences to occur special microscopic conditions are required: dealing with molecule-like mesogenic constituents, special anisotropic interactions have to be present.

We will discuss in this chapter, the symmetry structure and anisotropic interactions that are behind the D_{2h} uniaxial-biaxial phase descendence are actually perfectly compatible with all axial groups. As a consequence, the generalization of the special uniaxial-biaxial type of vestigial symmetry lowering is possible for this vast number of symmetries. Particularly, the gauge theory we introduced in Chapter 3 allows one to incorporate these generalized biaxial transitions in a natural and efficient manner.

5.1 The structure of nematic order parameters and generalized biaxial transitions

Three dimensional generalized nematics break the rotational group $O(3)$ down to a three-dimensional point group. By the Landau-de Gennes symmetry paradigm, phase transitions between any two nematic phases related by the subgroup structure of $O(3)$ are allowed, apart from transitions between the isotropic $O(3)$ phase and a generalized nematic phase. In this section, we will show that the order parameter structure of axial nematics provides a natural way to realize some of these allowed transitions. We then discuss how to realize these phase transitions by tuning the couplings in our lattice model in Section 5.2.

5.1.1 Point groups and nematic order parameters

Three-dimensional point groups are classified in terms of seven finite polyhedral groups, $\{T, T_d, T_h, O, O_h, I, I_h\}$, and seven infinite families of axial groups, $\{C_n, C_{nv}, S_{2n}, C_{nh}, D_n, D_{nh}, D_{nd}\}$ [131, 95]. The associated nematic order parameters are tensors that are invariant under the given point-group symmetry. We have discussed these order parameters and their derivation in Chapter 4. Now we review the results that are needed in the following.

Three dimensional orientation can be parametrized in terms of a $O(3)$ matrix

$$R = \begin{pmatrix} \mathbf{l} & \mathbf{m} & \mathbf{n} \end{pmatrix}^T. \tag{5.1}$$

The rows $\mathbf{n}^\alpha = \{\mathbf{l}, \mathbf{m}, \mathbf{n}\}$ of R form an orthonormal triad and satisfy the additional $O(3)$ constraint

$$\sigma = \det R = \epsilon_{abc}(\mathbf{l} \otimes \mathbf{m} \otimes \mathbf{n})_{abc} = \mathbf{l} \cdot (\mathbf{m} \times \mathbf{n}) = \pm 1, \tag{5.2}$$

where σ is the chirality or handedness of the triad $\mathbf{n}^\alpha$ associated with R.

The order parameter tensors are constructed from tensor products of R and we use the point group conventions as those in Chapter 4. In case of the polyhedral nematics $G = \{T, T_d, T_h, O, O_h, I, I_h\}$, the general form of the order parameter is given by $\mathbb{O}^G = \{\mathbb{O}^G[\mathbf{l}\ \mathbf{m}\ \mathbf{n}], \sigma\}$, where $\mathbb{O}^G[\mathbf{l}\ \mathbf{m}\ \mathbf{n}]$ describes the orientational order of the phase and σ is a chiral order parameter needed for the proper polyhedral groups $\{T, O, I\}$. The polyhedral groups have several higher order rotation axes and transform the triads $\{\mathbf{l}, \mathbf{m}, \mathbf{n}\}$ irreducibly: in these cases we only need one tensor to describe the orientational order.

On the other hand, the axial groups $\{C_n, C_{nv}, S_{2n}, C_{nh}, D_n, D_{nh}, D_{nd}\}$ are defined with respect to a symmetry plane involving rotations and/or reflections as well as a perpendicular, axial direction. Correspondingly, the order parameter tensors of the axial point groups have the general structure $\mathbb{O}^G = \{\mathbb{A}^G, \mathbb{B}^G, \sigma\}$, where $\mathbb{A}^G$ defines the ordering related to the orientation of the so-called primary axis perpendicular to the symmetry plane and $\mathbb{B}^G$ describes the in-plane ordering. We refer to $\mathbb{A}$ as the axial order and $\mathbb{B}$ as the in-plane (or just biaxial) order [32]. Similarly, σ is the chiral ordering for the proper axial groups $\{C_n, D_n\}$. Note that the $O(3)$ constraints can reduce the number of independent order parameter tensors in the set $\{\mathbb{A}^G, \mathbb{B}^G, \sigma\}$. Following the conventions in Chapter 4, $\mathbf{n}$ is chosen always to be along the primary axis. Then the axial order parameter tensor $\mathbb{A}^G = \mathbb{A}^G[\mathbf{n}]$ depends only on $\mathbf{n}$ by construction. It follows that the axial order parameter tensor $\mathbb{A}^G = \mathbb{A}^G[\mathbf{n}]$ depends only on $\mathbf{n}$ by construction. Similarly, the in-plane order parameter $\mathbb{B}^G = \mathbb{B}^G[\mathbf{l}, \mathbf{m}]$ depends only on $\{\mathbf{l}, \mathbf{m}\}$ for the symmetries $G = \{C_n, C_{nv}, C_{nh}, D_n, D_{nh}\}$, but is a tensor polynomial $\mathbb{B}^G = \mathbb{B}^G[\mathbf{l}, \mathbf{m}, \mathbf{n}]$ of all the three triads for the symmetries $\{S_{2n}, D_{nd}\}$. We have discussed these ordering tensors in Chapter 4, but for the convenience of the readers, in Table 5.1 we show a selection of axial nematic ordering tensors for the groups which are later encountered.

Moreover, because of the common structure of the axial point groups, the tensors $\mathbb{A}^G$ and $\mathbb{B}^G$ are not unique to a given symmetry, though the axial point group ordering can be uniquely defined by the full set of order

prarameters $\{\mathbb{A}^G, \mathbb{B}^G, \sigma\}$. For instance, the symmetry groups C_n and C_{nv} do not transform the primary axis $\mathbf{n}$, thus the axial ordering tensor for symmetries in these types is simply a vector,

$$\mathbb{A}^{C_n}[\mathbf{n}] = \mathbb{A}^{C_{nv}}[\mathbf{n}] = \mathbb{A}^{C_{\infty v}}[\mathbf{n}] = \mathbf{n}, \tag{5.3}$$

where $C_\infty \cong SO(2)$ is the continuous limit of C_n and $C_{\infty v} \cong O(2)$ is the continuous limit of C_{nv}. The symmetries $\{S_{2n}, C_{nh}, D_n, D_{nh}, D_{nd}\}$, however, transform $\mathbf{n}$ to $-\mathbf{n}$, and therefore have the same axial ordering tensor

$$\begin{aligned}\mathbb{A}^{D_{\infty h}}[\mathbf{n}] &= \mathbb{A}^{C_{\infty h}}[\mathbf{n}] = \mathbb{A}^{C_{nh}}[\mathbf{n}] = \mathbb{A}^{D_n}[\mathbf{n}] = \mathbb{A}^{D_{nh}}[\mathbf{n}] \\ &= \mathbb{A}^{D_{nd}}[\mathbf{n}] = \mathbb{A}^{S_{2n}}[\mathbf{n}] = \mathbf{n}\otimes\mathbf{n} - \frac{1}{3}\mathbb{1},\end{aligned} \tag{5.4}$$

which is just the well-known director order parameter for $D_{\infty h}$-uniaxial nematics. Note that $D_{\infty h}$ can be considered as the continuous limit of the finite groups D_{nh}, and D_{nd}, whereas $C_{\infty h}$ arises from the limit of C_{nh} and S_{2n}. Similarly, axial nematics with the same n-fold in-plane symmetries have the same ordering tensor $\mathbb{B}$,

$$\begin{aligned}&\mathbb{B}^{C_n}[\mathbf{l},\mathbf{m}] = \mathbb{B}^{C_{nh}}[\mathbf{l},\mathbf{m}], \\ &\mathbb{B}^{C_{nv}}[\mathbf{l},\mathbf{m}] = \mathbb{B}^{D_n}[\mathbf{l},\mathbf{m}] = \mathbb{B}^{D_{nh}}[\mathbf{l},\mathbf{m}].\end{aligned} \tag{5.5}$$

Note that, however, though the axial and the biaxial ordering tensors are distinct and transform irreducibly, they are not completely independent due to the $O(3)$ constraints of orthonormality and Eq. (5.2).

5.1.2 Generalized biaxial phases and transitions

The distinction between the primary axis $\mathbf{n}$ and the in-plane axes $\mathbf{l}$ and $\mathbf{m}$ for axial nematics allows the disordering of the axial and in-plane order separately.

A familiar example is the biaxial-uniaxial-isotropic liquid transitions of D_{2h}-biaxial liquid crystals [72–75, 86, 93]. The order parameter tensors of the D_{2h} nematic are defined by two linearly independent rank-2 tensors, $\mathbb{O}^{D_{2h}} = \{\mathbb{A}^{D_{2h}}[\mathbf{n}], \mathbb{B}^{D_{2h}}[\mathbf{l},\mathbf{m}]\}$, where $\mathbb{A}^{D_{2h}}[\mathbf{n}]$ has been give in Eq. (5.4), and $\mathbb{B}^{D_{2h}}[\mathbf{l},\mathbf{m}]$ is the well-known biaxial order parameter,

$$\mathbb{B}^{D_{2h}}[\mathbf{l},\mathbf{m}] = \mathbf{l}\otimes\mathbf{l} - \mathbf{m}\otimes\mathbf{m}. \tag{5.6}$$

Table 5.1. A selection of three-dimensional nematic order parameters. The first column specifies the symmetries, the second column specifies the type $\{\mathbb{A}, \mathbb{B}\}$ of the order, and the third column gives the explicit form of ordering tensors. Besides the tensor shown here, chial nematics C_2 and D_2 in addition have a chiral order parameter defined by σ.

Symmetry Groups	**Type**	**Ordering Tensors**
S_2	$\mathbb{B}[\mathbf{l}, \mathbf{m}, \mathbf{n}]$	$\mathbf{l} \otimes \mathbf{m},\ \mathbf{m} \otimes \mathbf{n},\ \mathbf{n} \otimes \mathbf{l}$
$C_2,\ C_{2h}$	$\mathbb{B}[\mathbf{l}, \mathbf{m}]$	$\mathbf{l} \otimes \mathbf{m}$
$C_{2v},\ D_2,\ D_{2h}$	$\mathbb{B}[\mathbf{l}, \mathbf{m}]$	$\mathbf{l} \otimes \mathbf{l} - \frac{1}{3}\mathbb{1},\ \mathbf{m} \otimes \mathbf{m} - \frac{1}{3}\mathbb{1}$
S_4	$\mathbb{B}[\mathbf{l}, \mathbf{m}, \mathbf{n}]$	$\Big(\mathbf{l} \otimes \mathbf{l} - \mathbf{m} \otimes \mathbf{m}\Big) \otimes \mathbf{n}$
D_{2d}	$\mathbb{B}[\mathbf{l}, \mathbf{m}, \mathbf{n}]$	$\Big(\mathbf{l} \otimes \mathbf{m} + \mathbf{m} \otimes \mathbf{l}\Big) \otimes \mathbf{n}$
$C_2, C_{2v}, C_{\infty v}$	$\mathbb{A}[\mathbf{n}]$	$\mathbf{n}$
$S_2, C_{2h}, D_2,$ $D_{2h}, D_{2d},\ D_{\infty h}$	$\mathbb{A}[\mathbf{n}]$	$\mathbf{n} \otimes \mathbf{n} - \frac{1}{3}\mathbb{1}$

In terms of the symmetries, the biaxial nematic order allows for the phase transitions

$$D_{2h} \to D_{\infty h} \to O(3), \tag{5.7}$$

upon increasing temperature. That is, upon increasing temperature, the biaxial order is destroyed first leading to the restoration of the in-plane $O(2)$ symmetry of uniaxial nematics before the transition to the fully disordered isotropic phase takes place.

Given the general order parameter structure of axial nematics discussed in Section 5.1.1, this transition sequence can be directly generalized to other axial symmetries. We will refer to the associated phase transitions as generalized biaxial transitions. Namely, by first destroying the in-plane order $\mathbb{B}$, the following generalized biaxial-uniaxial transition can be induced

$$\begin{aligned} &C_n, C_{nv} \to C_{\infty v}, \\ &S_{2n}, C_{nh}, D_n, D_{nh}, D_{nd} \to D_{\infty h}. \end{aligned} \tag{5.8}$$

Table 5.2. Generalized biaxial phase transitions. The first column specifies the generalized nematic symmetries and the second column the minimal set of order parameter tensors. Relations of the order parameters given by Eqs. (5.3)–(5.5) are indicated. For the explicit form of these order parameters see Table 4.1. The third and fourth column show the order parameter tensors involved in the generalized biaxial-uniaxial transitions in Eq. (5.8) and the biaxial-biaxial* transitions in Eq. (5.11), respectively. The symbol "$\to$" indicates the replacement of an order.

Symmetry	**Order Parameters**	**Uniaxial-biaxial Transitions**	**Biaxial-biaxial* (Uniaxial-uniaxial*) Transitions**
C_n	$\mathbb{A}^{C_n} = \mathbb{A}^{C_{\infty v}}[\mathbf{n}]$, $\mathbb{B}^{C_n} = \mathbb{B}^{C_{nh}}[\mathbf{l},\mathbf{m}]$, σ	$\mathbb{B}^{C_{nh}}[\mathbf{l},\mathbf{m}]$, σ	$\mathbb{A}^{C_{\infty v}}[\mathbf{n}] \to \mathbb{A}^{D_{\infty h}}[\mathbf{n}]$, σ
C_{nv}	$\mathbb{A}^{C_{nv}} = \mathbb{A}^{C_{\infty v}}[\mathbf{n}]$, $\mathbb{B}^{C_{nv}} = \mathbb{B}^{D_{nh}}[\mathbf{l},\mathbf{m}]$	$\mathbb{B}^{D_{nh}}[\mathbf{l},\mathbf{m}]$	$\mathbb{A}^{C_{\infty v}}[\mathbf{n}] \to \mathbb{A}^{D_{\infty h}}[\mathbf{n}]$
S_{2n}	$\mathbb{A}^{S_{2n}} = \mathbb{A}^{D_{\infty h}}[\mathbf{n}]$, $\mathbb{B}^{S_{2n}}[\mathbf{l},\mathbf{m},\mathbf{n}]$	$\mathbb{B}^{S_{2n}}[\mathbf{l},\mathbf{m},\mathbf{n}]$	$\mathbb{B}^{S_{2n}}[\mathbf{l},\mathbf{m},\mathbf{n}] \to \mathbb{B}^{C_{2nh}}[\mathbf{l},\mathbf{m}]$
C_{nh}	$\mathbb{A}^{C_{nh}} = \mathbb{A}^{D_{\infty h}}[\mathbf{n}]$, $\mathbb{B}^{C_{nh}}[\mathbf{l},\mathbf{m}]$	$\mathbb{B}^{C_{nh}}[\mathbf{l},\mathbf{m}]$	None
D_n	$\mathbb{A}^{D_n} = \mathbb{A}^{D_{\infty h}}[\mathbf{n}]$, $\mathbb{B}^{D_n} = \mathbb{B}^{D_{nh}}[\mathbf{l},\mathbf{m}]$, σ	$\mathbb{B}^{D_{nh}}[\mathbf{l},\mathbf{m}]$, σ	σ
D_{nh}	$\mathbb{A}^{D_{nh}} = \mathbb{A}^{D_{\infty h}}[\mathbf{n}]$, $\mathbb{B}^{D_{nh}}[\mathbf{l},\mathbf{m}]$	$\mathbb{B}^{D_{nh}}[\mathbf{l},\mathbf{m}]$	None
D_{nd}	$\mathbb{A}^{D_{nd}} = \mathbb{A}^{D_{\infty h}}[\mathbf{n}]$, $\mathbb{B}^{D_{nd}}[\mathbf{l},\mathbf{m},\mathbf{n}]$	$\mathbb{B}^{D_{nd}}[\mathbf{l},\mathbf{m},\mathbf{n}]$	$\mathbb{B}^{D_{nd}}[\mathbf{l},\mathbf{m},\mathbf{n}] \to \mathbb{B}^{D_{2nh}}[\mathbf{l},\mathbf{m}]$
$C_{\infty v}$	$\mathbb{A}^{C_{\infty v}}[\mathbf{n}]$	None	$\mathbb{A}^{C_{\infty v}}[\mathbf{n}] \to \mathbb{A}^{D_{\infty h}}[\mathbf{n}]$
$D_{\infty h}$	$\mathbb{A}^{D_{\infty h}}[\mathbf{n}]$	None	None

Note that in these cases we considered situations where the in-plane order has been completely disordered, leading to full $O(2)$ symmetry. Thus the chiral order σ for proper groups C_n and D_n has been simultaneously lost. Nevertheless, we can in principle also have the restorations of only the in-plane $SO(2)$ symmetry with the transitions

$$C_n \to C_\infty,\ D_n \to D_\infty. \tag{5.9}$$

where the chirality σ does not disorder [30]. However, since the handedness

field σ is a composite of $\{\mathbf{l}, \mathbf{m}, \mathbf{n}\}$ featuring also in-plane ordering, these transitions require more fine tuning in comparison to those in Eq. (5.8).

In the opposite limit, if the in-plane order with order parameter $\mathbb{B}$ is sufficiently strong in comparison to the axial ordering $\mathbb{A}[\mathbf{n}]$, we can disorder the primary axis $\mathbf{n}$ without destroying the in-plane order upon increasing the temperature. Note that due to the $O(3)$ constraint, the axial ordering is never fully independent in the presence of the perpendicular in-plane ordering that fixes $\mathbf{n}$ up to sign. Therefore, upon disordering the axial order, the symmetry of the phase is augmented by

$$\sigma_h = \begin{pmatrix} 1 & 0 & 0 \\ 0 & 1 & 0 \\ 0 & 0 & -1 \end{pmatrix}, \tag{5.10}$$

which is a simply a reflection with respect to the $(\mathbf{l}, \mathbf{m})$ plane that acts trivially on the in-plane ordering. Other symmetry operations transforming $\mathbf{n}$ to $-\mathbf{n}$, such as the inversion or a two-fold rotations about an axis in the $(\mathbf{l}, \mathbf{m})$-plane, however, these will simultaneously transform the in-plane order. If such symmetries belong to the original symmetry group G, they will lead to enhanced in-plane symmetries in combination with σ_h. Therefore the new symmetries due to the disordering of the axial order $\mathbb{A}^G[\mathbf{n}]$ are generated by the elements $\langle G, \sigma_h \rangle$ leading to either the direct product structure $G' \times \{\mathbb{1}, \sigma_h\}$ or the semi-direct product $G' \ltimes \{\mathbb{1}, \sigma_h\}$, where G' has either n-fold or $2n$-fold. These are transitions between phases with different "biaxial" orders $\mathbb{B}^G$ and $\mathbb{B}^{G^*}$, for convenience to be referred to as biaxial-biaxial* transitions, where superscript in G^* denotes the presence of the additional reflections in comparison with the low temperature symmetries G. The behavior of the associated orders in the generalized uniaxial-biaxial transitions Eq. (5.8) and biaxial-biaxial* transition are summarized in Table 5.2.

More specifically for the latter "biaxial-biaxial*" case, since σ_h is already contained in the groups C_{nh} and D_{nh}, the disordering of the primary axis with order parameter $\mathbb{A}^G[\mathbf{n}]$ will lead to the phase transition of the

generalized nematics with symmetries $\{C_n, C_{nv}, S_{2n}, D_n, D_{nh}, D_{nd}\}$

$$\begin{aligned} &C_n \to C_{nh}, \\ &S_{2n} \to C_{2nh}, \\ &C_{nv}, D_n \to D_{nh}, \\ &D_{nd} \to D_{2nh}, \end{aligned} \tag{5.11}$$

as follows from the subgroup structure of $O(3)$. Since σ_h is already contained in the groups C_{nh} and D_{nh}, the biaxial* phase is not present for these nematics.

Indeed, we see that these transitions have more interesting features than the generalized uniaxial-biaxial transitions in Eq. (5.8), because σ_h may be "fused" to the parent symmetries via a direct product or semi-direct product, leading to different effects on the original order. For instance, for C_n and C_{nv} nematics, whose axial order parameter $\mathbb{A}^G[\mathbf{n}]$ is simply the vector $\mathbf{n}$, disordering the primary axis in the presence of the in-plane order, i.e. adding the extra symmetry generator σ_h, will simply lift this vector to a director. Consequently, the original axial order is destroyed, but a new axial order will persist as long as $\mathbb{B}$ is ordered and lead to the nematic $\mathbb{B}^{G^*}$.

Moreover, as given in Eq. (5.4), the axial order parameter for D_n nematics is already fixed by the in-plane C_n rotations up to a sign, as well as being invariant under the dihedral π-rotations $\mathbf{m} \to -\mathbf{m}, \mathbf{n} \to -\mathbf{n}$. Therefore, perhaps counter intuitively, upon increasing the temperature and disordering the primary axis, i.e. adding σ_h to the symmetries of the phase, only leads to the vanishing of the chiral order parameter σ, while the axial order parameter $\mathbb{A}[\mathbf{n}]$ is still non-zero, albeit with reduction in its magnitude due to the higher temperature. Last but not the least, in the cases of S_{2n} and D_{nd} nematics, since the biaxial order parameter for these symmetries is a function of all the three triads, $\mathbb{B}^{S_{2n},D_{nd}} = \mathbb{B}^{S_{2n},D_{nd}}[\mathbf{l}, \mathbf{m}, \mathbf{n}]$, disordering $\mathbf{n}$ and promoting σ_h to the axial axis lifts their in-plane structure to a higher in-plane symmetry.

5.2 Gauge theory realization of generalized biaxial transitions

The generalized biaxial transitions in Eq. (5.8) and Eq. (5.11) generalize the biaxial-uniaxial transition of D_{2h} nematics into a much broader class.

These transitions can be readily realized by a gauge-theoretical description for generalized nematics discussed in Chapter 3. We now recollect the model and show how anisotropic couplings that do not break any symmetries serve as tuning parameters for the generalized nematic phase transitions in Sec. 5.1.2.

5.2.1 $O(3)/G$ lattice gauge theory for generalized nematics

In Chapter 3, we introduced a lattice model to describe nematic orders with an arbitrary three-dimensional point group symmetry. The model is a discrete non-Abelian gauge theory, generalizing from Z_2 Abelian Lammert-Rokshar-Toner model for $D_{\infty h}$-uniaxial nematic liquid crystals [25, 26]. In this model, instead of directly dealing with tensor order parameters, the symmetry of three dimensional nematic orders is realized by a point-group-symmetric gauge theory coupled to $O(3)$ matrices. Accordingly, the nematic phase and the isotropic phase are realized by the Higgs phase and the confined phase of the gauge theory, respectively. The model is defined by the Hamiltonian [23],

$$H = H_{\text{Higgs}} + H_{\text{gauge}}, \tag{5.12}$$

$$H_{\text{Higgs}} = -\sum_{\langle ij \rangle} \text{Tr}\left[R_i^T \mathbb{J} U_{ij} R_j\right], \tag{5.13}$$

$$H_{\text{gauge}} = -\sum_{\square} \sum_{\mathcal{C}_\mu} K_{\mathcal{C}_\mu} \delta_{\mathcal{C}_\mu}(U_\square) \text{Tr}\Big[U_\square\Big]. \tag{5.14}$$

H_{Higgs} is a Higgs term describing interactions between matter fields R_i and gauge fields U_{ij}. The matter fields R_i's live on the sites of a cubic lattice and are defined by the $O(3)$ matrix in Eq. (5.1). The gauge fields U_{ij}'s are of the symmetry of G and live on the link $\langle ij \rangle$. $\mathbb{J}$ is a coupling matrix determining how the local axises $\mathbf{n}_i^\alpha$ interact. This model is invariant under gauge transformations

$$R_i \to \Lambda_i R_i, \quad U_{ij} \to \Lambda_i U_{ij} \Lambda_j^T, \quad \forall \Lambda_i \in G, \tag{5.15}$$

which leads to the local identification

$$R_i \simeq \Lambda_i R_i, \quad \mathbf{n}^\alpha \simeq \Lambda_i^{\alpha\beta} \mathbf{n}_i^\beta, \quad \Lambda_i \in G. \tag{5.16}$$

Thus H_{Higgs} can effectively model the orientational interaction between two G-symmetric "mesogens". In addition, H_{Higgs} has the global $O(3)$-

rotation symmetry

$$R_i \to R_i \Omega^T,\ \Omega \in O(3). \tag{5.17}$$

Since gauge symmetries cannot be broken [28], the fully ordered Higgs phase of H_{Higgs} will develop long range order characterized by G-invariant tensor order parameters and thus realizes spontaneous symmetry breaking of Eq. (5.17) from an isotropic $O(3)$ liquid phase to a generalized nematic phase with the symmetry G [23].

H_{gauge} describes a point-group-symmetric gauge theory, where

$$U_\square = \prod_{\langle ij \rangle \in \square} U_{ij} \tag{5.18}$$

denotes the oriented products of gauge fields around plaquettes $\square$. Plaquettes with non-zero flux $U_\square \neq \mathbb{1}$ represent gauge defects. Gauge defects in the same conjugacy class are physically equivalent, correspondingly their core energy, $K_{\mathcal{C}_\mu}$, is a function of the conjugacy classes $\mathcal{C}_\mu$ of the group G. These gauge defects corresponding to the Volterra defects in nematics [23], thus one can in principle turn the topological defects in nematic via assigning these gauge fluxes a finite core energy. However, for the purpose of realizing the generalized biaxial transitions in Eqs. (5.8) and (5.11), the Hamiltonian H_{Higgs} is sufficient and for simplicity we will take $K_{\mathcal{C}_\mu} = 0$ in the following.

5.2.2 Anisotropic couplings and generalized biaxial transitions

In terms of $\mathbf{n}_i^\alpha = \{\mathbf{l}_i, \mathbf{m}_i, \mathbf{n}_i\}$, we can define a local triad vector $\mathbf{n}_j'^\beta = U_{ij}^{\beta\gamma} \mathbf{n}_j^\gamma$ at a site j, which has been brought ("parallel transported") into the same local gauge as $\mathbf{n}_i^\alpha$ at the site i, and express H_{Higgs} as

$$\begin{aligned} H_{\text{Higgs}} &= -\sum_{\langle ij \rangle} \mathbf{n}_i^\alpha \cdot \mathbb{J}^{\alpha\beta} (U_{ij})^{\beta\gamma} \mathbf{n}_j^\gamma \\ &= -\sum_{\langle ij \rangle} \mathbb{J}^{\alpha\beta} \mathbf{n}_i^\alpha \cdot \mathbf{n}_j'^\beta. \end{aligned} \tag{5.19}$$

This shows explicitly that $\mathbb{J}^{\alpha\beta}$ parametrizes the interaction between two local triads.

Table 5.3. Classification the coupling matrix $\mathbb{J}$. The coupling matrix $\mathbb{J}$ needs to be invariant under a given three-dimensional point group G, $\Lambda\mathbb{J}\Lambda^T = \mathbb{J}$, $\forall\Lambda \in G$. The possible forms of $\mathbb{J}$ can be found in from a standard textbook for solid state physics, e.g., Ref. [137].

Symmetry Groups	**Coupling Matrix**
C_1, $C_i \cong S_2$	$\begin{pmatrix} J_1 & J_{12} & J_{13} \\ J_{12} & J_2 & J_{23} \\ J_{13} & J_{23} & J_3 \end{pmatrix}$
$C_s \cong C_{1h} \cong C_{1v}$, C_2, C_{2h}	$\begin{pmatrix} J_1 & & J_{13} \\ & J_2 & \\ J_{13} & & J_3 \end{pmatrix}$
C_{2v}, D_2, D_{2h}	$\begin{pmatrix} J_1 & & \\ & J_2 & \\ & & J_3 \end{pmatrix}$
$C_{n\geq 3}, C_{(n\geq 3)v}$, $S_{2(n\geq 2)}$, $C_{(n\geq 3)h}$, $D_{n\geq 3}$, $D_{(n\geq 3)h}$, $D_{(n\geq 2)d}$	$\begin{pmatrix} J_1 & & \\ & J_1 & \\ & & J_3 \end{pmatrix}$
T, T_d, T_h, O, O_h, I, I_h	$\begin{pmatrix} J & & \\ & J & \\ & & J \end{pmatrix}$

Moreover, $\mathbb{J}$ has to respect the symmetry of the underlying "mesogens" (order parameter fields). In the language of the gauge theory, it needs to satisfy the constraint

$$\Lambda \mathbb{J} \Lambda^T = \mathbb{J}, \ \forall \Lambda \in G \tag{5.20}$$

for a given gauge group G. This heavily restricts the possible forms of $\mathbb{J}$. These possible forms can be found from a standard textbook for solid state physics like Ref. [137], and we tabulate the results in Table 5.3 for the convenience of the reader.

Table 5.3 shows that anisotropic couplings are allowed for axial nematics. This anisotropy is hardwired in the gauge theory Eq. (5.12) and do not break any additional symmetries. Although we have fixed the *local* point group action, i.e. the gauge symmetries, in terms of the triads $\{\mathbf{l}_i, \mathbf{m}_i, \mathbf{n}_i\}$, we can always diagonalize the symmetric matrix $\mathbb{J}^{\alpha\beta}$ by a global redefinition $R_i \to DR_i$, $U_{ij} \to DU_{ij}D^T$. Inspecting the allowed matrices $\mathbb{J}$, the only non-trivial case are the simple monoclinic symmetries $(C_s, C_2, C_{2h},)$, since in the case of C_1 and $C_i \simeq S_2 = \{\mathbb{1}, -\mathbb{1}\}$, there are no rotational gauge symmetries U_{ij} to begin with. It is easy to see that the monoclinic symmetries only introduce a common $\pm$ sign in the $(\mathbf{l}, \mathbf{m})$-plane with the non-diagonal couplings. Therefore without loss of generality we can diagonalize the couplings,

$$\mathbb{J} = \begin{pmatrix} J_1 & & \\ & J_2 & \\ & & J_3 \end{pmatrix} \tag{5.21}$$

with $J_1, J_2, J_3 \geq 0$ for nematic alignment. For the monoclinic symmetries, this requires $J_{13} \leq \sqrt{J_1 J_3}$ and we do not consider negative or "antinematic" couplings [138, 139].

The line of thought can actually be reversed in the sense that we can take couplings J_1, J_2, J_3 be a measure of the three dimensionality of the "mesogens". One realizes that they provide tuning parameters for the phase transitions involving the axial and in-plane ordering. For the purpose of realizing the transitions in Eq. (5.8) and Eq. (5.11), we can

consider the following form for simplicity,

$$\beta\mathbb{J} = \beta \begin{pmatrix} J_1 & & \\ & J_1 & \\ & & J_3 \end{pmatrix} = \beta J_3 \begin{pmatrix} \frac{J_1}{J_3} & & \\ & \frac{J_1}{J_3} & \\ & & 1 \end{pmatrix}$$
$$= \beta J_1 \begin{pmatrix} 1 & & \\ & 1 & \\ & & \frac{J_3}{J_1} \end{pmatrix}, \tag{5.22}$$

where J_1 specifies the coupling of the in-plane degrees of freedom and J_3 the coupling between the primary axes. Therefore this form of $\mathbb{J}$ is allowed for all axial groups and quantifies the anisotropy between the in-plane order and axial order, as the situation considered in Section 5.1.1.

The fact that the phase transitions are tuned with respect to the inversed temperature $\beta = 1/T$ reduces the the independent dimensionless couplings to two in terms of β and the anisotropy $\frac{J_1}{J_3}$ or $\frac{J_3}{J_1}$. The ratio $\frac{J_1}{J_3}$, or equivalently $\frac{J_3}{J_1}$, is in fact an analogue to the so-called biaxiality parameter of D_{2h} nematics [140–142, 71]. Accordingly, when $\frac{J_1}{J_3}$ is sufficiently small, upon increasing temperature we expect that the in-plane order will be lost while the axial order still persist, leading to the generalized biaxial-uniaxial transition given in Eq. (5.8). In the opposite limit, where $\frac{J_1}{J_3}$ is sufficiently large, it is possible to disorder the axial order while the in-plane order is still maintained, leading to the generalized biaxial-biaxial* transitions characterized by Eq. (5.11). Between these two limiting cases we expect direct transitions from the biaxial nematics to the $O(3)$ isotropic liquid. Note however that in general the "biaxial" in-plane order is much more fragile than the uniaxial order of the primary axial axis. Furthermore, the biaxial in-plane order reinforces the uniaxial order since it fixes the perpendicular axial order up to a sign. Conversely, the presence of the axial order reinforces the biaxial order much less, since ordering along $\mathbf{n}$ still leaves in-plane $SO(2)$ fluctuations before the full ordering sets in. As has been discovered in Chapter 3, the highly symmetric order parameter fields experience giant fluctuations and generalized biaxial nematics with a more symmetric in-plane structure require much

larger $\frac{J_1}{J_3}$ to stabilize the in-plane order.

Nevertheless, although $\frac{J_1}{J_3}$ parameterizes the anisotropy of the in-plane and axial order of general biaxial nematics, they are defined in the gauge theory, so their values do not directly describe the relative strength of the in-plane order and axial order. Therefore $\frac{J_1}{J_3} > 1$ does not necessary mean the in-plane order is favored, and vice versa. Moreover, in the gauge theoretical effective Hamiltonian Eq. (4.7) terms respecting all the symmetries appear order by order. Due to the $O(3)$ relations Eqs. (5.1) and (5.2), naturally only two of the orthonormal triads are fully independent. Therefore gauge invariant interactions such as $(\mathbf{l}_i \times \mathbf{m}_i) \cdot (\mathbf{l}_j \times \mathbf{m}_j) = \sigma_i\sigma_j \mathbf{n}_i \cdot \mathbf{n}_j$ or $(\mathbf{l}_i \cdot \mathbf{l}_j)^2 + (\mathbf{l}_i \cdot \mathbf{m}_j)^2 + (\mathbf{m}_i \cdot \mathbf{l}_j)^2 + (\mathbf{m}_i \cdot \mathbf{m}_j)^2 \sim (\mathbf{n}_i \cdot \mathbf{n}_j)^2$ will be present with coefficients parametrized by powers of J_1. Consequently, eventhough $J_3 = 0$, effective axial interactions $J_{3,\text{eff}}(J_1)\sigma_i\sigma_j \mathbf{n}_i \cdot \mathbf{n}_j$ or $J'_{3,\text{eff}}(J_1)(\mathbf{n}_i \cdot \mathbf{n}_j)^2$ will be generated if allowed by the symmetries. In particular this affects higher order axial symmetries that have high rank order parameter tensors with large fluctuations.

5.2.3 Temperature-anisotropy phase diagrams

Based on the discussions in Sections 5.1.2 and 5.2.2, we can now sketch the phase diagrams of biaxial nematics at different temperatures and anisotropies of $\mathbb{J}$ defined in Eq. (5.22). For simplicity, here we will restrict us to axial nematics whose in-plane structure is not very symmetric, so the induced effective axial coupling is not quite relevant. However, in the Appendix 5.A we will briefly discuss situations of highly symmetric axial nematics and the effect of the induced axial coupling.

The phase diagrams with respect to $\frac{J_1}{J_3}$ and $\frac{J_3}{J_1}$ are shown in Fig. 5.1 and Fig. 5.2, respectively. Since $\frac{J_1}{J_3}$ and $\frac{J_3}{J_1}$ are equivalent in measuring the anisotropy of $\mathbb{J}$, these two phase diagrams should be consistent.

Firstly, they should give the same phases and phase transitions. Concretely, in the $\frac{J_1}{J_3}$ phase diagram Fig. 5.1, we expect the generalized biaxial-uniaxial transitions in Eq. (5.8) to happen at small $\frac{J_1}{J_3}$, and the generalized biaxial-biaxial* transitions of Eq. (5.11) happen at large $\frac{J_1}{J_3}$. These phase transitions should respectively appear at large $\frac{J_3}{J_1}$ and small $\frac{J_3}{J_1}$ in the $\frac{J_3}{J_1}$ phase diagram Fig. 5.2.

Secondly, the anisotropies of $\mathbb{J}$ should also be consistent in these two types of phase diagrams. In the $\frac{J_1}{J_3}$ and $\frac{J_3}{J_1}$ phase diagrams, we can define a critical anisotropy $(\frac{J_1}{J_3})^U_c$ and $(\frac{J_3}{J_1})^U_c$ where the biaxial-uniaxial transition

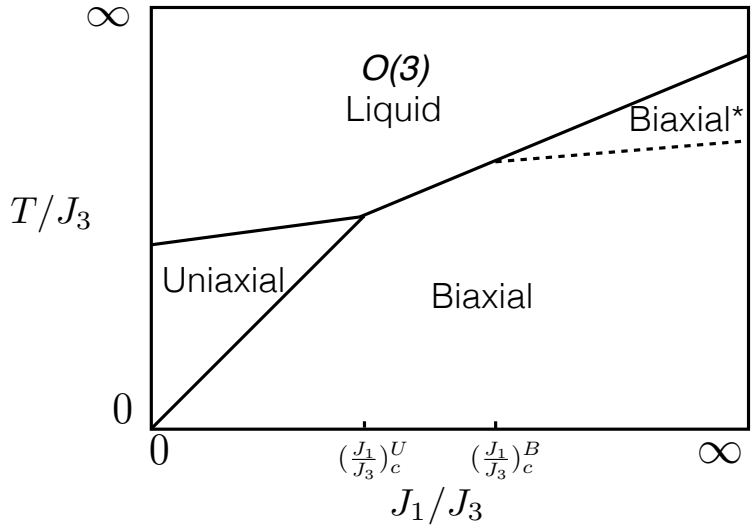

Figure 5.1. The schematic temperature-anisotropy phase diagrams for the axial nematics with not very large n, as a function of $\frac{J_1}{J_3}$. Small and large $\frac{J_1}{J_3}$ correspond to weak and strong in-plane coupling, respectively. $(\frac{J_1}{J_3})_c^U$ and $(\frac{J_1}{J_3})_c^B$ are the critical anisotropy where the generalized biaxial-uniaxial transitions in Eq. (5.8) and the biaxial-biaxial* transitions in Eq. (5.11) terminate, respectively. Solid lines in the figure are for all axial symmetries $\{C_n, C_{nv}, S_{2n}, C_{nh}, D_n, D_{nh}, D_{nd}\}$, while the dashed line is only for symmetries $\{C_n, C_{nv}, S_{2n}, D_n, D_{nd}\}$.

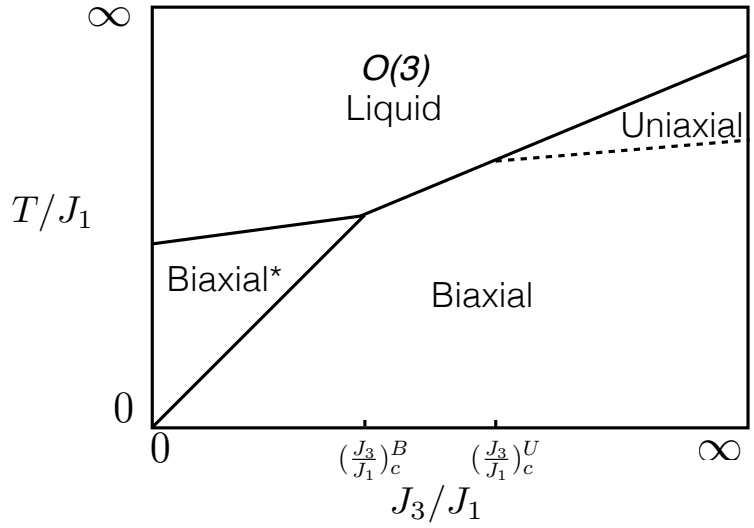

Figure 5.2. The schematic temperature-anisotropy phase diagrams for the axial nematics with not very large, as a function of $\frac{J_3}{J_1}$. Similarly to Fig. 5.1, but small and large $\frac{J_3}{J_1}$ correspond to strong and weak in-plane coupling, respectively.

line terminates, respectively. These two critical anisotropies should satisfy

$$(\tfrac{J_1}{J_3})_c^U = \left[(\tfrac{J_3}{J_1})_c^U\right]^{-1}, \tag{5.23}$$

since they correspond to the same anisotropy of $\mathbb{J}$. A critical anisotropy for the generalized biaxial-biaxial* transition can be defined in a similar way, as $(\frac{J_1}{J_3})_c^B$ and $(\frac{J_3}{J_1})_c^B$, and they in turn satisfy

$$(\tfrac{J_1}{J_3})_c^B = \left[(\tfrac{J_3}{J_1})_c^B\right]^{-1}. \tag{5.24}$$

Moreover, as we discussed in Section 5.2.2, biaxial nematics with a more symmetric in-plane structure require larger J_1 to stabilize the in-plane order. The critical anisotropy $(\frac{J_1}{J_3})_c^U$ for the uniaxial-biaxial transitions in the $\frac{J_1}{J_3}$ phase diagram Fig. 5.1 will therefore move to the right for biaxial nematics with a larger in-plane n-fold rotational symmetry or having more reflection planes acting on in-plane axes. One the other hand, since a weaker in-plane order in turn means a stronger axial order, the critical anisotropy $(\frac{J_1}{J_3})_c^B$ for the biaxial-biaxial* transitions will correspondingly move to the right. Accordingly, in these critical anisotropies of $\mathbb{J}$ will move to the opposite direction in the $\frac{J_3}{J_1}$ phase diagram Fig. 5.2

Lastly, although the gauge theoretical formulation is not realized microscopically in any condensed matter system, it encodes the mesogenic symmetries very efficiently and we expect the qualitative features and the topology of the phase diagrams to be applicable to many generalized nematic systems. This is clear from the biaxial-uniaxial phase diagrams for symmetries D_2 and D_{2h}, where all expected features of the mean-field phase diagram are recovered [140, 71], as will be discussed in more detail in Section 5.3.

5.3 Monte-Carlo simulations

We have simulated the $\frac{J_1}{J_3}$ and $\frac{J_3}{J_1}$ phase diagrams shown in Figs. 5.1 and 5.2 for nematics with symmetries $\{S_2, C_2, C_{2v}, C_{2h}, D_2, D_{2h}, D_{2d}\}$ which covers all types of axial symmetries. Moreover, we also checked the phase transitions in Eqs. (5.8)and (5.11) for many higher symmetries such as S_4, C_{3v}, D_3, D_{3h}, D_4, D_{4h}, D_6 and D_{6h}. We used the standard Metropolis Monte-Carlo algorithm, and the simulations were performed on lattices with the size $L^3 = 10^3, 12^3, 16^3$. Our results agree with the above scenario of generalized biaxial phase transitions.

Table 5.4. Generalized biaxial phase transitions for $\{S_2, C_2, C_{2v}, C_{2h}, D_2, D_{2h}, D_{2d}\}$ nematics. The first column specifies the symmetries and the second column specifies the type of the phase transition. The third and fourth column give the orders which have been destroyed and survive during the phase transition. The explicit from of the associated order parameters can be found in Table 5.1.

Symmetry Groups	Phase Transitions	Order Destroyed	Order Remained
S_2	$S_2 \to C_{2h}$	$\mathbb{B}_2^{S_2}$, $\mathbb{B}_3^{S_2}$	$\mathbb{A}^{D_{\infty h}}$, $\mathbb{B}_1^{S_2} = \mathbb{B}^{C_{2h}}$
	$S_2 \to D_{\infty h}$	$\mathbb{B}^{S_2}$	$\mathbb{A}^{D_{\infty h}}$
	$S_2 \to O(3)$	$\mathbb{A}^{D_{\infty h}}$, $\mathbb{B}^{S_2}$	None
C_2	$C_2 \to C_{2h}$	σ	$\mathbb{A}^{C_{\infty v}}$, $\mathbb{B}^{C_2} = \mathbb{B}^{C_{2h}}$
	$C_2 \to C_{\infty v}$	$\mathbb{B}^{C_2}$, σ	$\mathbb{A}^{C_{\infty v}}$
	$C_2 \to O(3)$	$\mathbb{A}^{C_{\infty v}}$, $\mathbb{B}^{C_2}$, σ	None
C_{2v}	$C_{2v} \to D_{2h}$	$\mathbb{A}^{C_{\infty v}}$	$\mathbb{A}^{D_{\infty h}}$, $\mathbb{B}^{C_{2v}} = \mathbb{B}^{D_{2h}}$
	$C_{2v} \to C_{\infty v}$	$\mathbb{B}^{C_{2v}}$	$\mathbb{A}^{C_{\infty v}}$
	$C_{2v} \to O(3)$	$\mathbb{A}^{C_{\infty v}}$, $\mathbb{B}^{C_{2v}}$	None
C_{2h}	$C_{2h} \to D_{\infty h}$	$\mathbb{B}^{C_{2h}}$	$\mathbb{A}^{D_{\infty h}}$
	$C_{2h} \to O(3)$	$\mathbb{A}^{D_{\infty h}}$, $\mathbb{B}^{C_{2h}}$	None
D_2	$D_2 \to D_{2h}$	σ	$\mathbb{A}^{D_{\infty h}}$, $\mathbb{B}^{D_2} = \mathbb{B}^{D_{2h}}$
	$D_2 \to D_{\infty h}$	$\mathbb{B}^{D_2}$, σ	$\mathbb{A}^{D_{\infty h}}$
	$D_2 \to O(3)$	$\mathbb{A}^{D_{\infty h}}$, $\mathbb{B}^{D_2}$, σ	None
D_{2h}	$D_{2h} \to D_{\infty h}$	$\mathbb{B}^{D_{2h}}$	$\mathbb{A}^{D_{\infty h}}$
	$D_{2h} \to O(3)$	$\mathbb{A}^{D_{\infty h}}$, $\mathbb{B}^{D_{2h}}$	None
D_{2d}	$D_{2d} \to D_{4h}$	$\mathbb{B}^{D_{2d}}$	$\mathbb{A}^{D_{\infty h}}$, $\mathbb{B}^{D_{4h}}$
	$D_{2d} \to D_{\infty h}$	$\mathbb{B}^{D_{2d}}$	$\mathbb{A}^{D_{\infty h}}$
	$D_{2d} \to O(3)$	$\mathbb{A}^{D_{\infty h}}$, $\mathbb{B}^{D_{2d}}$	None

5.3.1 Determination of the phases

To determine the symmetry of a nematic phase with the tensor order parameter $\mathbb{O}^G$, one in principle needs to consider all the entries of $\mathbb{O}^G$. However, for interactions favoring homogeneous distribution of the order parameter fields, such as the interaction in the gauge model Eq. (5.12), the symmetry of the phase can be revealed by the strength of the ordering which is a scalar order parameter defined as

$$q = \sqrt{(\mathbb{O}^G_{abc...})^2}, \tag{5.25}$$

where $\mathbb{O}^G = \frac{1}{L^3}\sum_i \mathbb{O}^G_i$ averages over the system and contractions for repeated indexes are assumed. This nematic ordering strength will develop a finite value in the ordered phase and vanish in the disordered phase (For more details of this method see Chapter 4.).

For axial nematics, we accordingly need to define the ordering strength for the axial order $\mathbb{A}^G$ and the in-plane order $\mathbb{B}^G$, respectively,

$$q_A = \sqrt{(\mathbb{A}^G_{ab...})^2}, \tag{5.26}$$

$$q_B = \sqrt{(\mathbb{B}^G_{ab...})^2}. \tag{5.27}$$

A transition is then identified by the peak of the associated susceptibility

$$\chi(q_{A,B}) = \frac{L^3}{T}(\langle q^2_{A,B}\rangle - \langle q_{A,B}\rangle^2). \tag{5.28}$$

where $\langle ...\rangle$ denotes the thermal average

In addition, we also computed the heat capacity and the susceptibility of the chiral order parameter, which are defined as the usual way,

$$C_v = \frac{1}{T^2 L^3}(\langle E^2\rangle - \langle E\rangle^2), \tag{5.29}$$

$$\chi(\sigma) = \frac{L^3}{T}(\langle \sigma^2\rangle - \langle \sigma\rangle^2). \tag{5.30}$$

where E is the internal energy of the system, and $\sigma = \frac{1}{L^3}\sum_i \sigma_i$ is the global chiral order parameter.

5.3.2 Numerical phase diagrams

Although $\frac{J_1}{J_3}$ and $\frac{J_3}{J_1}$ are equivalent in describing the anisotropy of the coupling matrix $\mathbb{J}$ in Eq. (5.22), there is nevertheless a preference for

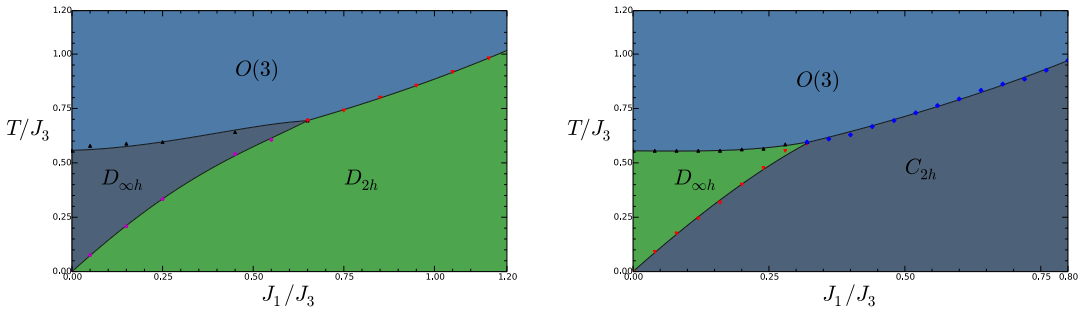

(a) D_{2h}, $\frac{J_1}{J_3}$ (b) C_{2h}, $\frac{J_1}{J_3}$

Figure 5.3. Temperature-anisotropy phase diagram of D_{2h} (a) and C_{2h} (b) nematics as a function of $\frac{J_1}{J_3}$. At small $\frac{J_1}{J_3}$, there is a sequence of biaixal-uniaxial-liquid transition with a vestigial $D_{\infty h}$ uniaxial phase. The vestigial uniaxial phase terminates at a tricritial or triple point, after which the transition sequence truns to a direct biaxial-liquid transition. There is no the biaxial-biaxial* transition in Eq. (5.11) in these two cases.

one or the other in practical simulations. We aimed at the generalized biaxial-uniaxial transitions in Eq. (5.8) by the $\frac{J_1}{J_3}$ phase diagram, since the biaxial* phase may require extremely large $\frac{J_1}{J_3}$ and is in general difficult to access in the $\frac{J_1}{J_3}$ phase diagram. On the other hand, we used the $\frac{J_3}{J_1}$ phase diagram.to discuss the generalized biaxial-biaxial* transitions.

The results are presented in Figs. 5.3 – 5.8. The associated order parameters and their behaviors in the phase transitions are collected in Table 5.1 and Table 5.4, respectively.

These phase diagrams correctly give the expected phase and phase transitions, inluding the well known biaxial-uniaxial transition of D_{2h} and D_2 nematics [140–142]. Particularly, in the $\frac{J_1}{J_3}$ phase digram for D_2 nematics in Fig. 5.4(a), we find that the transition between the D_2-biaxial nematic phase and the $O(3)$ isotropic liquid phase is first-order like. Both $\chi(q_B)$, $\chi(\sigma)$ and C_v exhibit a sudden peak at this transition, and the magnitude of their peak grows dramatically with the lattice size. This discontinuity continues to the biaxial-uniaxial transition line. Therefore, at where the three transition lines in Fig. 5.4(a) meet, we identify a triple point that the three phases can coexist. Moreover, in the middle of the biaxial-uniaxial transition line we find evidence for a tricritical point where the first order phase transition terminates and the transition becomes continous. These observation agree with the experiments results of

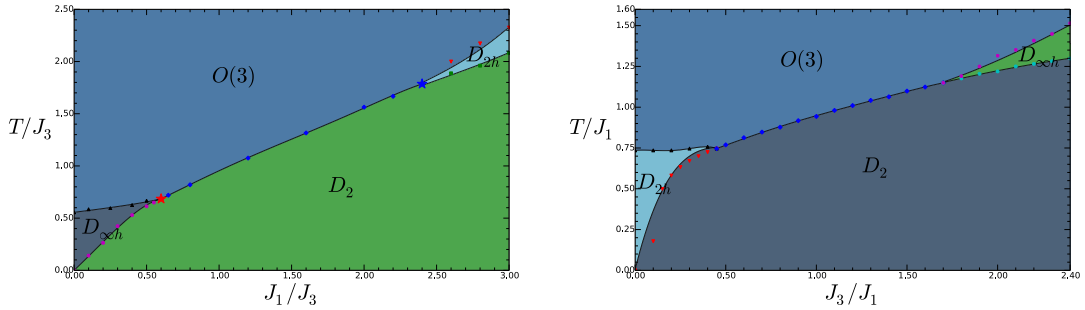

(a) D_2, $\frac{J_1}{J_3}$ (b) D_2, $\frac{J_3}{J_1}$

Figure 5.4. Temperature-anisotropy phase diagrams of D_2 nematics as a function of $\frac{J_1}{J_3}$ (a) and $\frac{J_3}{J_1}$ (b). In addition to a biaxial-liquid transition, there is a $D_2 \to D_{2h}$ biaixal-biaxial* transition at the large $\frac{J1}{J3}$ region.

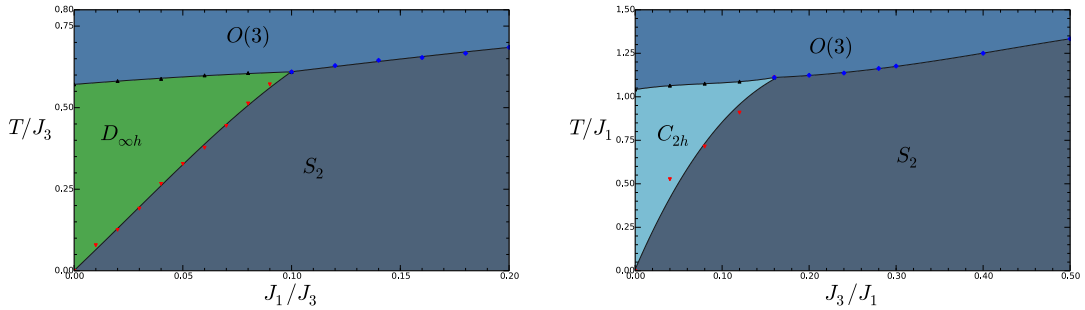

(a) S_2, $\frac{J_1}{J_3}$ (b) S_2, $\frac{J_3}{J_1}$

Figure 5.5. Temperature-anisotropy phase diagrams of S_2 nematics as a function of $\frac{J_1}{J_3}$ (a) and $\frac{J_3}{J_1}$ (b). The $S_2 \to D_{\infty h}$ biaxial-uniaxial transition at small $\frac{J1}{J3}$ region and the $S_2 \to C_{2h}$ biaxial-biaxial* transition at large $\frac{J1}{J3}$ region are shown by (a) and (b), respectively.

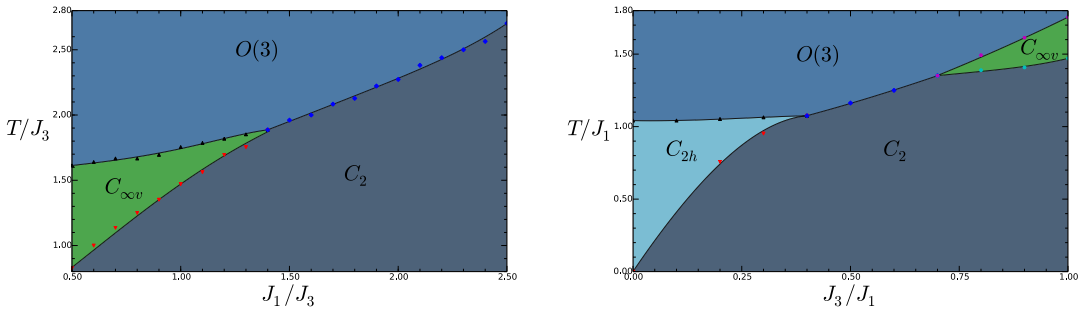

(a) C_2, $\frac{J_1}{J_3}$ (b) C_2, $\frac{J_3}{J_1}$

Figure 5.6. Temperature-anisotropy phase diagrams of C_2 nematics as a function of $\frac{J_1}{J_3}$ (a) and $\frac{J_3}{J_1}$ (b). The $C_2 \to C_{2h}$ biaxial-biaxial* transition is only shown in the $\frac{J_3}{J_1}$ phase diagram for practical convenience.

biaxial nematics in Ref. [98].

Moreover, these numerical phase diagrams demonstrate the consistency of the critical anisotropic couplings discussed in Section 5.2.3. Take the D_2 nematic as an example. As can be seen from Fig. 5.4(a), the critical anisotropy for the uniaxial-biaxial transition in the $\frac{J_1}{J_3}$ phase diagram in Fig. 5.4(a) is $(\frac{J_1}{J_3})_c^U \sim 0.6$. Consistently, the same anisotropy in the $\frac{J_3}{J_1}$ phase digram in Fig. 5.4(b) is given by $(\frac{J_3}{J_1})_c^U \sim 1.7$, satisfying Eq. (5.23).

Although we only show results for a small set of axial nematics, we can already see the tendency of the value of the critical anisotropies with respect to the in-plane symmetry of the order. Take D_2 and D_{2d} nematics as an example. These orders have the same axial structure, while the D_{2d} order has a four-fold in-plane rotational symmetry, as compared to the two-fold rotational symmetry in the D_2 phase. Therefore, we expect the critical anisotropies $(\frac{J_3}{J_1})_c^U$ and $(\frac{J_3}{J_1})_c^B$ of the D_2 order to be larger than those in the D_{2d} case, which is indeed the case in Fig. 5.4(b) and Fig. 5.8(b). As another example, both C_2 and D_2 symmetry have a two-fold in-plane rotations. However, the latter one is more symmetric in its axial order. This in turn means that the axial order in the C_2 case is stronger relative to its in-plane order. Therefore, we expect the critical anisotropies $(\frac{J_3}{J_1})_c^U$ and $(\frac{J_3}{J_1})_c^B$ of the C_2 order to be smaller than those in the D_2 order, as compared to those in the D_2 case, which is indeed the case in Figs. 5.6(b) and 5.4(b).

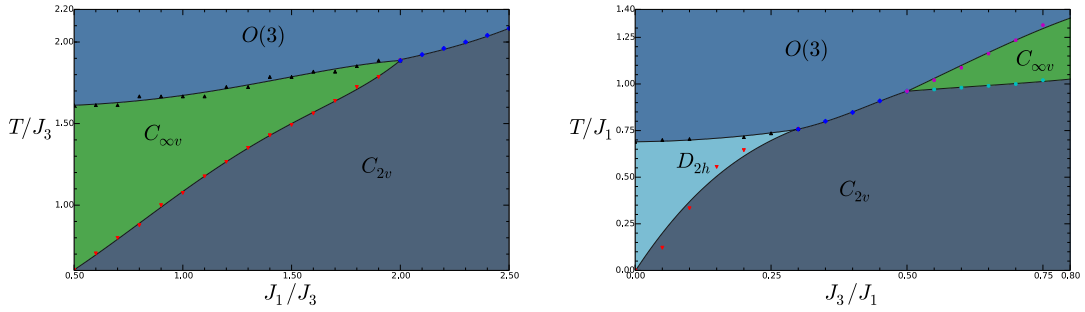

(a) C_{2v}, $\frac{J_1}{J_3}$ (b) C_{2v}, $\frac{J_3}{J_1}$

Figure 5.7. Temperature-anisotropy phase diagrams of C_{2v} nematics as a function of $\frac{J_1}{J_3}$ (a) and $\frac{J_3}{J_1}$ (b). The $C_{2v} \to D_{2h}$ biaxial-biaxial* transition is only shown in the $\frac{J_3}{J_1}$ phase diagram for practical convenience.

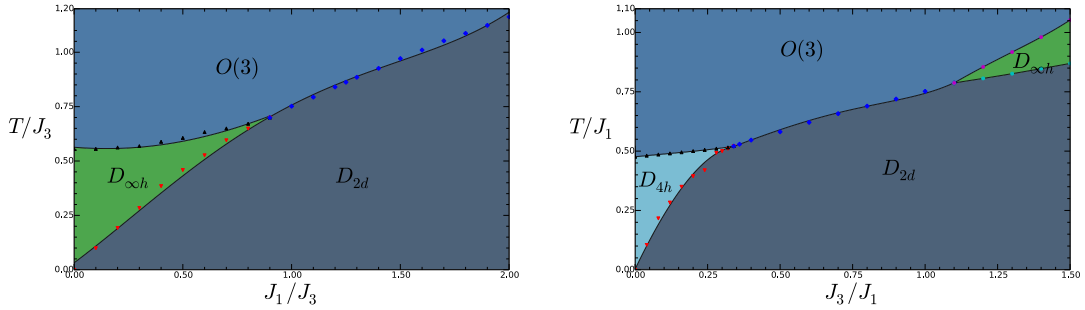

(a) D_{2d}, $\frac{J_1}{J_3}$ (b) D_{2d}, $\frac{J_3}{J_1}$

Figure 5.8. Temperature-anisotropy phase diagrams of D_{2d} nematics as a function of $\frac{J_1}{J_3}$ (a) and $\frac{J_3}{J_1}$ (b). The $D_{2d} \to D_{4h}$ biaxial-biaxial* transition is only shown in the $\frac{J_3}{J_1}$ phase diagram for practical convenience.

5.4 Concluding remarks

There is a rich landscape of unexplored generalized nematics, entailing not only a diversity of orientational phases in terms of their symmetry but also an abundance in possible vestigial phases. In this chapter, we have discussed the anisotropy-induced vestigial uniaxial and biaxial phases for nematics characterized by axial point-group symmetries and studied their phase transitions. Our results generalize the well-studied biaxial-uniaxial transition of D_{2h} nematics to a much broader class, that can be directly accessed within our earlier proposed gauge theoretical formulation of generalized nematics and follow from a-priori symmetry arguments. This framework allows us in particular to compare nematics and vestigial phases with different symmetries in one common reference. Utilizing this formalism, we found that, in comparison to the familiar D_{2h} biaxial nematic phase, nematic phases with high axial symmetries require much lower temperature to stabilize their order. This motivates the fact that biaxial phases with high symmetry are difficult to realize in reality and have not yet been experimentally encountered: before reaching the low temperature demanded by the biaxial order, crystallization may already start playing a role. Consequently, columnar, smectic and/or crystalline phases may occur instead of a generalized nematic phase. These challenges not withstanding, the advances in the fabrication and manipulation of colloidal systems of nanoparticles appear in fact promising with regards to stabilizing generalized nematic phases in the laboratory in the near future [80, 77, 81, 78, 83].

Besides these generalized biaxial transitions, there may be more vestigial phases and transitions in the gauge model Eq. (5.12). Those phases are associated with the defects in the model, which have been ignored in this work by setting $H_{\text{gauge}} = 0$ in Eq. (5.12), describing the confined and Higgs phases of the model. From the point of view of topological melting, phase transitions may be understood as a proliferation of topological defects [26, 30, 31]. To illustrate this further we can take the D_{2h}-biaxial nematic as an example. According to homotopy theory, topological defects of D_{2h} nematics are classified by the five conjugacy classes of the quaternion group Q_8 [143, 19, 20, 116]. Among these defects, there are only three elementary ones, which are the π-disclinations in the three orthogonal planes of the three dimensional space. In the transition of the nematic phase to the $O(3)$ liquid phase, all these defects proliferate. In the biaxial-uniaxial transition, however, one of them stays gapped. This

implies that a phase transition can be affected by the tuning of the energy cost of topological defects. The gauge model Eq. (5.12) provides a natural way to do this. Concretely, when the H_{gauge} term is set to be zero, topological defects in the model only cost elastic energy by the H_{Higgs} term. By tuning on the H_{gauge} term, however, we can introduce a finite core energy to a particular class of topological defects, and therefore modify the nature of the phase transition. While such defect terms $H_{\text{gauge}} \neq 0$ have been identified to be important in the melting of many quantum nematics [60, 61, 58, 59, 16, 144], they have not yet been discovered to play a role in the realm of classical nematics and melting [145]. The rich physics associated with these ideas leave many interesting avenues of for future research in the generalized nematic systems.

5.A Phase diagrams for axial nematics with high symmetries

So far we have focused on axial nematics with a not very symmetric in-plane structure, where the induced axial coupling does not have profound effects. For axial nematics with high symmetries, the induced axial coupling becomes more relevant and may stabilize a uniaxial phase always before the underlying biaxial phase. Here we will briefly discuss the general feature of these situations. For more details, see Ref. [32].

In Fig. 5.9, we show the J_1-J_3 phase diagram for D_{2h}, D_{3h} and D_{4h} nematics. Let us first focus on the D_{2h} case in Fig. 5.9(a). As in the temperature-anisotropy phase diagram in Fig. 5.3(a), in the region with small J_1 and large J_3 there is a vestigial uniaxial phase sandwiched between the fully ordered biaxial phase and the disordered liquid phase. The critical anisotropy where the vestigial uniaxial phase starts appearing is consistent with that of Fig. 5.3(a), up to our numerical accuracy. Moving to D_{3h} case, the increased in-plane symmetry requires a larger in-plane coupling (lower temperature and larger $\frac{J_1}{J_3}$ anisotropy) to stabilize the biaxial order, due to the more severe fluctuations. The biaxial phase is therefore squeezed by the liquid phase and the vestigial uniaxial phase.

The squeezing of the biaxial phase is even more prominent for the D_{4h} nematics, where the in-plane symmetry is increased further. In particular, since very large in-plane coupling is required to stabilize the highly symmetric D_{4h} order, before the biaxial phase is realized, the induced axial coupling is always sufficiently strong for the uniaxial order. This leads to a vestigial uniaxial phase realized for all non-negative values of the "bare" axial coupling J_3, while the direct biaxial-liquid transition is absent. The same is true for the more symmetric D_{6h} nematics, with a even larger region of the vestigial uniaxial phase.

However, one should not interpret this as a no-go theorem for a direct biaxial-liquid transition in the case of highly symmetric biaxial nematics. Instead, this simply means that in order to realize this transition, one needs to consider a model with "anti-nematic" coupling for the axial order to offset the induced axial coupling.

The above discussions can similarly be verified for D_2, D_3 and D_4 nematics as well, as shown in Fig. 5.10. Nonetheless, since the biaxial-biaxial* transition is possible for these cases, in the small J_3 region, there is in addition a vestigial biaxial* phase. This phase is also squeezed as

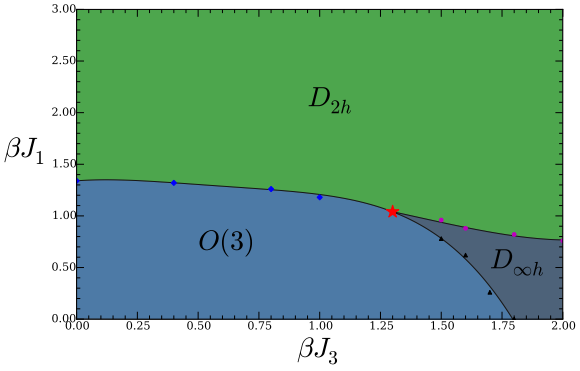

(a) D_{2h} phase diagram

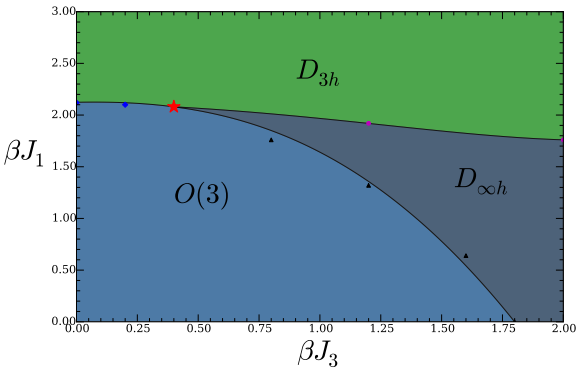

(b) D_{3h} phase diagram

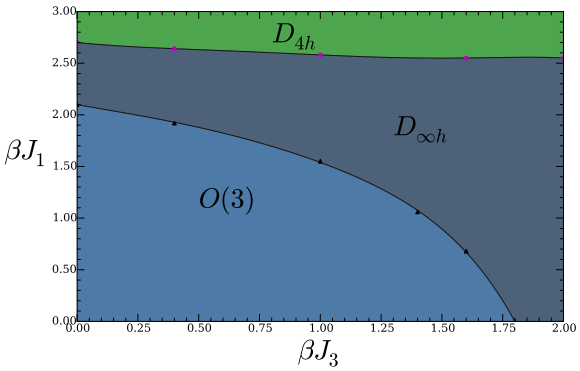

(c) D_{4h} phase diagram

Figure 5.9. The J_1-J_3 phase diagram of (a) D_{2h}, (b) D_{3h} and (c) D_{4h} nematics. Similar to the temperature-anisotropy phase diagram in Fig. 5.3(a), there is a vestigial uniaxial phase appearing from the region with small J_1 and large J_3 (small $\frac{J_1}{J_3}$), realizing the generalized biaxial-uniaxial transition in Eq. (5.8). As the symmetry increases, this vestigial uniaxial phase becomes more prominent and the fully ordered biaxial phase is remarkably squeezed. When the symmetry is sufficiently high, the vestigial uniaxial phase appears adjacent to the isotropic liquid due to the symmetry allowed axial terms. The red star in the D_{2h} and D_{3h} case highlights a tricritical/triple point where the three transition lines meet.

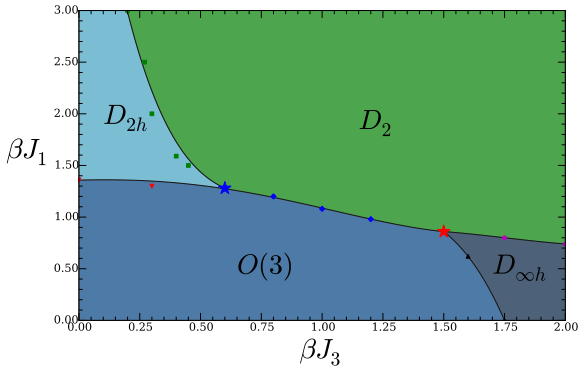

(a) D_2 phase diagram

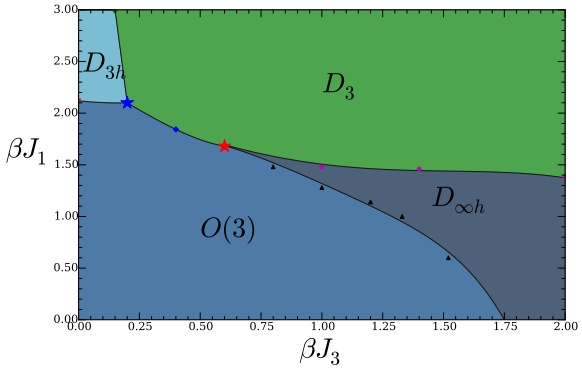

(b) D_3 phase diagram

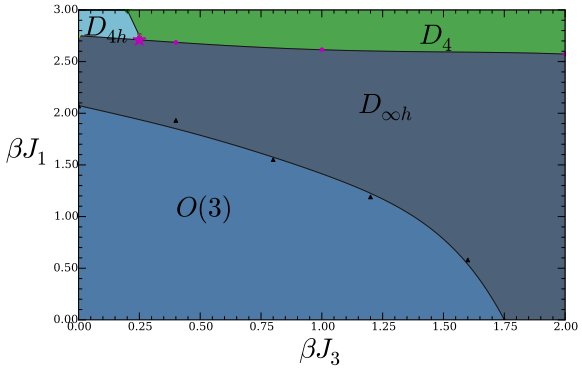

(c) D_4 phase diagram

Figure 5.10. The J_1-J_3 phase diagram of D_2 (a), D_3 (b) and D_4 (c) nematics. Similar to Fig. 5.9, but there is in addition a vestigial biaxial* phase at small J_3 region, realizing the generalized biaxial-biaxial* transition in Eq. (5.11). Both this vestigial biaxial* phase and the fully ordered biaxial phase are squeezed considerably as the symmetry increases. The associated tricritical/triple points at where transition lines meet are highlighted by large stars.

symmetries increase, as in the case of the fully ordered biaxial phase. Moreover, in cases of D_2 and D_3, there are direct transitions from the fully ordered biaxial phase or vestigial biaxial phase to the liquid phase. For the highly symmetric D_4 case, however, these transitions are replaced by a biaxial-uniaxial or a biaxial*-uniaxial transition, since a vestigial uniaxial phase exists for all non-negative values of J_3 as in the D_{4h} case due to the induced axial couplings.

Chapter 6

Conclusion and outlook

The central result of our study in this thesis is the introduction of the $O(3)/G$ gauge theory. This theory utilizes a tool from high energy physics, non-Abelian gauge theory, to describe the statistical physics of nematic orders with an intrinsic three-dimensional point group symmetry. These orders are ubiquitous in condensed matter physics. However, due to the intrinsic symmetry, they require tensor order parameters of unprecedented complexity. Traditional approaches, like the Landau theory and order-parameter-based lattice models, are thus practically not implementable in general. The gauge theory we introduced, on the other hand, fits these nematic orders in a unified framework in an efficient way.

A physical theory should be able to produce useful results. It has been shown that this $O(3)/G$ gauge theory can act as an order parameter generator. Accordingly, we have derived the order parameters for the physically most interesting point-group symmetries. They are anticipated to be helpful for characterizing novel phases in quantum and classical magnets, spinor atoms and assemblies of molecules.

A physical theory should also be able to make testable predictions. With this gauge theory, we have identified the giant fluctuations of highly symmetric orientational orders, and, more interestingly, the emergence of a fluctuation-induced classical chiral liquid phase. We have also generalized the biaxial-uniaxial transition of plate like mesogens to a much broader class of biaxial transitions. This include seven types of biaxial-uniaxial transitions and five types of transitions between different biaxial phases. Given the rapid progress in the tailoring nanoparticles with particular shapes, these phases and phase transitions might well find their way to the laboratory in a near future. Additionally, they can also be verified by numerical experiments such as molecule dynamics where interactions with a certain symmetry can be readily modeled.

Other than these results, the power of the $O(3)/G$ gauge theory has far from been fully mobilized.

This theory provides a platform to chase possible new universality

classes from $O(3)$ breaking. As has been discussed in the beginning of this thesis, phase transitions which break $O(3)$ symmetry may have distinct critical behaviors and the nature of most of them remain to explore. Though in principle these critical properties can also be examined in terms of traditional Landau methods, there one will encounter obstacles raised from the tensor structure of associated order parameters. These obstacles are largely avoided with the $O(3)/G$ gauge theory since it does not directly deal with order parameter fields. For the purpose of chasing new universality classes, among the three-dimensional point groups, polyhedral symmetries $\{T_h, O, O_h, I, I_h\}$ require an even rank ordering tensor, thus a first order phase transition is generically expected; finite axial groups require two ordering tensors and the associated phase transitions may depend on the way how these two tensors couple. The tetrahedral-T and -T_d symmetry, on the other hand, require only a single odd rank ordering tensor, and thereby these can be a good starting point.

Moreover, the $O(3)/G$ gauge theory provides a scheme to study competing exchange interactions of general orientational orders as well. Competition often leads to new physics, such as frustration. We have a model for the ferromagnetic interaction of general orientational orders at hand, and by re-defining the inner product in the model, the ferromagnetic interaction can be modified to non-ferromagnetic interactions. Thus a model of competing interactions of general orientational orders can be constructed. Given the exotic properties of frustrated Ising and Heisenberg magnets, one may expect to find richer physics from the competition between general orientational orders.

Furthermore, this theory is convenient for controlling topological defects in the system. Via the Yang-Mills plaquette term, we can insert certain types of defects into the system, or suppress them, and examine their influence on thermaldynamic quantities and phase transitions. This may even lead to intermediate phases besides the chiral liquid phase and those in the generalized biaxial transitions. From the view of defect melting, the biaxial-uniaxial transition of axial nematics can be understood as defects of different topological charges are proliferated separately. Therefore, it should not be a surprise by assigning distinct core energies to these defects (in terms of coefficients of the Yang-Mills plaquette term), different intermediate phases will be preferred.

Finally, there is a rich landscape of non-Abelian topological orders in the $O(3)/G$ gauge theory. So far we have mainly focused on physics of

matter fields. Discrete gauge theories, however, are topological field theories in the sense that their deconfined phase has non-trivial ground state degeneracy and supports fractionalized excitations. Studies in literatures of discrete gauge theories are often limited to Z_N type Abelian theories. The $O(3)/G$ gauge theory, which inherits the topological properties of discrete gauge theories, is a natural exciting extension of this to non-Abelian realms.

Bibliography

[1] W. Heisenberg, "Mehrkörperproblem und resonanz in der quantenmechanik," Zeitschrift für Physik **38**, 411–426 (1926).

[2] L. D. Landau, "On the theory of phase transitions. i." Zh. Eksp. Teor. Fiz. **11**, 19 (1937).

[3] L. Landau, "Theory of the superfluidity of helium ii," Phys. Rev. **60**, 356–358 (1941).

[4] A. J. Leggett, "A theoretical description of the new phases of liquid ^{3}He," Rev. Mod. Phys. **47**, 331–414 (1975).

[5] L. D. Landau and V. Ginzburg, "On the theory of superconductivity," Zh. Eksp. Teor. Fiz. **20**, 1064 (1950).

[6] L. P. Gor'kov, "Microscopic derivation of the ginzburg-landau equations in the theory of superconductivity," Sov. Phys. JETP **9**, 1364–1367 (1959).

[7] P. W. Anderson, "Plasmons, gauge invariance, and mass," Phys. Rev. **130**, 439–442 (1963).

[8] F. Englert and R. Brout, "Broken symmetry and the mass of gauge vector mesons," Phys. Rev. Lett. **13**, 321–323 (1964).

[9] P. W. Higgs, "Broken symmetries and the masses of gauge bosons," Phys. Rev. Lett. **13**, 508–509 (1964).

[10] G. S. Guralnik, C. R. Hagen, and T. W. B. Kibble, "Global conservation laws and massless particles," Phys. Rev. Lett. **13**, 585–587 (1964).

[11] P. de Gennes and J. Prost, *The Physics of Liquid Crystals*, International Series of Monographs on Physics (Clarendon Press, 1995).

[12] S. A. Kivelson, E. Fradkin, and V. J. Emery, "Electronic liquid-crystal phases of a doped mott insulator," Nature **393**, 550–553 (1998).

[13] E. Fradkin, S. A. Kivelson, M. J. Lawler, J. P. Eisenstein, and A. P. Mackenzie, "Nematic fermi fluids in condensed matter physics," Annual Review of Condensed Matter Physics **1**, 153–178 (2010).

[14] J. Zaanen, Z. Nussinov, and S. Mukhin, "Duality in 2+1D quantum elasticity: superconductivity and quantum nematic order," Ann. Phys. **310**, 181–260 (2004), arXiv:cond-mat/0309397 .

[15] A. Andreev and I. Grishchuk, "Spin nematics," Sov. Phys. JETP **60**, 267 (1984).

[16] D. Podolsky and E. Demler, "Properties and detection of spin nematic order in strongly correlated electron systems," New Journal of Physics **7**, 59 (2005).

[17] P. Anderson, *Basic Notions of Condensed Matter Physics*, Basic Notions of Condensed Matter Physics Series (Benjamin/Cummings, 1984).

[18] D. R. Nelson and J. Toner, "Bond-orientational order, dislocation loops, and melting of solids and smectic-a liquid crystals," Physical Review B **24**, 363 (1981).

[19] N. D. Mermin, "The topological theory of defects in ordered media," Rev. Mod. Phys. **51**, 591–648 (1979).

[20] L. Michel, "Symmetry defects and broken symmetry. configurations hidden symmetry," Rev. Mod. Phys. **52**, 617–651 (1980).

[21] O. Lehmann, "Über fliessende krystalle," Z. phys. Chem **4**, 462–472 (1889).

[22] G. Friedel, "The mesomorphic states of matter," Annales de Physique **18**, 273 (1922).

[23] K. Liu, J. Nissinen, R.-J. Slager, K. Wu, and J. Zaanen, "Generalized liquid crystals: giant fluctuations and the vestigial chiral order of I, O and T matter," arXiv preprint arXiv:1512.07822 (2015).

[24] C. N. Yang and R. L. Mills, "Conservation of isotopic spin and isotopic gauge invariance," Phys. Rev. **96**, 191–195 (1954).

[25] P. E. Lammert, D. S. Rokhsar, and J. Toner, "Topology and nematic ordering," Phys. Rev. Lett. **70**, 1650–1653 (1993).

[26] P. E. Lammert, D. S. Rokhsar, and J. Toner, "Topology and nematic ordering. i. a gauge theory," Phys. Rev. E **52**, 1778–1800 (1995).

[27] E. Fradkin and S. H. Shenker, "Phase diagrams of lattice gauge theories with higgs fields," Phys. Rev. D **19**, 3682–3697 (1979).

[28] S. Elitzur, "Impossibility of spontaneously breaking local symmetries," Phys. Rev. D **12**, 3978–3982 (1975).

[29] K. Liu, J. Nissinen, R.-J. Slager, K. Wu, and J. Zaanen, "Classification of point-group-symmetric orientational ordering tensors," arXiv preprint arXiv:1603.04794 (2016).

[30] K. Liu, J. Nissinen, Z. Nussinov, R.-J. Slager, K. Wu, and J. Zaanen, "Classification of nematic order in $2+1$ dimensions: Dislocation melting and $o(2)/Z_N$ lattice gauge theory," Phys. Rev. B **91**, 075103 (2015).

[31] A. J. Beekman, J. Nissinen, K. Wu, K. Liu, R.-J. Slager, Z. Nussinov, V. Cvetkovic, and J. Zaanen, "Dual gauge field theory of quantum liquid crystals in two dimensions," arXiv preprint arXiv:1603.04254 (2016).

[32] K. Liu, J. Nissinen, J. de Boer, R.-J. Slager, and J. Zaanen, "Hierarchy of orientational phases and axial anisotropies in the gauge theoretical description of generalized nematics," arXiv preprint arXiv:1606.04507 (2016).

[33] H. Kleinert, *Gauge Fields in Condensed Matter, Vol.II Stress and Defects* (World Scientific, Singapore, 1989).

[34] M. Kleman and J. Friedel, "Disclinations, dislocations, and continuous defects: A reappraisal," Rev. Mod. Phys. **80**, 61–115 (2008).

[35] J. M. Burgers, *Some considerations on the fields of stress connected with dislocations in a regular crystal lattice. I* (Royal Dutch Academy of Sciences, 1939).

[36] F. C. Frank, "I. liquid crystals. on the theory of liquid crystals," Discuss. Faraday Soc. **25**, 19–28 (1958).

[37] B. Halperin and D. Nelson, "Theory of two-dimensional melting," Phys. Rev. Lett. **41**, 121–124 (1978).

[38] H. Kleinert and J. Zaanen, "Nematic world crystal model of gravity explaining absence of torsion in spacetime," Phys. Lett. A **324**, 361–365 (2004), arXiv:cond-mat/0309379 .

[39] V. Cvetkovic, Z. Nussinov, and J. Zaanen, "Topological kinematic constraints: dislocations and the glide principle," Philosophical Magazine **86**, 2995–3020 (2006).

[40] P. Ehrenfest, "Bemerkung über die angenäherte Gültigkeit der klassischen Mechanik innerhalb der Quantenmechanik," Zeit. Phys. **45**, 455–457 (1927).

[41] M. Fisher, P. Weichman, G. Grinstein, and D. Fisher, "Boson localization and the superfluid–insulator transition," Phys. Rev. B **40**, 546–570 (1989).

[42] M. Fisher and D. Lee, "Correspondence between two-dimensional bosons and a bulk superconductor in a magnetic field," Phys. Rev. **B39**, 2756–2759 (1989).

[43] V. Cvetkovic, *Quantum Liquid Crystals*, Ph.D. thesis, Leiden University (2006), http://hdl.handle.net/1887/4456 .

[44] J. Goldstone, A. Salam, and S. Weinberg, "Broken symmetries," Physical Review **127**, 965–970 (1962).

[45] A. J. Beekman, K. Wu, V. Cvetkovic, and J. Zaanen, "Deconfining the rotational Goldstone mode: The superconducting quantum liquid crystal in (2+1) dimensions," Phys. Rev. B **88**, 024121 (2013).

[46] J.-M. Park and T. C. Lubensky, "Topological defects on fluctuating surfaces: General properties and the kosterlitz-thouless transition," Phys. Rev. E **53**, 2648–2664 (1996).

[47] M. Henneaux and C. Teitelboim, *Quantization of Gauge Systems* (Princeton University Press, Princeton, NJ, 1992).

[48] X. Wen, *Quantum Field Theory of Many-Body Systems: From the Origin of Sound to an Origin of Light and Electrons*, Oxford Graduate Texts (OUP Oxford, 2004).

[49] F. J. Wegner, "Duality in generalized ising models and phase transitions without local order parameters," Journal of Mathematical Physics **12**, 2259–2272 (1971).

[50] J. B. Kogut, "An introduction to lattice gauge theory and spin systems," Rev. Mod. Phys. **51**, 659–713 (1979).

[51] D. Horn, M. Weinstein, and S. Yankielowicz, "Hamiltonian approach to Z_N lattice gauge theories," Phys. Rev. D **19**, 3715–3731 (1979).

[52] G. Bhanot and M. Creutz, "Phase diagram of $z(n)$ and u(1) gauge theories in three dimensions," Phys. Rev. D **21**, 2892–2902 (1980).

[53] O. Borisenko, V. Chelnokov, G. Cortese, M. Gravina, A. Papa, and I. Surzhikov, "Critical behavior of 3d lattice gauge theories at zero temperature," Nuclear Physics B **879**, 80 – 97 (2014).

[54] K. Gregor, D. A. Huse, R. Moessner, and S. L. Sondhi, "Diagnosing deconfinement and topological order," New Journal of Physics **13**, 025009 (2011).

[55] W. Janke and H. Kleinert, "How good is the villain approximation?" Nuclear Physics B **270**, 135 – 153 (1986).

[56] J. V. José, L. P. Kadanoff, S. Kirkpatrick, and D. R. Nelson, "Renormalization, vortices, and symmetry-breaking perturbations in the two-dimensional planar model," Phys. Rev. B **16**, 1217–1241 (1977).

[57] Villain, J., "Theory of one- and two-dimensional magnets with an easy magnetization plane. ii. the planar, classical, two-dimensional magnet," J. Phys. France **36**, 581–590 (1975).

[58] Z. Nussinov and J. Zaanen, "Stripe fractionalization i: The generation of ising local symmetry," J. Phys. IV France **12**, 245–250 (2002).

[59] J. Zaanen and Z. Nussinov, "Stripe fractionalization: the quantum spin nematic and the abrikosov lattice," physica status solidi (b) **236**, 332–339 (2003).

[60] T. Senthil and M. P. A. Fisher, "Z_2 gauge theory of electron fractionalization in strongly correlated systems," Phys. Rev. B **62**, 7850–7881 (2000).

[61] T. Senthil and M. P. A. Fisher, "Fractionalization, topological order, and cuprate superconductivity," Phys. Rev. B **63**, 134521 (2001).

[62] T. Grover and T. Senthil, "Quantum phase transition from an antiferromagnet to a spin liquid in a metal," Phys. Rev. B **81**, 205102 (2010).

[63] S. V. Isakov, R. G. Melko, and M. B. Hastings, "Universal signatures of fractionalized quantum critical points," Science **335**, 193–195 (2012).

[64] L. Onsager, "The effects of shape on the interaction of colloidal particles," Annals of the New York Academy of Sciences **51**, 627–659 (1949).

[65] W. Maier and A. Saupe, "Eine einfache molekular-statistische theorie der nematischen kristallinflüssigen phase. teil l1." Zeitschrift für Naturforschung A **14**, 882–889 (1959).

[66] P. A. Lebwohl and G. Lasher, "Nematic-liquid-crystal order?a monte carlo calculation," Physical Review A **6**, 426 (1972).

[67] L. Yu and A. Saupe, "Observation of a biaxial nematic phase in potassium laurate-1-decanol-water mixtures," Physical Review Letters **45**, 1000 (1980).

[68] K. Severing and K. Saalwächter, "Biaxial nematic phase in a thermotropic liquid-crystalline side-chain polymer," Physical review letters **92**, 125501 (2004).

[69] B. R. Acharya, A. Primak, and S. Kumar, "Biaxial nematic phase in bent-core thermotropic mesogens," Phys. Rev. Lett. **92**, 145506 (2004).

[70] L. A. Madsen, T. J. Dingemans, M. Nakata, and E. T. Samulski, "Thermotropic biaxial nematic liquid crystals," Physical review letters **92**, 145505 (2004).

[71] G. R. Luckhurst and T. J. Sluckin, eds., *Biaxial Nematic Liquid Crystals: Theory, Simulation and Experiment* (John Wiley & Sons, 2015).

[72] M. J. Freiser, "Ordered states of a nematic liquid," Phys. Rev. Lett. **24**, 1041–1043 (1970).

[73] R. Alben, "Phase transitions in a fluid of biaxial particles," Physical Review Letters **30**, 778 (1973).

[74] J. P. Straley, "Ordered phases of a liquid of biaxial particles," Physical Review A **10**, 1881 (1974).

[75] F. Biscarini, C. Chiccoli, P. Pasini, F. Semeria, and C. Zannoni, "Phase diagram and orientational order in a biaxial lattice model: A monte carlo study," Phys. Rev. Lett. **75**, 1803–1806 (1995).

[76] E. Matijevic, "Monodispersed metal (hydrous) oxides - a fascinating field of colloid science," Accounts of Chemical Research **14**, 22–29 (1981).

[77] F. Li, D. P. Josephson, and A. Stein, "Colloidal assembly: The road from particles to colloidal molecules and crystals," Angewandte Chemie International Edition **50**, 360–388 (2011).

[78] A. G. Mark, J. G. Gibbs, T.-C. Lee, and P. Fischer, "Hybrid nanocolloids with programmed three-dimensional shape and material composition," Nat Mater **12**, 802–807 (2013).

[79] M. Huang, C.-H. Hsu, J. Wang, S. Mei, X. Dong, Y. Li, M. Li, H. Liu, W. Zhang, T. Aida, W.-B. Zhang, K. Yue, and S. Z. D. Cheng, "Selective assemblies of giant tetrahedra via precisely controlled positional interactions," Science **348**, 424–428 (2015).

[80] S. C. Glotzer and M. J. Solomon, "Anisotropy of building blocks and their assembly into complex structures," Nature materials **6**, 557–562 (2007).

[81] P. F. Damasceno, M. Engel, and S. C. Glotzer, "Predictive self-assembly of polyhedra into complex structures," Science **337**, 453–457 (2012).

[82] G. van Anders, D. Klotsa, N. K. Ahmed, M. Engel, and S. C. Glotzer, "Understanding shape entropy through local dense packing," Proceedings of the National Academy of Sciences **111**, E4812–E4821 (2014).

[83] V. N. Manoharan, "Colloidal matter: Packing, geometry, and entropy," Science **349** (2015), 10.1126/science.1253751.

[84] L. E. Hough, M. Spannuth, M. Nakata, D. A. Coleman, C. D. Jones, G. Dantlgraber, C. Tschierske, J. Watanabe, E. Kï£¡rblova, D. M. Walba, J. E. Maclennan, M. A. Glaser, and N. A. Clark, "Chiral isotropic liquids from achiral molecules," Science **325**, 452–456 (2009).

[85] C. Dressel, T. Reppe, M. Prehm, M. Brautzsch, and C. Tschierske, "Chiral self-sorting and amplification in isotropic liquids of achiral molecules," Nature chemistry **6**, 971–977 (2014).

[86] D. W. Allender, M. A. Lee, and N. Hafiz, "Landau theory of biaxial and uniaxial nematic liquid crystals," Molecular Crystals and Liquid Crystals **124**, 45–52 (1985).

[87] E. F. Gramsbergen, L. Longa, and W. H. de Jeu, "Landau theory of the nematic-isotropic phase transition," Physics Reports **135**, 195–257 (1986).

[88] M. V. Jarić, "Landau theory of long-range orientational order," Nuclear Physics B **265**, 647–670 (1986).

[89] L. G. Fel, "Tetrahedral symmetry in nematic liquid crystals," Phys. Rev. E **52**, 702–717 (1995).

[90] L. Radzihovsky and T. C. Lubensky, "Fluctuation-driven 1st-order isotropic-to-tetrahedratic phase transition," EPL (Europhysics Letters) **54**, 206 (2001).

[91] T. C. Lubensky and L. Radzihovsky, "Theory of bent-core liquid-crystal phases and phase transitions," Phys. Rev. E **66**, 031704 (2002).

[92] B. Mettout, "Macroscopic and molecular symmetries of unconventional nematic phases," Phys. Rev. E **74**, 041701 (2006).

[93] D. Allender and L. Longa, "Landau–de gennes theory of biaxial nematics reexamined," Physical Review E **78**, 011704 (2008).

[94] M. Jarić, L. Michel, and R. Sharp, "Zeros of covariant vector fields for the point groups: invariant formulation," Journal de Physique **45**, 1–27 (1984).

[95] L. Michel and B. Zhilinskiı, "Symmetry, invariants, topology. basic tools," Physics Reports **341**, 11–84 (2001).

[96] S. Romano, "Computer simulation study of a simple cubatic mesogenic lattice model," Physical Review E **74**, 011704 (2006).

[97] S. Romano, "Computer simulation study of a simple tetrahedratic mesogenic lattice model," Physical Review E **77**, 021704 (2008).

[98] K. Merkel, A. Kocot, J. Vij, R. Korlacki, G. Mehl, and T. Meyer, "Thermotropic biaxial nematic phase in liquid crystalline organosiloxane tetrapodes," Physical review letters **93**, 237801 (2004).

[99] C. Tschierske and D. J. Photinos, "Biaxial nematic phases," J. Mater. Chem. **20**, 4263–4294 (2010).

[100] J. Toner, "Ordered phases that scatter light strongly," Phys. Rev. A. **27**, 1157 (1983).

[101] J. R. Podgornik, H. H. Strey, K. Gawrisch, D. C. Rau, A. Rupprecht, and V. A. Parsegian, "Bond orientational order, molecular motion, and free energy of high-density dna mesophasesy," PNAS **93**, 4261 (1996).

[102] H. Takezoe and Y. Takanishi, "Bent-core liquid crystals: Their mysterious and attractive world," Japanese Journal of Applied Physics **45**, 597 (2006).

[103] N. W. Ashcroft and N. D. Mermin, *Solid State physics* (Saunders, Philadelphia, 1976).

[104] J. Friedel, *Dislocations* (Pergamon, 1964).

[105] L. Longa, G. Pajak, and T. Wydro, "Chiral symmetry breaking in bent-core liquid crystals," Physical Review E **79**, 040701 (2009).

[106] P. R. Gerber and M. E. Fisher, "Critical temperatures of classical n-vector models on hypercubic lattices," Physical Review B **10**, 4697 (1974).

[107] R. M. Fernandes, A. V. Chubukov, and J. Schmalian, "What drives nematic order in iron-based superconductors?" Nat. Phys. **10**, 97–104 (2014).

[108] Y. Kamiya, N. Kawashima, and C. Batista, "Dimensional crossover in the quasi-two-dimensional ising-o (3) model," Physical Review B **84**, 214429 (2011).

[109] D. W. Johnson and K. N. Raymond, "The self-assembly of a $[Ga_4L_6]^{12-}$ tetrahedral cluster thermodynamically driven by host-guest interactions." Inorg. Chem. **40**, 5157–5161 (2001).

[110] E. K. Honarmand, E. Bill, P. L. Hagedoorn, and W. R. Hagen, "The catalytic center of ferritin regulates iron storage via fe(ii)-fe(iii) displacement." Nat. Chem. Biol. **8**, 941–948 (2012).

[111] R. Zandi, D. Reguera, R. F. Bruinsma, W. M. Gelbart, and J. Rudnick, "Origin of icosahedral symmetry in viruses." PNAS **101**, 15556–15560 (2004).

[112] M. Kumar and D. Blaas, "Human rhinovirus subviral a particle binds to lipid membranes over a twofold axis of icosahedral symmetry," J. Virol **87**, 11309–11312 (2013).

[113] A. Kitaev, "Anyons in an exactly solved model and beyond," Annals of Physics **321**, 2 – 111 (2006), january Special Issue.

[114] X. G. Wen, "Mean-field theory of spin-liquid states with finite energy gap and topological orders," Phys. Rev. B **44**, 2664–2672 (1991).

[115] R. S. Andrist, H. G. Katzgraber, H. Bombin, and M. A. Martin-Delgado, "Tricolored lattice gauge theory with randomness: fault tolerance in topological color codes," New Journal of Physics **13**, 083006 (2011).

[116] C. Xu and A. W. W. Ludwig, "Topological quantum liquids with quaternion non-abelian statistics," Phys. Rev. Lett. **108**, 047202 (2012).

[117] T. Frankel, *The geometry of physics: an introduction* (Cambridge University Press, 2011).

[118] P. Chaikin and T. Lubensky, *Principles of Condensed Matter Physics* (Cambridge University Press, 2000).

[119] E. Fradkin, S. A. Kivelson, M. J. Lawler, J. P. Eisenstein, and A. P. Mackenzie, "Nematic Fermi fluids in condensed matter physics," Ann. Rev. Cond. Mat. Phys. **1**, 153–178 (2010).

[120] R. Rosso, "Orientational order parameters in biaxial nematics: Polymorphic notation," Liquid Crystals **34**, 737–748 (2007).

[121] P. J. Steinhardt, D. R. Nelson, and M. Ronchetti, "Icosahedral bond orientational order in supercooled liquids," Phys. Rev. Lett. **47**, 1297–1300 (1981).

[122] P. J. Steinhardt, D. R. Nelson, and M. Ronchetti, "Bond-orientational order in liquids and glasses," Phys. Rev. B **28**, 784–805 (1983).

[123] M. V. Jarić, "Long-range icosahedral orientational order and quasicrystals," Phys. Rev. Lett. **55**, 607–610 (1985).

[124] A. Haji-Akbari and S. C. Glotzer, "Strong orientational coordinates and orientational order parameters for symmetric objects," Journal of Physics A: Mathematical and Theoretical **48**, 485201 (2015).

[125] Y. Sun and Y. Xia, "Shape-controlled synthesis of gold and silver nanoparticles," Science **298**, 2176–2179 (2002).

[126] M. H. Huang and P.-H. Lin, "Shape-controlled synthesis of polyhedral nanocrystals and their facet-dependent properties," Advanced Functional Materials **22**, 14–24 (2012).

[127] L. Messio, C. Lhuillier, and G. Misguich, "Lattice symmetries and regular magnetic orders in classical frustrated antiferromagnets," Phys. Rev. B **83**, 184401 (2011).

[128] T. Grover and T. Senthil, "Non-abelian spin liquid in a spin-one quantum magnet," Phys. Rev. Lett. **107**, 077203 (2011).

[129] R. Barnett, A. Turner, and E. Demler, "Classifying novel phases of spinor atoms," Phys. Rev. Lett. **97**, 180412 (2006).

[130] T. Zibold, V. Corre, C. Frapolli, A. Invernizzi, J. Dalibard, and F. Gerbier, "Spin-nematic order in antiferromagnetic spinor condensates," Phys. Rev. A **93**, 023614 (2016).

[131] S. Sternberg, *Group theory and physics* (Cambridge University Press, 1995).

[132] D. Litvin, "The icosahedral point groups," Acta Crystallographica Section A: Foundations of Crystallography **47**, 70–73 (1991).

[133] X. Zheng and P. Palffy-Muhoray, "Eigenvalue decomposition for tensors of arbitrary rank," electronic-Liquid Crystal Communications (2007).

[134] S. S. Turzi and F. Bisi, "Determination of the symmetry classes of orientational ordering tensors," arXiv preprint arXiv:1602.06413 (2016).

[135] D. R. J. Chillingworth, R. Lauterbach, and S. S. Turzi, "Molien series and low-degree invariants for a natural action of $\mathrm{SO}(3) \wr \mathrm{Z}_2$," Journal of Physics A: Mathematical and Theoretical **48**, 015203 (2015).

[136] S. S. Turzi, "On the cartesian definition of orientational order parameters," Journal of Mathematical Physics **52**, 053517 (2011).

[137] J. Nye, *Physical Properties of Crystals: Their Representation by Tensors and Matrices*, Oxford science publications (Clarendon Press, 1985).

[138] S. Romano and G. De Matteis, "Orientationally ordered phase produced by fully antinematic interactions: A simulation study," Physical Review E **84**, 011703 (2011).

[139] F. Bisi, G. De Matteis, and S. Romano, "Calamitic and antinematic orientational order produced by the generalized straley lattice model," Physical Review E **88**, 032502 (2013).

[140] A. M. Sonnet, E. G. Virga, and G. E. Durand, "Dielectric shape dispersion and biaxial transitions in nematic liquid crystals," Phys. Rev. E **67**, 061701 (2003).

[141] G. De Matteis and E. G. Virga, "Tricritical points in biaxial liquid crystal phases," Physical Review E **71**, 061703 (2005).

[142] G. De Matteis, S. Romano, and E. G. Virga, "Bifurcation analysis and computer simulation of biaxial liquid crystals," Physical Review E **72**, 041706 (2005).

[143] G. Volovik and V. Mineev, "Investigation of singularities in superfluid he3 in liquid crystals by the homotopic topology methods," Zh. Eksp. Teor. Fiz **72**, 22562274 (1977).

[144] D. F. Mross and T. Senthil, "Stripe melting and quantum criticality in correlated metals," Phys. Rev. B **86**, 115138 (2012).

[145] J. Toner, P. E. Lammert, and D. S. Rokhsar, "Topology and nematic ordering. ii. observable critical behavior," Phys. Rev. E **52**, 1801–1810 (1995).

Samenvatting

De ordening van alle mogelijke kristalstructuren in twee en drie dimensies behelst een van de wetenschappelijke hoogtepunten van de 19e eeuw. Dergelijke tastbare kristallen breken, wiskundig gezien, de translatie- en rotatiesymmetrie van de onderliggende ruimte en worden beschreven middels een zogenaamde ruimtegroep. Vloeibare kristallen, daarentegen, breken alleen de rotatiesymmetrieën en zouden a priori dus op eenzelfde manier moeten kunnen worden ingedeeld in termen van alle mogelijke puntgroepen, i.e. de ondergroepen van de volledig isotrope orthogonale groep $O(3)$. Desalniettemin is traditiegetrouw de wetenschappelijke aandacht voor vloeibare kristallen vooral gefocust op uniaxiale nematische fasen, die één hoofdas bezitten en beschreven worden door puntgroep $D_{\infty h}$, en systemen waarbij ook in een tweede richting orde optreedt, de biaxiale vloeibare kristallen met D_{2h}-symmetrie. Dit is echter slechts een greep uit het totaal aantal mogelijkheden; in drie ruimtelijke dimensies bestaan er zeven oneindige families van axiale en polyhedrale groepen en elke puntgroep kan in principe met een nematische fase corresponderen. De gebruikelijke orderparametermethodiek om deze fasen te bestuderen, i.e. de Landau-de Gennes theorie, is echter zeer gecompliceerd en gaat gepaard met onhanteerbare tensoren van hoge orde. In dit proefschrift worden dergelijk systemen daarom belicht vanuit een alternatief perspectief dat gebaseerd is op een ijktheoretische beschrijving van vloeibare kristallen en corresponderende faseovergangen.

De onderliggende theorie betreft een niet-Abelse discrete ijktheorie waarin $O(3)$ materie wordt gekoppeld aan een ijkveld. Dit ijkveld incorporeert effectief de onderliggende puntgroepsymmetrie met een overeenkomst in fysische vrijheidsgraden tussen de nematische fase in kwestie en de beschrijving als resultaat: de $O(3)$ materie met locale ijksymmetrie fungeert als een orderparameterveld. Dergelijke ijktheorieën alsmede de bijbehorende fasen zijn veelvuldig bestudeerd in de context van de deeltjesfysica en de vloeibare kristal en isotrope vloeibare fasen corresponderen respectievelijk met de welbekende Higgs en confined fase van de ijktheorie. Omdat in deze aanpak de onderliggende puntgroepsymmetrie direct wordt meegnomen in de formulering kunnen de resultaten komende uit de standaard Landau-de Gennes theorie worden gereproduceerd zonder dat de

gecompliceerde tensoren daadwerkelijk hoeven worden te berekend. Bovendien biedt de ijktheoretische beschrijving een algemeen raamwerk dat alle nematische fasen eenduidig en efficient kan bestuderen.

De ijktheoretische beschrijving kan verder de orderparametertensoren expliciet *genereren*, dit in tegenstelling tot de traditionele Landau-de Gennes verhandelingen waar vooraf de concrete vorm met behulp van symmetrieoverwegingen moet worden bepaald. Dit betekent dat men eerst de zeer complexe orderparamatertensor moet construeren alvorens het model en alle relevante interacties kunnen worden bepaald voor het specifieke geval in kwestie. Met de ijktheoretische beschrijving in handen kunnen we echter alle orderparameters eenduidig vinden met de onderliggende symmetrie als enige invoer. Een belangrijk resultaat in dit proefschrift betreft dan ook een systematische categorisering van alle orderparameters voor alle interessante symmetriegevallen, inclusief alle kristallijne puntgroepen, axiale puntgroepen en het geval van icosahedrale symmetrie. Deze systematiek in het landschap van mogelijk nematische fasen is, voor zover wij weten, tot op heden niet ontdekt, hoewel de onderliggende theorie al aandacht geniet sinds de jaren 70.

Daarnaast stelt de bovengenoemde beschrijving ons in staat om alle nematische fasen in een referentiekader te vergelijken. Zodoende kunnen we de orderparameterfluctaties eenduidig vergelijken en vinden we dat deze monotonisch toenemen voor toenemende symmetrie. Een bijbehorend order-by-disorder mechanisme leidt vervolgens tot de mogelijkheid van nieuwe rudimentaire fasen, waarvan een fase gekenmerkt door slechts chiraliteit het meest in het oog springt. We ontdekken dat, met name hoog in de hiërarchische structuur van de puntgroepen, de fluctuaties geassocieerd met nematische orde dramatisch aangroeien. Voor scenarios betreffende polyhedrale groepen met een chiraliteit, i.e. situaties waar de spiegelsymmetrie van de isotrope ruimte is gebroken, kunnen dergelijke fluctuaties de spiegel- en rotatiesymmetrie onafhankelijk breken en zodoende aanleiding geven tot de formatie van een rudimentaire fase die alleen een chirale orde heeft. Deze ontdekkingen zijn dus met nadruk gestoeld op de voordelen van de ijktheoretische beschrijving, aangezien Landau-de Gennes theorieën voor verschillende symmetrieën niet eenduidig te vergelijken zijn.

Tenslotte vinden we dat we eveneens op natuurlijke wijze anisotropieën tussen de componenten langs en loodrecht op de hoofdas in de beschrijving van axiale nematische fasen kunnen toevoegen in de ijktheoretische

beschrijving. Dit stelt ons in staat om nieuwe faseovergangen te voorspellen en reeds bekende faseovergangen te verifiëren. In essentie kan dit worden opgevat als een generalisatie van de welbekende uniaxiale-biaxiale transitie naar algemene axiale puntgroepsymmetrische nematische fasen en brengt zodoende nieuwe mogelijkheden in kaart.

Summary

Crystals break both the translational and rotational symmetry of isotropic space, and are classified by space groups. On the other hand, nematic liquid crystals, which only break the rotational symmetry but are invariant under translations, should be in principle classified by point groups, i.e. subgroups of the full rotational group $O(3)$ of isotropic space. Traditionally, the study of nematic phases has mainly been focused on uniaxial nematics with $D_{\infty h}$-point group symmetry and biaxial nematics with D_{2h}-point group symmetry. However, in three spatial dimensions, point groups encompass seven infinite families of axial groups and seven polyhedral groups. Each point group can correspond to a nematic phase. The conventional approaches to study these phases, such as Landau-de Gennes theory or associated lattice models, involve order parameter tensors of high rank and complicated form, and are in general too unwieldy in practice. This thesis is devoted to a gauge theoretical description of nematic phases and the associated phase transitions.

The underlying theory is a non-Abelian discrete gauge theory which is formulated by a point-group-symmetric gauge theory coupled to $O(3)$ matter. The gauge symmetry in the theory identifies the orientations of the $O(3)$ degrees of freedom under given local point group transformations, and thus realizing the rotational symmetries associated with nematic order. The $O(3)$ matter with local gauge symmetries can be interpreted as coarse-grained order parameter fields. Similar lattice gauge theories have been extensively studied in particle physics and the phase structure and broken symmetry phases have been enumerated. Accordingly, the nematic phase and the isotropic liquid phase are realized by the so called Higgs phase and the confined phase of the gauge theory, respectively. Since this approach emphasizes the symmetries from the outset, it circumvents the global Landau-de Gennes order parameter description, but does not directly depend on the complex high-rank order parameter tensors. Moreover, this theory can fit nematics with any three-dimensional point-group symmetries into a unified framework and treat all of them on a general footing in an efficient way.

The proposed gauge theory can act as a generator of nematic order parameter tensors. This is a significant advantage in comparison with the

traditional Landau-de Gennes theory and the associated lattice models. Those methods require order parameters as a priori degrees of freedom. As a consequence, before one can explicitly formulate a Landau-de Gennes theory or an associated lattice model, one first needs to construct the highly non-trivial order parameters for each symmetry and then enumerate their couplings case-by-case. However, with the gauge theory, we are in principle able to derive the minimal set of order parameter tensors allowed by the symmetries for all point groups, and have enumerated the explicit form of those tensors for many physically interesting symmetries including all the crystallographic point groups, the icosahedral groups as well as all infinite axial groups. The derivation also allows one to elucidate their general structure and interrelations. To the best of my knowledge, this has never been done before in such a general and systematic way, although this problem has been intensively discussed in the liquid crystal community since the 1970s.

Furthermore, this gauge theory allows us to compare different nematic symmetries against a common reference. We were therefore able to quantify the orientational fluctuations of nematic orders with increasing symmetry and identified an order-by-disorder mechanism for a vestigial chiral liquid phase. We discovered that toward the top of the three-dimensional point-group hierarchy, the fluctuations associated with the nematic order increase tremendously. For the chiral polyhedral nematics, for which the left-right hand symmetry of isotropic space is broken, fluctuations in orientations may become sufficiently severe, such that the orientational order and the chiral order can be destroyed separately, with the ramification that room opens for a vestigial liquid phase breaking only chirality. In these observations we again benefit from the gauge theoretical description offering a common microscopic reference making it possible to compare nematics with different symmetries. In the framework of traditional Landau-de Gennes theory, however, the theoretical description of different nematic phases are formulated in terms of different order parameter tensors and/or couplings, rendering such comparisons to be rather ad hoc and obscure.

Finally, we also show that the gauge theory provides a convenient way to access the anisotropy between the axial and in-plane order of axial nematics. We were therefore able to predict and verify many anisotropy-induced vestigial phases. This extends the extensively studied biaxial-uniaxial transition of D_{2h} biaxial nematics to a much broader class, identifying generalized biaxial-uniaxial transitions for all nematics with a finite

axial-point-group symmetry as well as additional transitions between two different but related biaxial nematics and different two uniaxial nematics.

List of Publications

1. *Quantum phase transition in an array of coupled dissipative cavities*, Ke Liu, Lei Tan, Chun-Hai Lv and Wu-Ming Liu, Phys. Rev. A **83**, 063840 (2011).

2. *Extended dual description of Mott transition beyond two-dimensional space*, Yin Zhong, Ke Liu and Hong-Gang Luo, Phys. Rev. B **85**, 075106 (2012).

3. *Alternative Kondo breakdown mechanism: Orbital-selective orthogonal metal transition*, Yin Zhong, Ke Liu, Yong-Qiang Wang and Hong-Gang Luo, Phys. Rev. B **86**, 115113 (2012).

4. *Correlated metallic state in honeycomb lattice: Orthogonal Dirac semimetal*, Yin Zhong, Ke Liu, Yong-Qiang Wang and Hong-Gang Luo, Phys. Rev. B **86**, 165134 (2012).

5. *Half-filled Kondo lattice on the honeycomb lattice*, Yin Zhong, Ke Liu, Yu-Feng Wang, Yong-Qiang Wang and Hong-Gang Luo, Eur. Phys. J. B **86**, 1-8 (2013).

6. *Classification of nematic order in* $2+1$ *dimensions: Dislocation melting and* $O(2)/Z_N$ *lattice gauge theory*, Ke Liu, Jaakko Nissinen, Zohar Nussinov, Robert-Jan Slager, Kai Wu and Jan Zaanen, Phys. Rev. B, **91**, 075103 (2015).
Chapter 2

7. *Generalized liquid crystals: giant fluctuations and the vestigial chiral order of* I*,* O *and* T *matter*, Ke Liu, Jaakko Nissinen, Robert-Jan Slager, Kai Wu and Jan Zaanen, arXiv: 1512.07822, submitted to Phys. Rev. X.
Chapter 3

8. *Dual gauge field theory of quantum liquid crystals in two dimensions*, Aron J. Beekman, Jaakko Nissinen, Kai Wu, Ke Liu, Robert-Jan Slager, Zohar Nussinov, Vladimir Cvetkovic and Jan Zaanen, arXiv: 1603.04254, submitted to Physics Reports.
Chapter 2

9. *Classification of point-group-symmetric orientational ordering tensors*, Jaakko Nissinen, Ke Liu*, Robert-Jan Slager, Kai Wu and Jan Zaanen, arXiv: 1603.04794, accepted by Phys. Rev. E.
Chapter 4

10. *Hierarchy of orientational phases and axial anisotropies in the gauge theoretical description of generalized nematics*, Ke Liu, Jaakko Nissinen, Josko de Boer, Robert-Jan Slager and Jan Zaanen, arXiv: 1606.04507, submitted to Phys. Rev. E.
Chapter 5

Curriculum Vitæ

I was born in 1987 in the village Futudian in Jize, a village in the northern part of China. I did my primary-school studies in the village, but in 1999 I went to Shijiazhuang, the capital of my home province, for middle-school education. Since then I have moved to several places. My high school was in Qingdao. That is a seaside city in the east of China and produces my favorite green tea Laoshan, named by the region where it grows. My first university was in Shijiazhuang again, and I received the bachelor's degree after another four years there. Then I moved to Lanzhou, the geometric center of China, for the master's degree. That city is famous for two things, ramen and the university, and they were combined well in my everyday life there. In 2012, I moved to Leiden to do my PhD with a four-year state scholarship from China.

Acknowledgments

I feel privileged to study and work at the Lorentz Institute, a place filled with interesting people coming from around the world working at the frontier of a wide array of modern physics. The traditional boundary between different branches of physics are very much weakened there. String theorists and cosmologists may work on problems in condensed matter physics, while condensed-matter physicists and soft-matter physicists are equipped with skills which used to be known only to hard-core high energy physicists. I hereby thank all the professors and junior scientists in the institute for creating this special atmosphere, as well as the Chinese Scholarship Council for financially supporting me.

Furthermore, I would like to extend my thanks to my supervisor, prof. Jan Zaanen, and my collaborators, with special mention of Jaakko Nissinen and Robert-Jan Slager, for their help and stimulation in my development as a scientist. I am also grateful to prof. Henk Blöte for his kind help in improving my numerical skills, and the secretaries in the institute — Trudy, Fran and Marianne — for their help in many aspects, as well as all the members in the dissertation committee for their time and assistance.

Friends deserve special thanks. I thank current and former members of the stripe-string club, particularly Balazs, Petter, Nick, Andrey, Louk, Miggy, Bartek, Aron, Vincenzo, Josko, Yan and Yawen, and friends in other groups, especially Qiang, Shuo, Lei, Dapeng, Yujie, Zhihong, Jean Charles, Benny and Debu, as well as all my housemates and friends scattered around other departments of the university. I am pleased with the time and memories we shared.

Finally, my deepest gratitude goes to my family — my grandmother, my parents, my uncles and aunts, my sister and my cousins — for their constant and endless support and care.